UNCLASSIFIED

AD NUMBER

AD006741

NEW LIMITATION CHANGE

TO

Approved for public release, distribution unlimited

FROM

Distribution authorized to U.S. Gov't. agencies and their contractors; Administrative/Operational Use; 30 SEP 1952. Other requests shall be referred to Office of Naval Research, Washington, DC.

AUTHORITY

onr ltr, 9 nov 1977

THIS PAGE IS UNCLASSIFIED
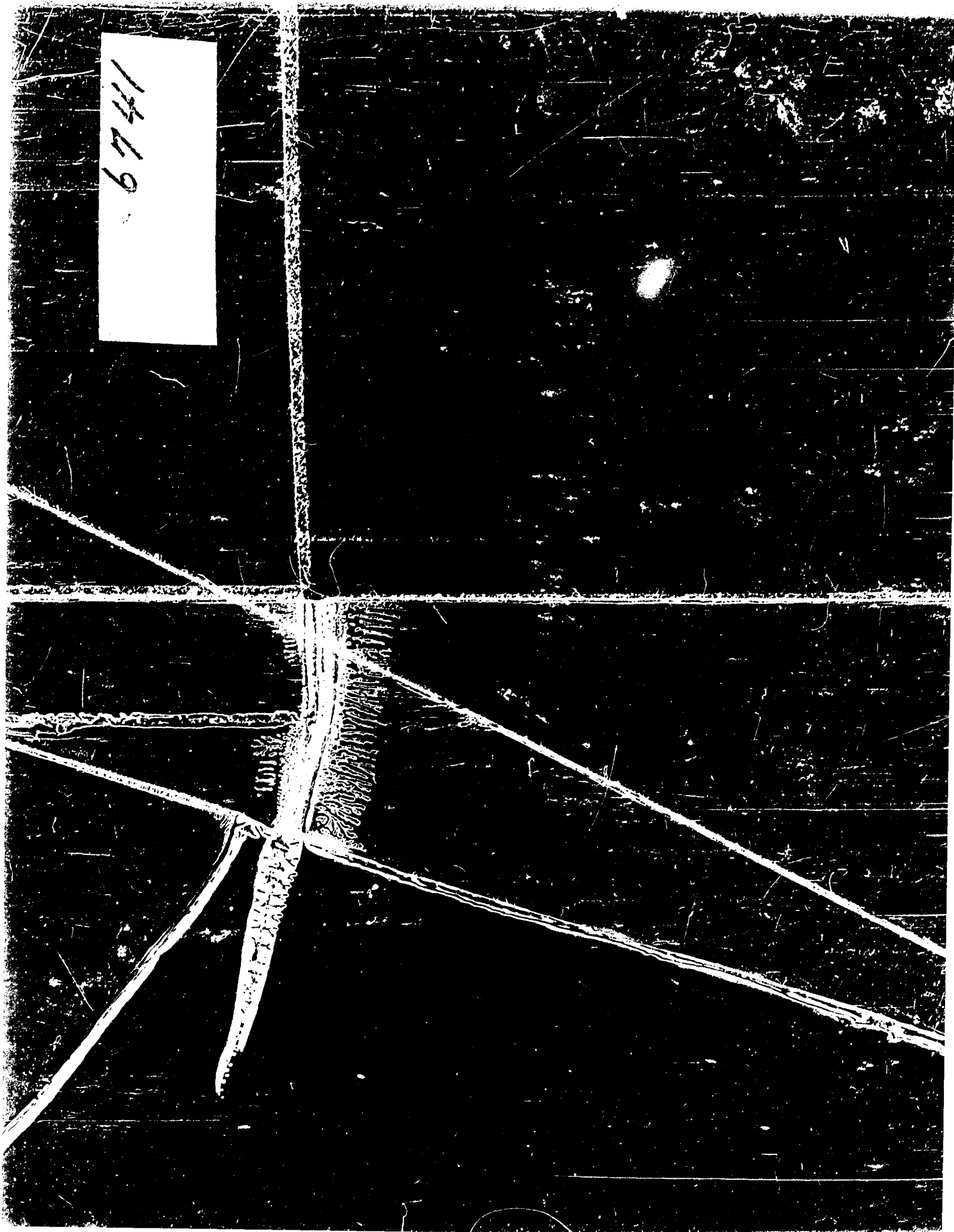
NORTHWESTERN UNIVERSITY

Evanston, Illinois

The Technological Institute   September 30, 1952
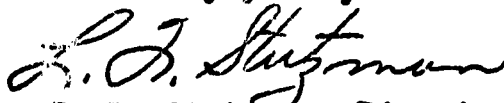
Letter of Transmittal

Chief of Naval Research
EXOS:ONR: N66
Serial No. 20450
Washington 25, D. C.

Attention: Commander Thompson

Dear Sir:

    Attached is the tri-monthly report for the period June 1-
September 30, 1952 (inclusive) for Project NR 266-001 at North-
western University. This report covers work done here principally
in the past three months and which is at a satisfactory stage
for reporting. Other phases which are not reported here but
on which work is progressing are noted in the introductory
summary.

                            Sincerely yours,

                            L. F. Stutzman, Director
                            Project 130
                            Chemical Engineering Department

LFS:ml

CHEMICAL ENGINEERING DEPARTMENT

NORTHWESTERN TECHNOLOGICAL INSTITUTE

Evanston, Illinois

TRI-MONTHLY REPORT

(July 1 - September 30, 1952)

NR 266-001
(N6-ori-158)

Respectfully submitted,

September 30, 1952

Director

Assistant Director

TABLE OF CONTENTS

LIST OF FIGURES

LIST OF TABLES

DISTRIBUTION LIST

The following offices are being sent copies of this report in the amount shown.

Office	No. of Copies
Commanding Officer, Office of Naval Research 495 Summer Street, Boston 10, Massachusetts	1
Commanding Officer, Office of Naval Research 346 Broadway, New York 13, N. Y.	1
Commanding Officer, Office of Naval Research 801 Donahue Street, San Francisco 24, California	1
Commanding Officer, Office Naval Research 1030 Green Street, Pasadena 1, California	1
Officer in Charge, Office of Naval Research, Branch Office, London Navy Number 100, Fleet Post Office, New York, N. Y.	2
Chief of Naval Research, Department of the Navy Attn: Code 466, Washington 25, D. C.	25
Commanding Officer, Office of Naval Research 844 North Rush Street, Chicago 11, Illinois	2
*Chief of the Bureau of Ships (Code 649) Department of the Navy, Washington 25, D. C.	3
*Commander, Mare Island Naval Shipyard (Code 371), Vallejo, California	1
*Science Division, Navy Research Section Library of Congress, Washington 21, D. C.	5
Officer in Charge, U. S. Naval Medical Research Laboratory U S. Naval Submarine Base, New London, Connecticut	1
Director of Research, Northwestern Technological Institute Evanston, Illinois	1
Chemical Engineering Department Northwestern Technological Institute, Evanston, Illinois	1

*The offices so marked are at present not being supplied direct. They are
are being supplied by Chief of Naval Research from their supply.

INTRODUCTORY SUMMARY

The present tri-monthly report covers three of the methods for removal of CO_2 from air which are under investigation by Project N6-ori 158. These methods are: the removal of CO_2 by reaction with a regenerative type solid; the freezing out of CO_2 by lowering the air temperature, this temperature lowering being accomplished by compressing the air, cooling the air back to approximately room temperature and expanding back to one atmosphere pressure; and the absorption of CO_2 in regenerative solvents at below room temperature.

The information available on the regenerative type solid indicates that silver oxide is the best such material to be used. Theoretical mechanism equations have been derived for two modes of operation of the absorption step of a regenerative CO_2-removal process using silver oxide as the absorbent. These equations have been solved for the case of CO_2 absorption at a rate of 7.5 lb/hr from air of 21% CO_2 content, by volume, and the results are presented in graphical form.

Experiments have been carried out on a small-scale fixed-bed absorption unit in order to evaluate the constants of the derived mechanism equations. Such experimental runs have indicated the repeatability of absorption - desorption cycle; i.e. - absorption at room temperature from air of 1% CO_2 content, and desorption by decomposition of the carbonate at 125°C and 5 mm. Hg. Further work will support the conclusion of feasibility indicated by these preliminary experiments and will result finally in a complete process design for an operating unit.

The freeze out method feasibility study has been completed. This process does not lend itself readily to simple research techniques and construction of a unit, even in a small size was outside the present scope of the project. This process does have possibilities and investigation should continue further with the construction of a test unit to determine what difficulties, if any, might be encountered in making the process work.

The low temperature absorption method requires the determination and interpretation of data on the solubility of CO_2 in solvents at various temperatures. The latest data and interpretation are presented in this report. More such data and data on rate of absorption and heat exchange studies, also in progress, will be presented at a later date.

Other studies in progress are.

Absorption of CO_2 in sea water

Absorption of CO_2 on charcoal

Absorption of CO_2 on solid NaOH

Freezing out of CO_2 with outside mechanical refrigeration

Freezing out of CO_2 with liquid oxygen

These problems will be covered in later reports.

SECTION I

CO_2 ABSORPTION WITH Ag_2O

INTRODUCTION

One of the most promising regenerative chemical methods for removal of CO_2 from air is by reaction with silver oxide to form silver carbonate, which can later be regenerated to the original silver oxide. This method, along with many others, was listed in the complete survey of CO_2-removal methods presented in a recent report of Project NR 266-001, dated March 31, 1952. The same general reaction will occur with many metal oxides, but silver oxide seems to offer the best possibility of easy reversibility, thus making possible a regenerative process for CO_2 removal.

During the past three months, considerable effort has been expended on a study of the possibilities of the silver oxide-silver carbonate system as a CO_2-removal process. Theoretical mathematical expressions have been developed which represent the CO_2 addition step for two different modes of operation. In addition, several small-scale runs have been made to indicate the applicability of the theoretical expressions to the actual system and to determine the rate of CO_2 removal in such a system. This report will outline the results of the work to date and indicate the direction to be taken by future studies.

THERMODYNAMIC DATA

Addition of CO_2 to silver oxide, or to any other metal oxide, will occur only when the partial pressure of the CO_2 in contact with the solid is greater than the equilibrium value determined by:

$$eq\ p_{CO_2} = \frac{1}{K_{eq}}$$

where:
$$\ln K_{eq} = -\frac{\Delta G_T^\circ}{RT}$$

(In these expressions, K_{eq} is the equilibrium constant for the reaction, ΔG_T° is the standard free energy change of the reaction at temperature $T^\circ K$, and R is the gas constant.)

Similarly, decomposition of the metal carbonate will take place only when the partial pressure of the CO_2 in contact with solid is less than the above equilibrium value.

The reaction for the proposed silver oxide process is as follows:

$$Ag_2O + CO_2 \rightleftharpoons Ag_2CO_3$$

Basic data for the various components are tabulated in Table I. In addition, heat capacity data are plotted on Figure 1; where necessary, extrapolations have been made.

Values for K_{eq} at various values of temperature have been calculated from the basic data presented, making use of the following relationships:

$$\Delta \overline{C}_p = \overline{C}_p\ (Ag_2CO_3) - \overline{C}_p\ (Ag_2O) - \overline{C}_p\ (CO_2)$$

$$\Delta (\Delta H_f^\circ) = \Delta \overline{C}_p \int_{291}^{T} dT$$

$$\Delta (\Delta S^\circ) = \Delta \overline{C}_p \int_{298}^{T} dT/T$$

$$\Delta G_T^\circ = \Delta H_{f,T}^\circ - T \Delta S_T^\circ$$

.Results of these calculations are plotted on Figure 2, as $\log_{10} K_{eq}$ vs. $1/T(^\circ K)$. In additon, since eq. $p_{CO_2} = 1/K_{eq}$, values of the equilibrium p_{CO_2} have been calculated and are plotted on Figure 3 vs. $1/T(^\circ K)$. This latter plot will be of use in predicting the pressure-temperature combinations at which decomposition of the carbonate should take place.

TABLE I

BASIC THERMODYNAMIC DATA

System: $Ag_2O + CO_2 \rightleftharpoons Ag_2CO_3$
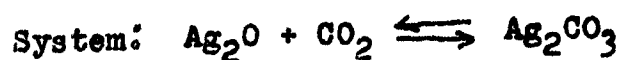
Temperature		C_p (cal/gm mol - °K)		
(°K)	(°F)	CO_2 [1]	Ag_2O [2]	Ag_2CO_3 [2]
10	-442	----	1.08	0.49
25	-415	----	5.26	3.90
50	-370	----	8.44	10.22
100	-280	----	10.75	16.95
150	-190	----	12.47	20.79
200	-100	----	13.93	23.20
298.1	77	9.17	15.75	26.83
350	170	9.53	----	----
400	260	9.86	----	----
450	350	10.19	----	----
500	440	10.43	----	----

	CO_2	Ag_2O	Ag_2CO_3
$S^°_{298.1°K}$ (cal/gm mol, °K)	51.1 [3]	29.1 [2]	40.0 [2]
$\Delta H^°_{f, 291.1°K}$ (kcal/gm mol)	-94.03 [3]	-6.95 [3]	-120.5 [3]

[1] Hougen and Watson - Chemical Process Principles, Vol. I, p. 214

[2] K. K. Kelley - Bu. Mines Bull. 434 (1941)

[3] Lange - Handbook of Chemistry

FIGURE 1

HEAT CAPACITY DATA

Ag_2CO_3

Ag_2O

CO_2

C_p (CAL/GM-MOL °K)

TEMP. (°K.)
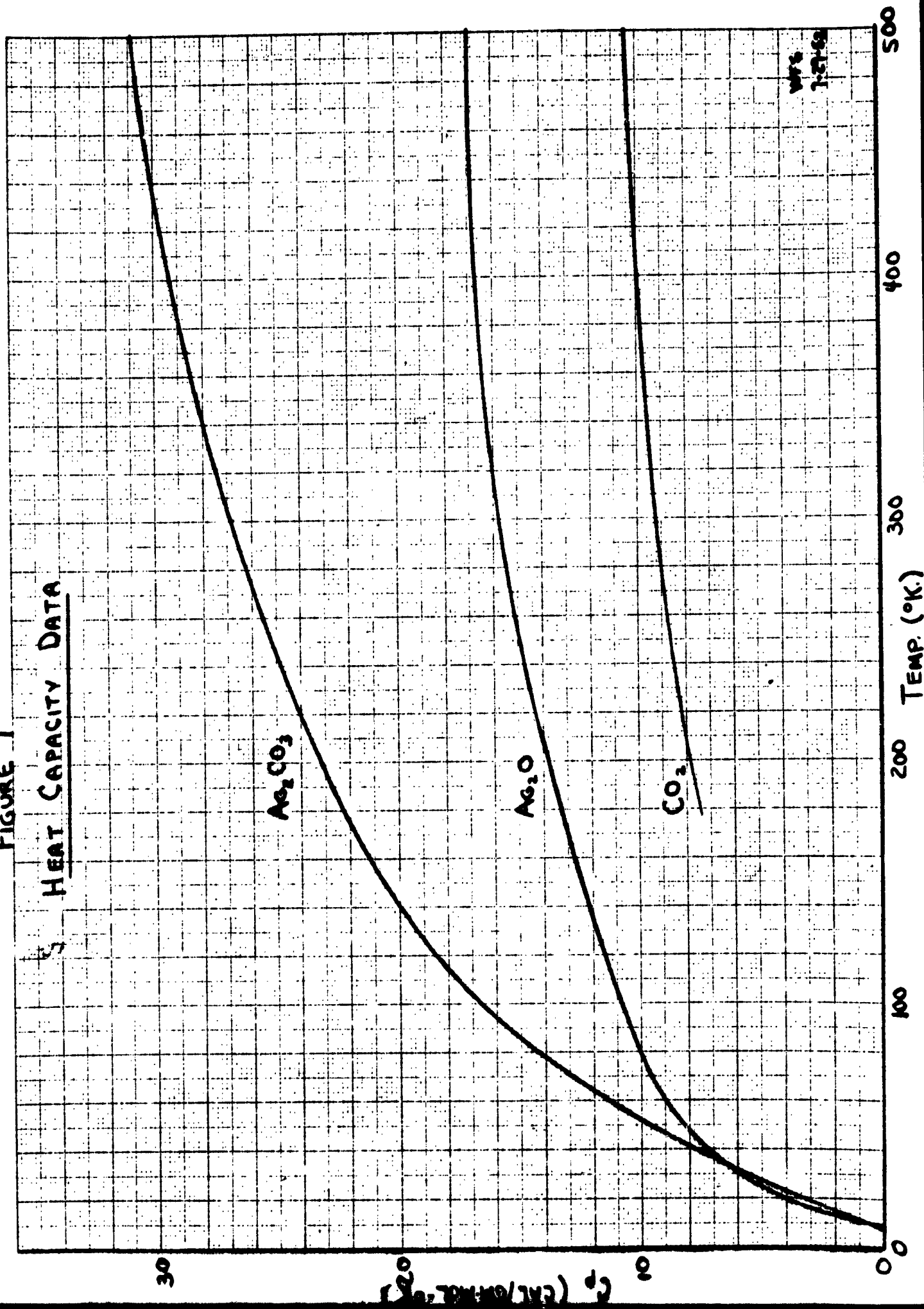
FIGURE 2

$$\text{LOG}_{10} \, K \quad \text{vs.} \quad \frac{1}{T(^\circ K)}$$

FOR THE SYSTEM:

$$Ag_2O + CO_2 \rightleftharpoons Ag_2CO_3$$

NOTE –
$$K = \frac{1}{p_{CO_2}}$$

WFS
7-29-52

133
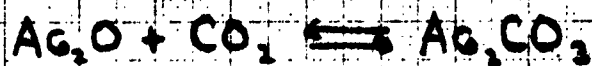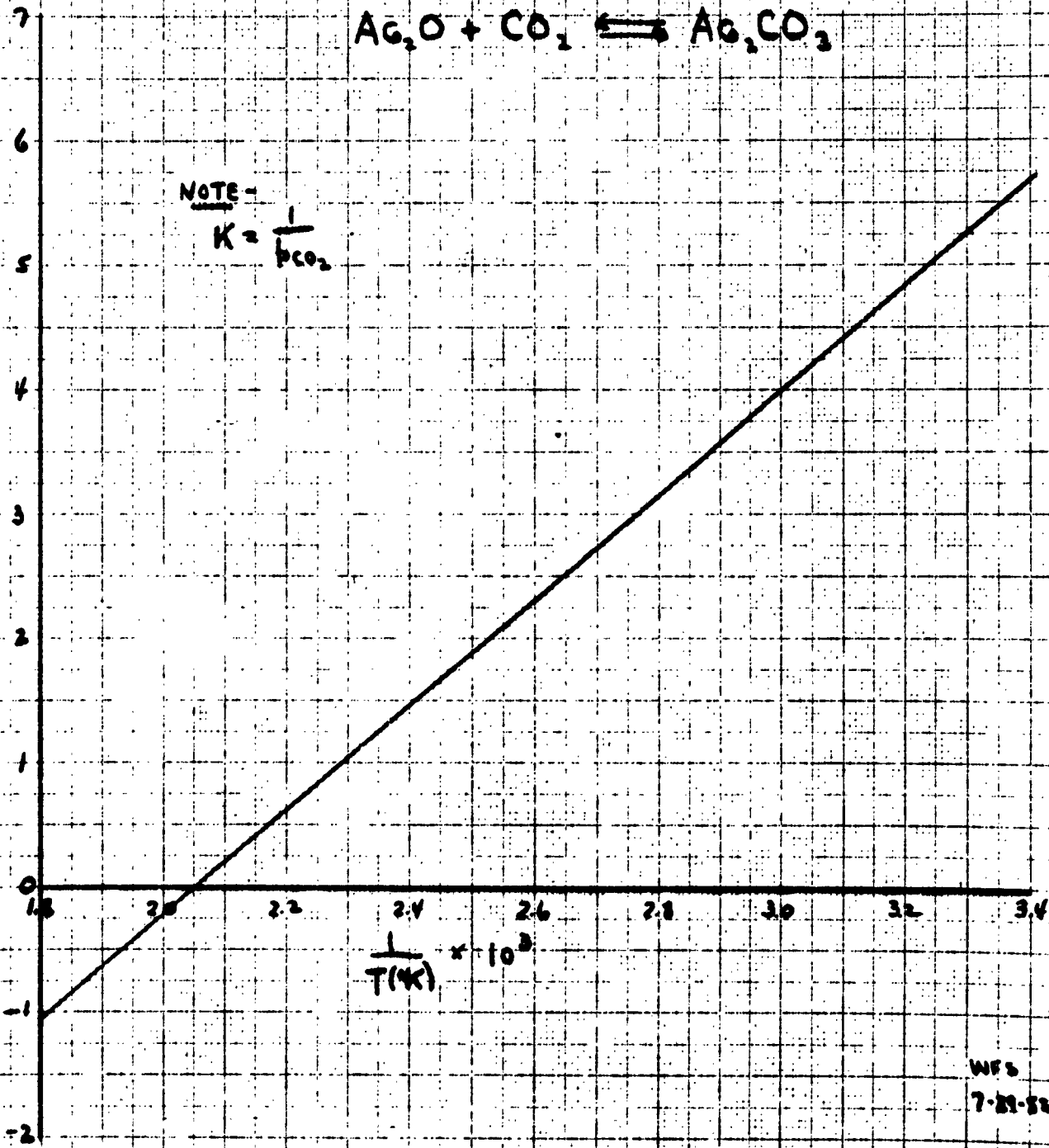
FIGURE 3

EQUILIBRIUM PRESSURE OF CO_2

FOR THE SYSTEM :
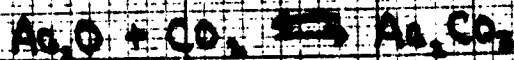
$Ag_2O + CO_2 \rightleftharpoons Ag_2CO_3$

WFS
7-30-62
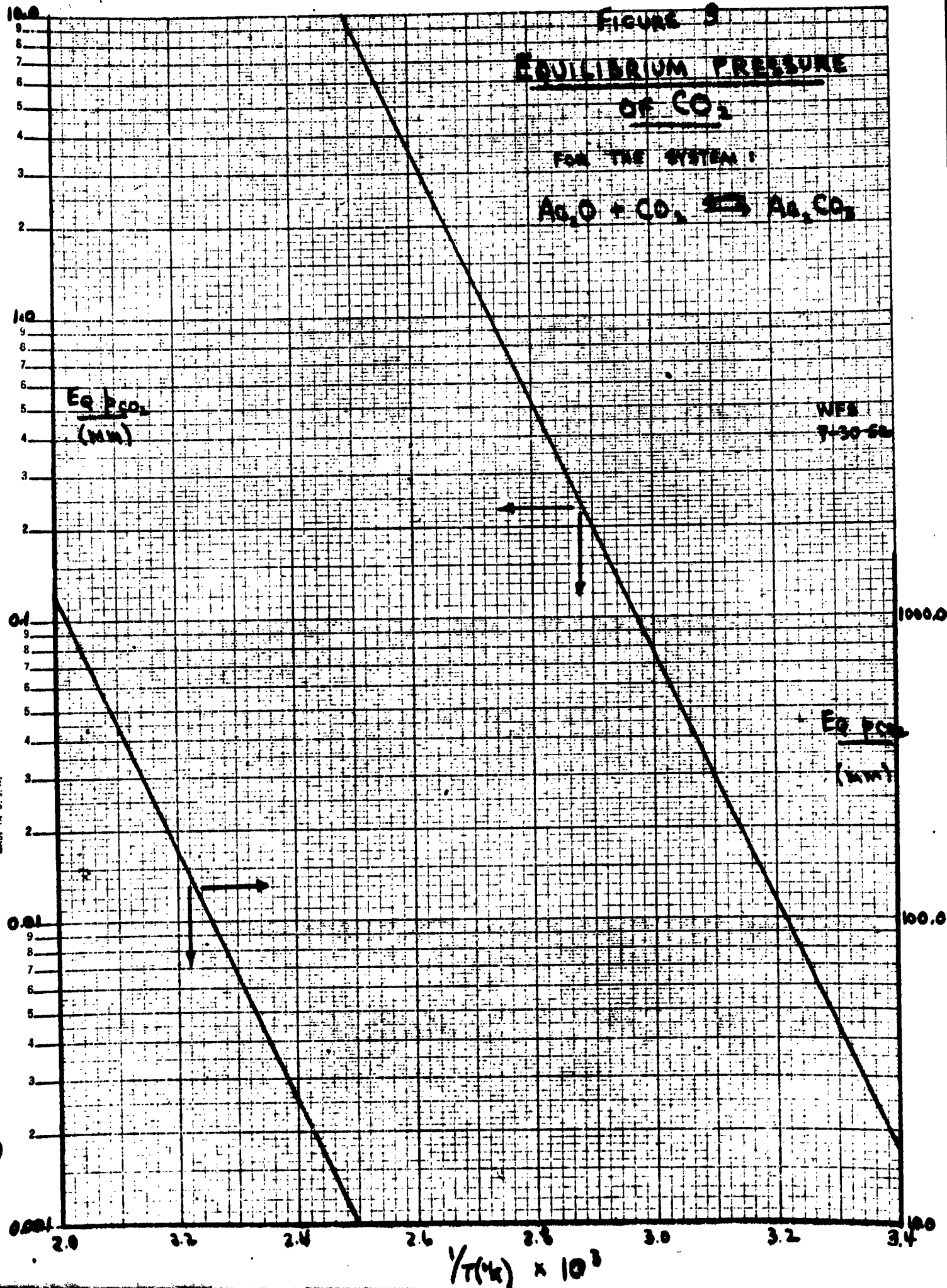
. PROPOSED UNIT

Assuming that alternate absorption of CO_2 and decomposition of carbonate can take place over many cycles with little decrease in the activity of the silver oxide for further CO_2 absorption, there are several possible mechanical arrangements which might be employed for a full-scale unit. A final choice of the best method to use would be difficult to make at this time. Instead, three different processes will be proposed and their advantages and disadvantages pointed out. Then, at the completion of experimental work now in progress, a complete design will be presented, based on the most promising system of operation.

The investigation to date has shown the following modes of operation to be possible:

1) Employ two identical packed beds of silver oxide. Use one for CO_2 absorption while the other is being regenerated under heat and vacuum.

Advantages - Operation can be made completely automatic; no handling of solid required.

Disadvantages - Entire bed must be alternately heated and cooled to effect regeneration; complex automatic controls required; absorption and regeneration steps must remain in balance.

2) Use only one packed bed of silver oxide; and add fresh and remove spent solid continuously, countercurrent to the gas flow. Regenerate the spent solid at a separate location at any convenient time.

Advantages - No balance of absorption and regeneration steps required; less heat load.

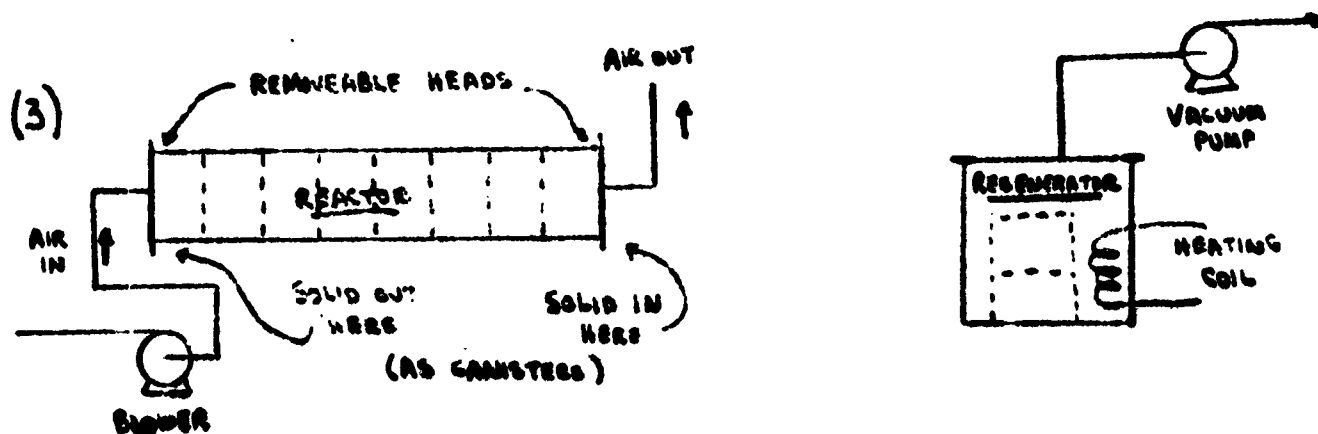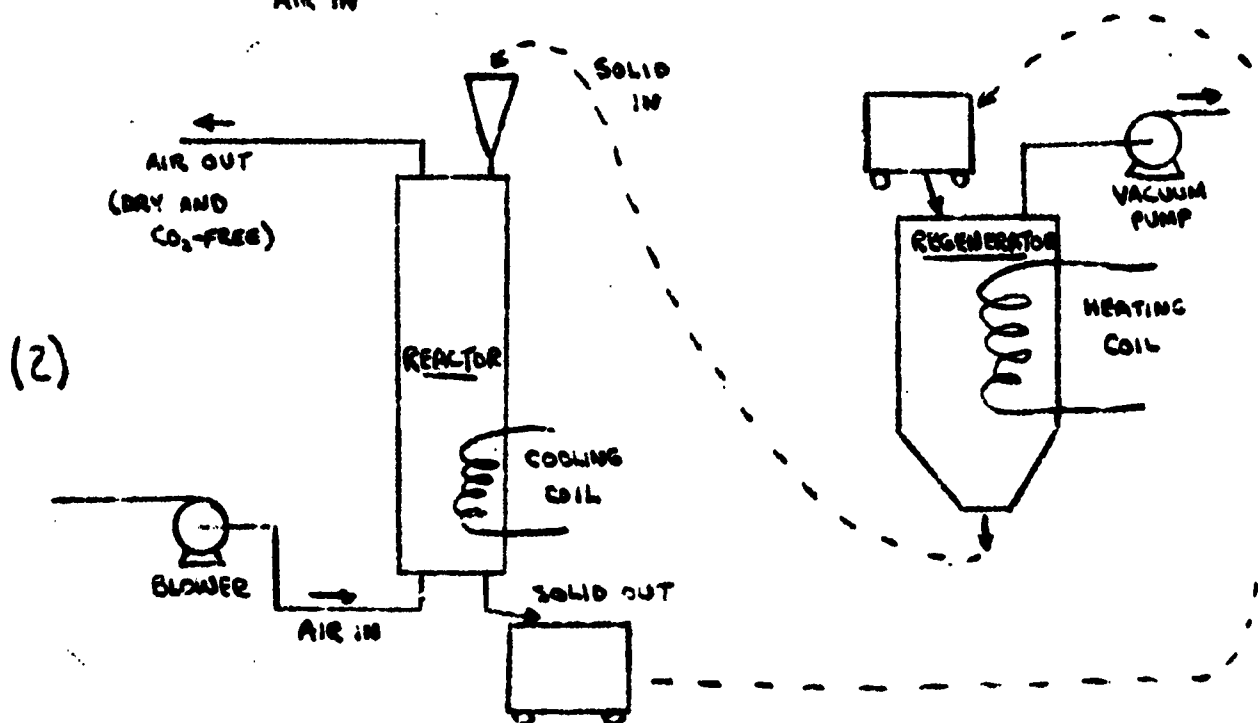Disadvantage - Complex solids handling procedure will be necessary.

3) A combination of the first two; i.e., use only one packed bed, but add and remove solid at regular intervals, manually.

Advantages - Simple solids handling; less complex controls required.

Disadvantage - Requires services of an operator, at least part time.

A simplified sketch of each of these modes of operation can be found on the next page, Figure 4.

FIGURE 4

(1)

AIR OUT (DRY AND CO₂-FREE)

BLOWER

AIR IN

COOLING COIL

#1

HEATING COIL

#2

COOLING COIL

HEATING COIL

VACUUM PUMP

CO₂ AND H₂O, OVERBOARD

VALVES AS SHOWN — #1 IS REACTOR AND IS BEING COOLED; #2 IS REGENERATING AND IS BEING HEATED.

(2)

AIR OUT (DRY AND CO₂-FREE)

SOLID IN

REACTOR

BLOWER

AIR IN

COOLING COIL

SOLID OUT

REGENERATOR

HEATING COIL

VACUUM PUMP

(3)

REMOVEABLE HEADS

AIR OUT

REACTOR

AIR IN

SOLID OUT HERE

SOLID IN HERE

(AS CANISTERS)

REGENERATOR

HEATING COIL

VACUUM PUMP

PROCESS DETAILS

WFS
9-9-52

MATHEMATICAL DEVELOPMENTS

The three possible modes of operation suggested in the previous section are in reality only two independent methods, since (3) is a combination of (1) and (2). A theoretical mathematical expression has been developed for the absorption step of each of the independent modes.

I - Fixed solid bed - steady flow of gas with constant
   inlet composition.

II - Moving solid bed of constant inlet composition - with
    countercurrent flow of constant inlet composition gas.

In the derivation of these expressions it has been necessary to make several simplifying assumptions. Such assumptions will be pointed out as they are encountered during the developments. None of these assumptions is a major one, and none affects the general applicability of the final solution.

Case I - Fixed Solid Bed - Steady Gas Flow

For the reaction: $Ag_2O + CO_2 \rightleftharpoons Ag_2CO_3$

Consider a packed bed, as follows:
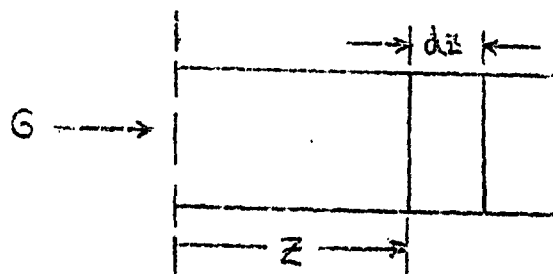
For a unit cross section (CO_2 balance):

$$G \, y \, d \, t = G \, (y + \frac{\partial y}{\partial z} d z) \, d t + (-\frac{\partial x}{\partial t}) \, d z \, d t \qquad (1)$$

(input)   (output)   (accumulation
                                          on solid)

where G = lb moles total air/ft^2-hr

      y = mole fraction CO_2 in total air

      t = time, hours

      z = distance down bed from inlet, feet

      x = concentration of Ag_2O, lb moles/ft^3 of reactor

(Neglect change of CO_2 content of the bed voids. This is OK for a flow process where bed volume is negligible compared with volume of fluid passed through.)

It will be assumed that:

$$r = k_A \, p_{CO_2} \, C_{Ag_2O} - k_D \, C_{Ag_2CO_3} \qquad (2)$$
$$= k_A \, \pi \, y \, x - k_D \, (x_o - x)$$

where: C_{Ag_2O} = concentration of Ag_2O, lb moles/ft^3 of reactor

$C_{Ag_2CO_3}$ = concentration of Ag_2CO_3, lb moles/ft^3 of reactor

k_D = desorption rate constant, hr^{-1}

And, further, it will be assumed that absorption is taking place under conditions where the reverse reaction is negligible.

Therefore: $\quad r_A = k_A \, \pi \, y \, x = - \dfrac{\partial x}{\partial t} \qquad (3)$

where: $\quad k_A$ = absorption rate constant, atm^{-1} - hr^{-1}

π = absorption pressure, atmospheres

r_A = absorption rate, lb moles CO_2/hr-ft^3 reactor

From (1): $\quad \dfrac{\partial x}{\partial t} = G \dfrac{\partial y}{\partial z}$

So we have:
$$\left. \begin{aligned} \frac{\partial y}{\partial z} &= B \, x \, y \\ \frac{\partial x}{\partial t} &= D \, x \, y \end{aligned} \right\} \qquad (4)$$

where: $\quad B = - \dfrac{k_A \, \pi}{G} \qquad\qquad D = - k_A \, \pi$

At this point, a change of variable is to be introduced:

Define: $\quad S_V = \dfrac{60 \, F}{V}$

$V = A Z; \quad 60 \, F = 359 \, GA$

F = gas feed rate, std CFM

V = reactor volume, ft^3

A = cross section area of bed, ft^2

Therefore: $\quad \dfrac{60 \, F}{V} = \dfrac{359 \, G}{Z} \qquad$ or: $\dfrac{Z}{G} = 359 \, (1/S_V)$

So: $B\ Z = -\dfrac{k_A\ \pi\ Z}{G} = -359\ k_A\ \pi\ (1/S_V) = B'\ (1/S_V)$

and therefore:

$$\dfrac{\partial\ y}{\partial(1/S_V)} = B'\ x\ y$$

$$\dfrac{\partial\ x}{\partial\ t} = D\ x\ y$$

(4a)

where: $\quad B' = -359\ k_A\ \pi \qquad y\ (o,\ t) = y_o$

$\qquad\qquad D = -k_A\ \pi \qquad x\ (1/S_V,\ o) = x_o$

$\qquad\qquad 1/S_V = \dfrac{V}{60\ F}$

The solution for this pair of simultaneous partial differential equations is: (see pp. 21 ff. for details)

$$\dfrac{x}{x_o} = \dfrac{1}{1 + j\ (h - 1)}$$

$$\dfrac{y}{y_o} = \dfrac{j\ h}{1 + j\ (h - 1)}$$

(5)

where:

$\qquad j = e^M$

$\qquad h = e^N$

$\qquad M = B'\ x_o\ (1/S_V) = -359\ k_A\pi\ x_o\ (1/S_V)$

$\qquad N = -D\ y_o\ t = k_A\ \pi\ y_o\ t$

Graphical presentations of this general solution are included on the following pages:

y/y_o vs N at various values of M - Figure 5

y/y_o vs -M at various values of N - Figure 6

-M vs N at various values of y/y_o - Figure 7

It should be pointed out that there is an interesting relationship between $\dfrac{y}{y_o}$ and $\dfrac{x}{x_o}$. For a given value of M and N, there is a definite value for y/y_o, as shown on Figure 5. For example, at M = -2.0 and N = 3.0, y/y_o = 0.76. The value of x/x_o at these same values of M and N can also be obtained from this same Figure 5, by determining the value of y/y_o at M = -N and N = -M (i.e.. at M = -3.0 and N = 2.0), which gives x/x_o = 0.273. Therefore, the graphs supplied for y/y_o values may also be used for
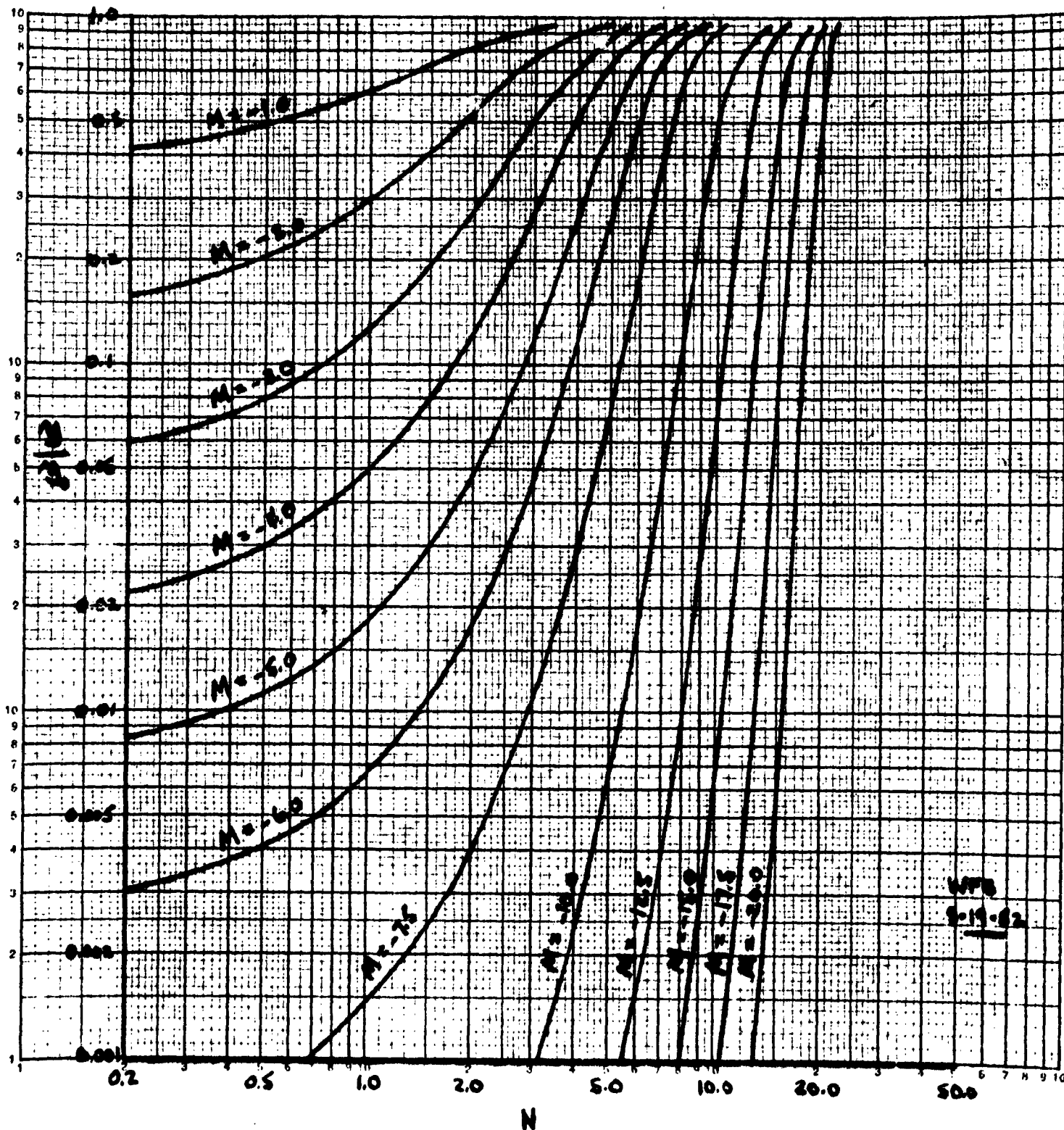
FIGURE 5

GENERAL SOLUTION OF:

$$\frac{y}{y_0} = \frac{jh}{1+j(h-1)}$$

where: $j = e^M$
$h = e^N$

For CO_2 absorption on Ag_2O:

$$M = -359 \, k_A \pi x_0 \left(\frac{1}{s_v}\right) \quad \text{(DIMENSIONLESS DISTANCE VARIABLE)}$$

$$N = k_A \pi y_0 t \quad \text{(DIMENSIONLESS TIME VARIABLE)}$$

FIGURE 6

GENERAL SOLUTION OF:

$$\frac{y}{y_0} = \frac{h}{1+g(h-1)}$$
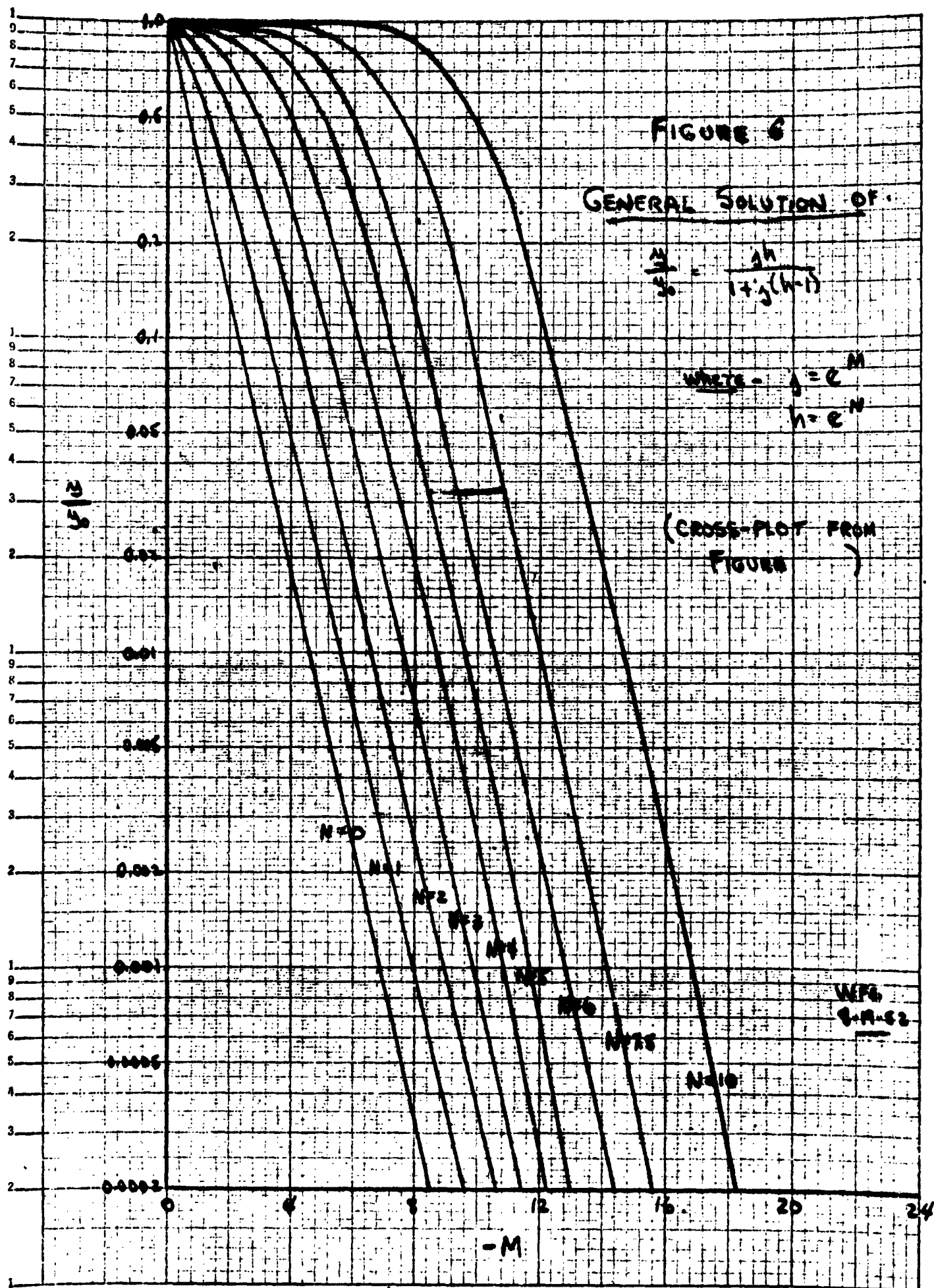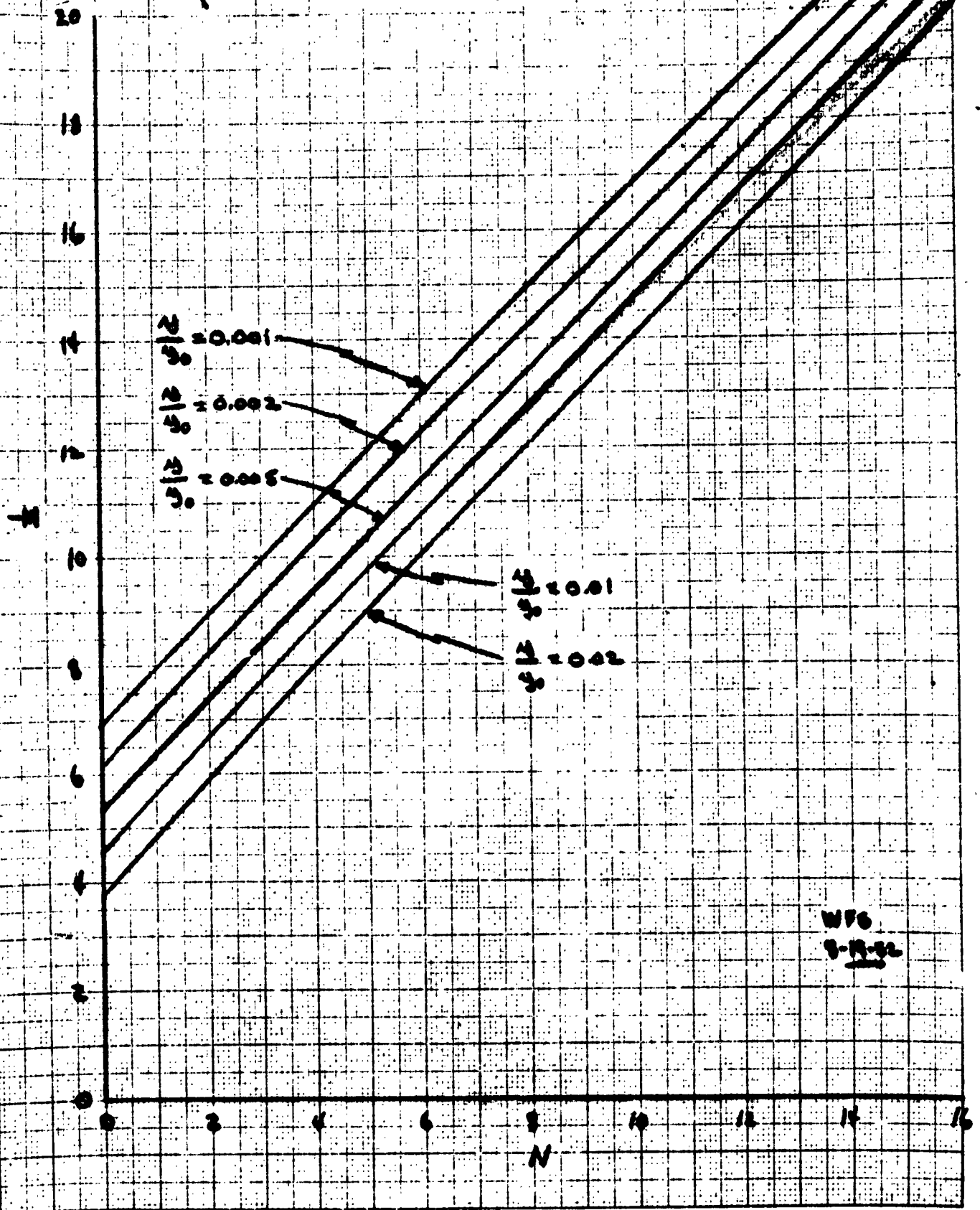
WHERE: $g = e^{-M}$
$h = e^{-N}$

(CROSS-PLOT FROM FIGURE)

FIGURE 7

CROSS-PLOT OF:
-M vs. N
(@ constant N/g_0)

$\frac{N}{g_0} = 0.001$

$\frac{N}{g_0} = 0.002$

$\frac{N}{g_0} = 0.005$

$\frac{N}{g_0} = 0.01$

$\frac{N}{g_0} = 0.02$

WFG
9-15-52

x/x_0 values, providing M and N are redefined properly. This can be proved as follows:

$$\frac{x}{x_0} = \frac{1}{1 + j(h-1)} = \frac{1}{1 + e^{M_x}(e^{N_x} - 1)} \qquad \text{at } M_x, N_x$$

$$\frac{y}{y_0} = \frac{1}{1 + j h (h-1)} = \frac{e^{M_y} e^{N_y}}{1 + e^{M_y}(e^{N_y} - 1)} \qquad \text{at } M_y, N_y$$

Let: $M_y = -N_x$

$N_y = -M_x$

Therefore: $\dfrac{y}{y_0} = \dfrac{e^{-N_x} e^{-M_x}}{1 + e^{-N_x}(e^{-M_x} - 1)} = \dfrac{1}{1 + e^{-N_x} e^{-M_x} - e^{-N_x}} \cdot \dfrac{1}{e^{N_x} e^{M_x}}$

at $-N_x, -M_x$

And: $\dfrac{y}{y_0} = \dfrac{1}{e^{N_x} e^{M_x} + 1 - e^{M_x}} = \dfrac{1}{1 + e^{M_x}(e^{N_x} - 1)} = \dfrac{x}{x_0}$ at M_x, N_x

At this stage of the investigation, sufficient experimental work has been done to give a good idea of the rate of the absorption step of the process. This work and the results therefrom will be summarized in a later section. Here it is sufficient to state that the value of k_A in the previous relation has been determined to be of the order of 800 atm^{-1}-hr^{-1}. With this result, it is of considerable interest to solve the general relationship for the special case of CO_2 absorption from air at 1.0% CO_2 by volume. For this purpose, it will be assumed that the reaction will be carried out in such a manner that y/y_0 at the reactor outlet will be approximately zero during the absorption step. As soon as $y/y_0 = 0.01$, the reactors will be switched and freshly regenerated silver oxide will take over the CO_2 removal job. Air feed rate will be set at 110 std CFM, carrying 8.1 lb/hr of CO_2 through the unit. This will be essentially all removed during most of the cycle, so approximately four minutes out of every hour can be employed in switching and still operate with 7.5 lb/hr over-all CO_2 removal.

In general:

$$M = -359\ k_A\ \pi\ x_o\ (1/S_V)$$

$$N = k_A\ \pi\ y_o\ t$$

$$1/S_V = V/60\ F$$

For this particular case:

$$k_A = 800\ atm^{-1}\text{-}hr^{-1}$$

$$\pi = 1.0\ atm$$

$$y_o = 0.01\ mole/mole$$

$$F = 110\ std\ CFM$$

outlet $y/y_o = 0.01$, at switch time

Therefore:

$$M = (-359)(800)(1.0)(1/60)(1/110)\ x_o\ V$$

$$N = (800)(1.0)(0.01)\ t$$

or:

$$M = -43.52\ x_o\ V$$

$$N = 8\ t$$

at $y/y_o = 0.01$

$$-M = 4.6 \quad \text{when } N=0 \quad \text{(From Figure 7)}$$

Therefore:

$$-M = 4.6 + N$$

or:

$$43.52\ x_o\ V = 4.6 + 8\ 5$$

and, finally:

$$V = \frac{0.1057}{x_o} + \frac{0.1838}{x_o}\ t$$

and:

$$t = 5.44\ x_o\ V - 0.575$$

Curves representing these two equations have been plotted and are included as Figures 8 and 9. With these curves it is possible to read off the reactor volume required for operation at a definite switching interval, or the switching interval required when operating with a particular silver oxide initial concentration. It can be seen that the reactor volumes required and the switching interval indicated will be within reason, even at very low values of initial silver oxide concentration. Further experimental work will substantiate these preliminary conclusions and make possible the final design of an operating unit.

FIGURE 8

REACTOR VOLUME AS A
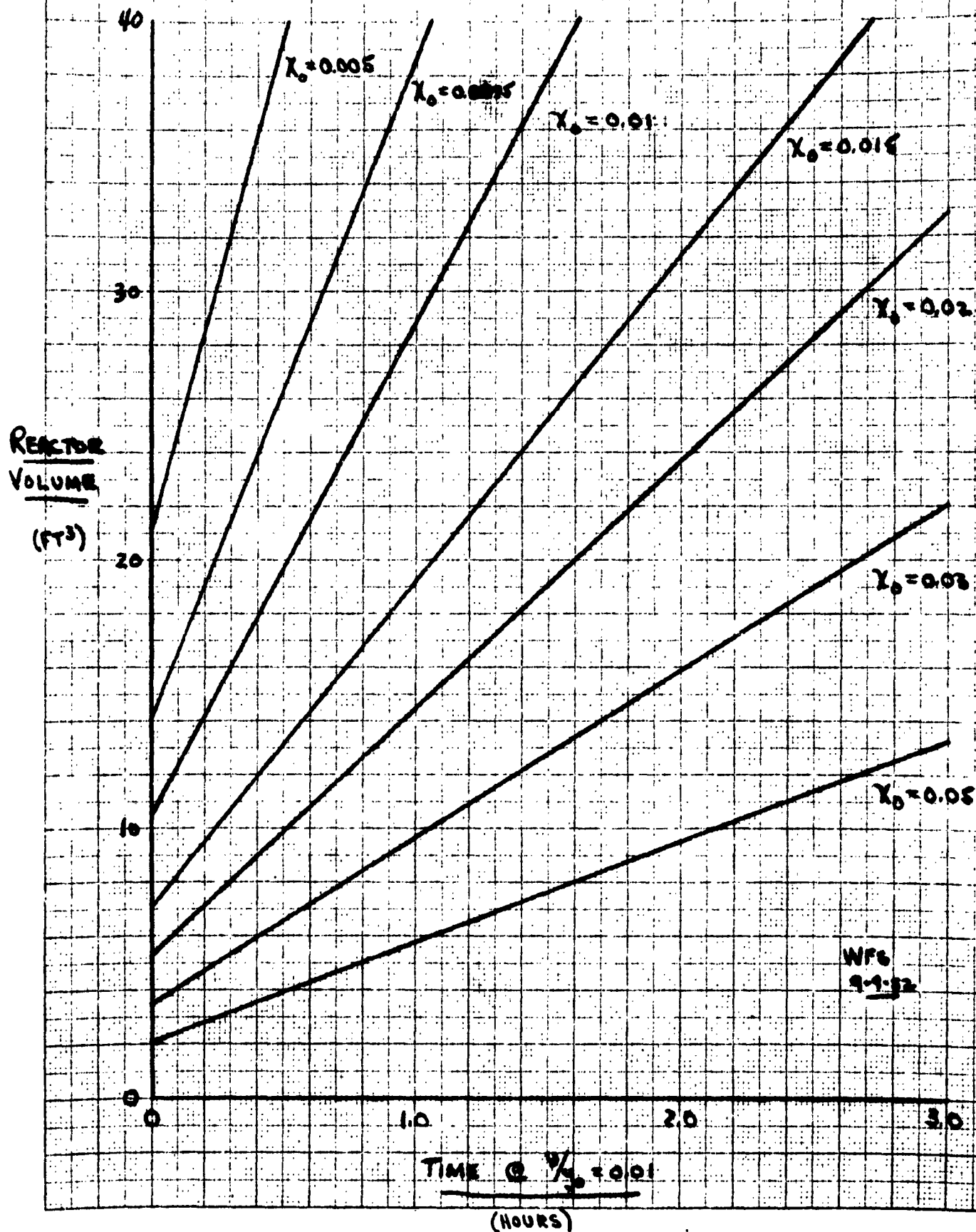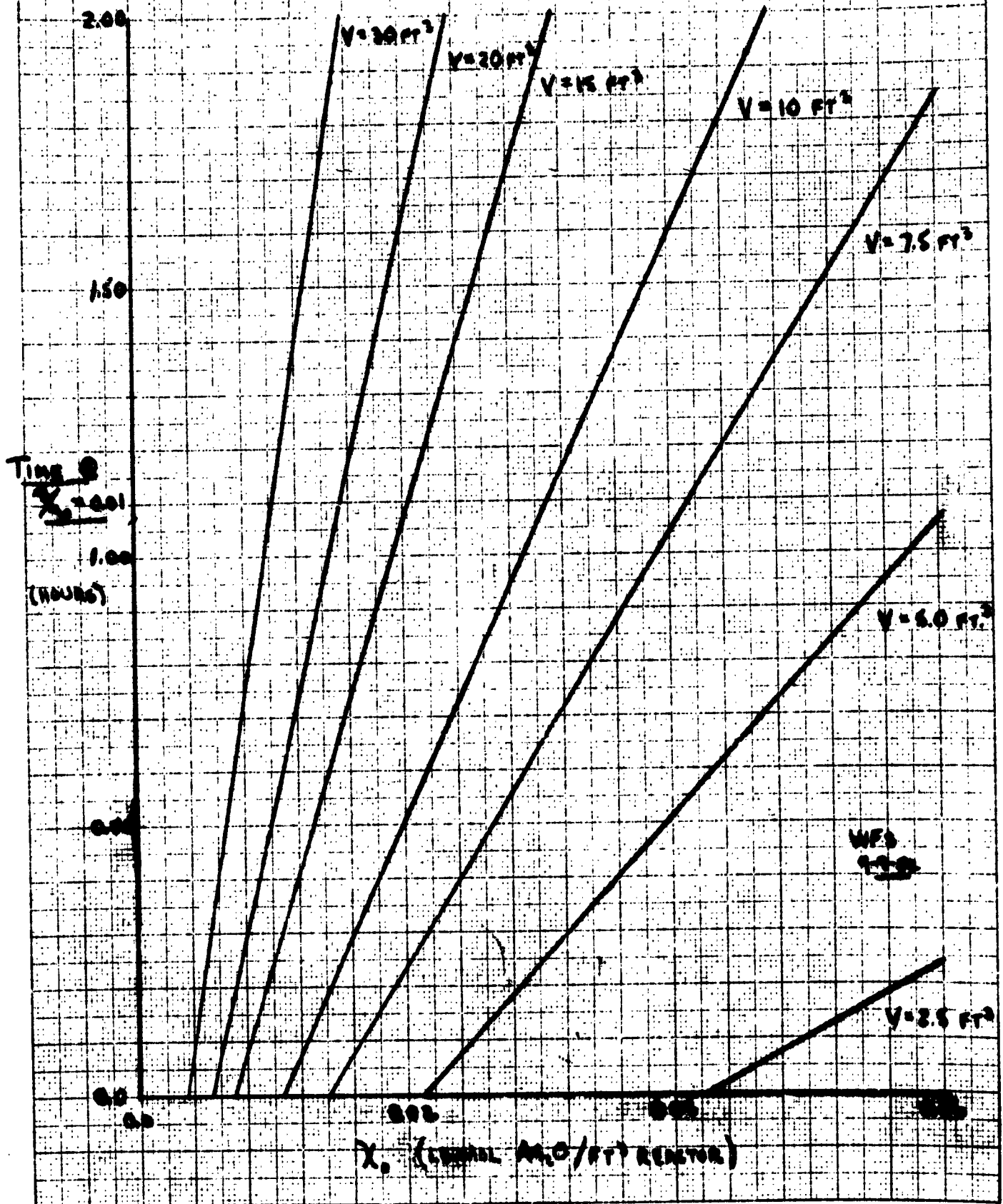FUNCTION OF
SWITCHING INTERVAL

FIGURE 9

SWITCHING TIME AS A
FUNCTION OF
INITIAL SOLID CONCENTRATION

Case I. Fixed Solid Bed, Solution

$$\frac{\partial y}{\partial (1/S_V)} = B' \, x \, y \quad \Bigg\}$$

$$\frac{\partial x}{\partial t} = D \, x \, y \quad \Bigg\} \qquad (4a)$$

$$x \, (1/S_V, 0) = x_0 \quad \Bigg\}$$

$$y \, (0, \, t) = y_0 \quad \Bigg\} \qquad (6)$$

Put: $U = y \qquad\qquad X = 1/S_V \qquad\qquad a = B'$

$ V = x \qquad\qquad Y = t \qquad\qquad b = D$

$$\frac{\partial U}{\partial X} = a \, U \, V$$

$$\frac{\partial V}{\partial Y} = b \, U \, V \qquad (4b)$$

$$V \, (X, \, 0) = V_0$$

$$U \, (0, \, Y) = U_0 \qquad (6a)$$

Solve (4b) for U V and equate:

$$\frac{1}{a} \frac{\partial U}{\partial X} = \frac{1}{b} \frac{\partial V}{\partial Y}$$

or:
$$\frac{\partial (a \, V)}{\partial Y} = \frac{\partial (b \, U)}{\partial X} \qquad (7)$$

$\therefore \quad a \, V \, d \, X + b \, U \, d \, Y$ is an exact differential

and: $\quad f \, (X, \, Y)$ exists such that:

$$U = \frac{1}{b} \frac{\partial f}{\partial Y} \qquad\qquad V = \frac{1}{a} \frac{\partial f}{\partial X} \qquad (8)$$

$$\frac{\partial U}{\partial X} = \frac{1}{b} \frac{\partial^2 f}{\partial X \partial Y} = a \, U \, V = a \, \frac{1}{b} \frac{\partial f}{\partial Y} \, \frac{1}{a} \frac{\partial f}{\partial X}$$

$$\therefore \quad \frac{\partial^2 f}{\partial X \partial Y} = \frac{\partial f}{\partial Y} \frac{\partial f}{\partial X}$$

or:
$$\frac{\partial f}{\partial Y} = \frac{\partial^2 f}{\partial X \partial Y} \Bigg/ \frac{\partial f}{\partial X} \qquad (9)$$

Put:
$$h = \frac{\partial f}{\partial X} \qquad \therefore \quad \frac{\partial h}{\partial Y} = \frac{\partial^2 f}{\partial X \partial Y}$$

and:
$$\frac{\partial f}{\partial Y} = \frac{1}{h} \frac{\partial h}{\partial Y} = \frac{\partial}{\partial Y} (\ln h) = \frac{\partial}{\partial Y} \left(\ln \frac{\partial f}{\partial X} \right)$$

Integrate:
$$f = \ln \frac{\partial f}{\partial X} + \phi(X)$$

or:
$$\frac{\partial f}{\partial X} = e^{[f - \phi(X)]} \tag{10}$$

From (6a) and (8):
$$\frac{\partial f}{\partial X} = a V \qquad \frac{\partial f}{\partial X}(X, 0) = a V_0$$

$$f = a V X + \ln C \qquad f(X, 0) = a V_0 X + \ln C$$

Therefore:
$$a V_0 = e^{[a V_0 X + \ln C - \phi(X)]}$$
$$\ln a V_0 = a V_0 x + \ln C - \phi(X)$$

Therefore:
$$\phi(X) = \ln \frac{C}{a V_0} + a V_0 X \tag{11}$$

so:
$$\frac{\partial f}{\partial X} = \frac{a V_0}{C} e^{[f - a V_0 X]} \tag{12}$$

Ordinary D.E. corresponding to (12) is:
$$\frac{d F}{d X} = \frac{a V_0}{C} e^{[F - a V_0 X]} \tag{13}$$

Separate variables:
$$e^{-F} d F - \frac{a V_0}{C} e^{-a V_0 X} d X = 0$$

$$-e^{-F} + \frac{1}{C} e^{-a V_0 X} = \text{constant} \tag{14}$$

Or general solution of (12) is:
$$-e^{-f} + \frac{1}{C} e^{-a V_0 X} = \psi(Y) \tag{15}$$

From (6a) and (8):
$$\frac{\partial f}{\partial Y} = b V \qquad \frac{\partial f}{\partial Y}(0, Y) = b V_0$$

$$f = b U Y + K \qquad f(0, Y) = b U_0 Y + K$$

$$\therefore -e^{-b U_0 Y - k} + \frac{1}{C} = \psi(Y) \tag{16}$$

From (8) and (12):
$$a V = \frac{a V_0}{C} e^{[f - a V_0 X]}$$

$$C \frac{V}{V_0} = e^{[f - a V_0 X]}$$

$$\ln C \frac{V}{V_0} = f - a V_0 X$$

$$\therefore \quad f = \ln \ C \ \frac{V}{V_o} + a \ V_o \ X \tag{17}$$

Put (17) and (16) into (15):

$$- \frac{1}{C} \ \frac{V_o}{V} \ e^{-a \ V_o \ X} + \frac{1}{C} \ e^{-a \ V_o \ X} = \frac{1}{C} - e^{-k} \ e^{-b \ U_o \ Y}$$

and apply: $V \ (X, \ 0) = V_o$

$$- \frac{1}{C} \ e^{-a \ V_o \ X} + \frac{1}{C} \ e^{-a \ V_o \ X} = \frac{1}{C} - e^{-k}$$

$$\therefore \quad e^{-k} = \frac{1}{C}$$

and:

$$e^{-a \ V_o \ X} \left[1 - \frac{V_o}{V} \right] = 1 - e^{-b \ U_o \ Y} \tag{18}$$

Differentiate (18) with respect to Y:

$$e^{-a \ V_o \ X} \ \frac{V_o}{V^2} \ \frac{\partial V}{\partial Y} = b \ U_o \ e^{-b \ U_o \ Y}$$

Put in: $\quad \frac{\partial V}{\partial Y} = b \ U \ V$

$$\frac{V_o}{V} \ e^{-a \ V_o \ X} = \frac{U_o}{U} \ e^{-b \ U_o \ Y}$$

Therefore:

$$\frac{U}{U_o} = \frac{V}{V_o} \ e^{a \ V_o \ X} \ e^{-b \ U_o \ Y} \tag{19}$$

$$\left[\frac{V_o}{V} - 1 \right] = e^{a \ V_o \ X} \left[e^{-b \ U_o \ Y} - 1 \right] \tag{20}$$

Put:
$$e^{a \ V_o \ X} = j$$
$$e^{-b \ U_o \ Y} = h$$

Then:
$$\frac{V_o}{V} = 1 + j \ (h - 1)$$

or:
$$\frac{V}{V_o} = \frac{1}{1 + j \ (h - 1)}$$

and:
$$\frac{U}{U_o} = \frac{j \ h}{1 + j \ (h - 1)}$$

$$\left. \right\} \tag{21}$$

Replacing original variables:

$$\frac{x}{x_o} = \frac{1}{1 + j(h - 1)}$$

$$\frac{y}{y_o} = \frac{j h}{1 + j(h - 1)}$$

(5)

where:

$$j = e^M$$

$$h = e^N$$

$$M = B' x_o (1/S_V) = -359 k_A \pi_o (1/S_V)$$

$$N = -D y_o t = k_A \pi y_o t$$

Case II - Countercurrent Gas and Solid Flow

For the reaction: $Ag_2O + CO_2 \rightleftarrows Ag_2CO_3$
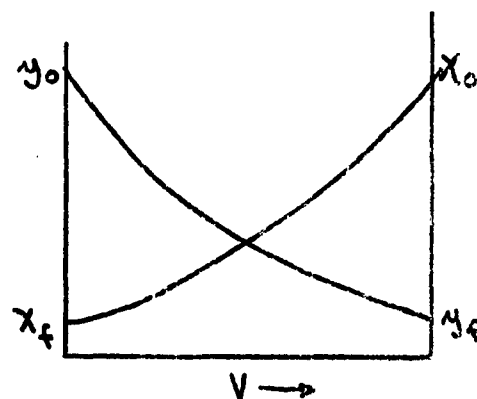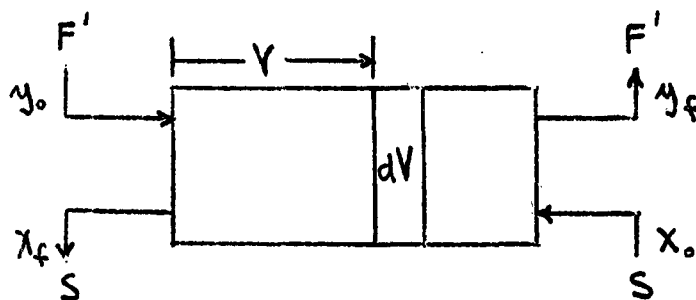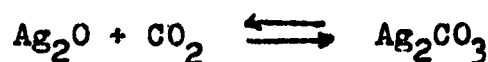
F' = gas rate (over-all), lb moles/hr = $\frac{60 F}{359}$

S = solid rate (over-all), ft^3/hr

y = moles CO_2/mole total gas

x = moles of Ag_2O/ft^3 of solid

V = volume of reactor, ft^3

At steady state: $F' (y_o - y_f) = S (x_o - x_f) = R$

R = removal rate (lb mol/hr)

or: $\quad -F' d y = S d x \quad$ (in general)

By material balance on small section above (d V):

$$F' y - F' (y + \frac{d\,y}{d\,V} d V) = S (x + \frac{d\,x}{d\,V} d V) - S x$$

$$= \text{moles } CO_2 \text{ transferred/ hr-ft}^3 \text{ of reactor}$$

or: $\quad -F' \frac{d\,y}{d\,V} = S \frac{d\,x}{d\,V}$

Also, it will be assumed that:

$$\text{moles } CO_2 \text{ transferred/hr-ft}^3 = r_A = k_A \pi y x$$
$$\text{(as before)}$$

Therefore: $\quad -F' \frac{d\,y}{d\,V} = k_A \pi y x$

or: $\quad \frac{d\,y}{y\,x} = - \frac{k_A \pi}{F'} d V$

Now, replace F' by $\frac{60 F}{359}$, its equivalent, and since $\frac{1}{S_V} = \frac{V}{60 F}$

$$\frac{d\,V}{F'} = \frac{359}{60 F} d V = 359 \, d (1/S_V)$$

Therefore: $\quad \frac{d\,y}{y\,x} = -359 \, k_A \pi \, d (1/S_V)$

At any volume V: $\quad F' (y_0 - y) = S (x - x_f)$

Therefore: $\quad x = x_f + \frac{F'}{S} (y_0 - y)$

$$\frac{d\,y}{y\,[x_f + \frac{F'}{S} (y_0 - y)]} = -359 \, k_A \pi \, d (1/S_V)$$

or: $\quad \frac{S}{F'} \int_{y_0}^{y} \frac{d\,y}{y\,[(\frac{S}{F'} x_f + y_0) - y]} = -359 \, k_A \pi \int_{0}^{1/S_V} d(1/S_V)$

So consider: $\int_{y_0}^{y} \frac{d\,y}{y\,(A - y)} = \int_{y_0}^{y} \frac{d\,y}{A_y - y^2}$

$$= \frac{1}{A} \ln \frac{-2\,y + A - A}{-2\,y + A + A} \Big|_{y_0}^{y} = \frac{1}{A} \ln \frac{y}{y - A} \Big|_{y_0}^{y}$$

$$= \frac{1}{A} \ln \frac{y(y_0 - A)}{y_0(y - A)} = \frac{1}{S/F' \; x_f + y_0} \ln \frac{y(-S/F' \; x_f)}{y_0(y - y_0 - S/F' \; x_f)}$$

where: $A = \frac{S}{F'} x_f + y_0$

and then: $\dfrac{S/F'}{S/F' \; x_f + y_0} \ln \dfrac{y(S/F' \; x_f)}{y_0(S/F' \; x_f + y_0 - y)} = -359 \; k_A \; \pi \; (1/S_V)$

From first material balance: $x_f = x_0 - \frac{R}{S}$

Therefore: $\dfrac{S/F'}{S/F' \; (x_0 - R/S) + y_0} \ln \dfrac{y \; S/F' \; (x_0 - R/S)}{y_0 \; / (x_0 - R/S) \; S/F' + y_0 - y /}$

$$= \frac{S/F'}{(S/F' \; x_0 + y_0) - R/F'} \ln \frac{y \; (S/F' \; x_0 - R/F')}{y_0 \left\{ /(S/F' \; x_0 + y_0) - R/F' / - y \right\}}$$

or: $\dfrac{1}{S_V} = \dfrac{1}{359 \; k_A \; \pi} \dfrac{q}{(q \; x_0 + y_0) - T} \ln \dfrac{y_0 \left\{ /(q \; x_0 + y_0) - T/ - y \right\}}{y \; (q \; x_0 - T)}$

$$q = S/F' \qquad T = \frac{R}{F'} = y_0 - y$$

Rearranging:

$$-359 \; k_A \; \pi \; (1/S_V) = \frac{q}{q + \dfrac{y_0 - T}{x_0}} \ln \frac{y \; (q - T/x_0)}{y_0 \; / (q + \dfrac{y_0 - T}{x_0}) - \dfrac{y}{x_0} /}$$

Substitute: $M = -359 \; k_A \; \pi \; x_0 \; (1/S_V)$

$$T = y_0 - y$$

So: $M = \dfrac{q}{q + y/x_0} \ln \dfrac{y \; (q - \dfrac{y_0 - y}{x_0})}{y_0 \; q} = \dfrac{q}{q + y/x_0} \ln \dfrac{y \; /(q + y/x_0) - y_0/x_0}{q \; y_0}$

$$= \frac{q \dfrac{x_0}{y_0}}{q \dfrac{x_0}{y_0} + y/y_0} \ln \frac{\dfrac{y}{y_0} \; / (q \dfrac{x_0}{y_0} + \dfrac{y}{y_0}) - 1 /}{q \dfrac{x_0}{y_0}}$$

Let: $P = q \dfrac{x_0}{y_0}$

Then: $M = 2.303 \dfrac{P}{P + y/y_0} \log \dfrac{y/y_0 \; /(P - 1) + y/y_0 /}{P}$ (Final solution)

where: $M = -359 \; k_A \; \pi \; x_0 \; (1/S_V)$

$$P = q \; x_0/y_0$$

$$q = S/F'$$

A graphical presentation of this solution can be found in Figure 10 next page.

FIGURE 10

GENERAL SOLUTION OF —

$$M = 2.303 \frac{\rho}{\rho + y/y_0} \log \frac{y/y_0 \left[(\rho - 1) + y/y_0 \right]}{\rho}$$

NOTE — FOR VALUES OF $\rho < 1.00$, y/y_0 CURVE IS ASYMPTOTIC TO SOME VALUE OF $y/y_0 \neq 0.0$.

E.G. — FOR $\rho = 0.99$, ASYMPTOTE IS $y/y_0 = 0.01$

WFS
9-10-52

(ALL CURVES ARE ASYMPTOTIC TO $y/y_0 = 0.0$)

$P = 5.0$
$P = 3.0$
$P = 2.0$
$P = 1.5$
$P = 1.2$
$P = 1.05$
$P = 1.00$

—M

WHERE — $M = -2.303 \log_{10} \Psi I_0 (y/y_0)$

$P = q \, x_0/y_0$

$q = S/P$

As in Case I, it will be of interest to solve the general relationship of Case II for the special situation of CO_2 absorption from air at 1% CO_2 by volume. As yet no experiments have been run using countercurrent gas and solid flow. However, the value of k_A (800 atm^{-1}-hr^{-1}) determined from fixed-bed experiments will be assumed to hold in countercurrent operation as well. A gas flow of 110 std. CFM will be assumed, to allow comparison with Case I. For such a gas flow, a removal rate of 7.5 lb/hr will result if y/y_o at the reactor outlet is kept at 0.072.

In general:

$$M = -359 \, k_A \, \pi \, x_o \, (1/S_V)$$

$$P = q \, x_o / y_o$$

$$1/S_V = V/60 \, F$$

$$q = S/F'$$

For this particular case:

$$k_A = 800 \text{ atm}^{-1}\text{-hr}^{-1}$$

$$\pi = 1.0 \text{ atm}$$

$$y_o = 0.01 \text{ mole/mole}$$

$$F = 110 \text{ std CFM}$$

outlet $y/y_o = 0.072$

Therefore:

$$M = (-359)(800)(1.0)(1/60)(1/110) \, x_o \, V$$

$$P = (359)(1/60)(1/110)(1/0.01) \, S \, x_o$$

or:

$$M = -43.52 \, x_o \, V \qquad P = 5.45 \, S \, x_o$$

Values of x_o have been assumed and corresponding values of M and P determined from Figure 10 at $y/y_o = 0.072$. Then values for V and S are calculated. Results of these calculations are plotted on the next page, Figure 11. From this set of curves, it is possible to determine the reactor volume required for operation with a particular solid feed rate and initial solid concentration. It can be seen that the solid feed rate will need to be fairly high, especially if x_o, the inlet solid concentration is low. Further experimental work on this particular mode of operation will help to substantiate these preliminary conclusions.

FIGURE 11

REACTOR VOLUME AS A FUNCTION
OF SOLID FEED RATE

(Air Feed Rate = 110 STD CFM)

(CO_2 Feed Rate = 7.5 lb/hr)

SOLID FEED RATE (lb/hr)
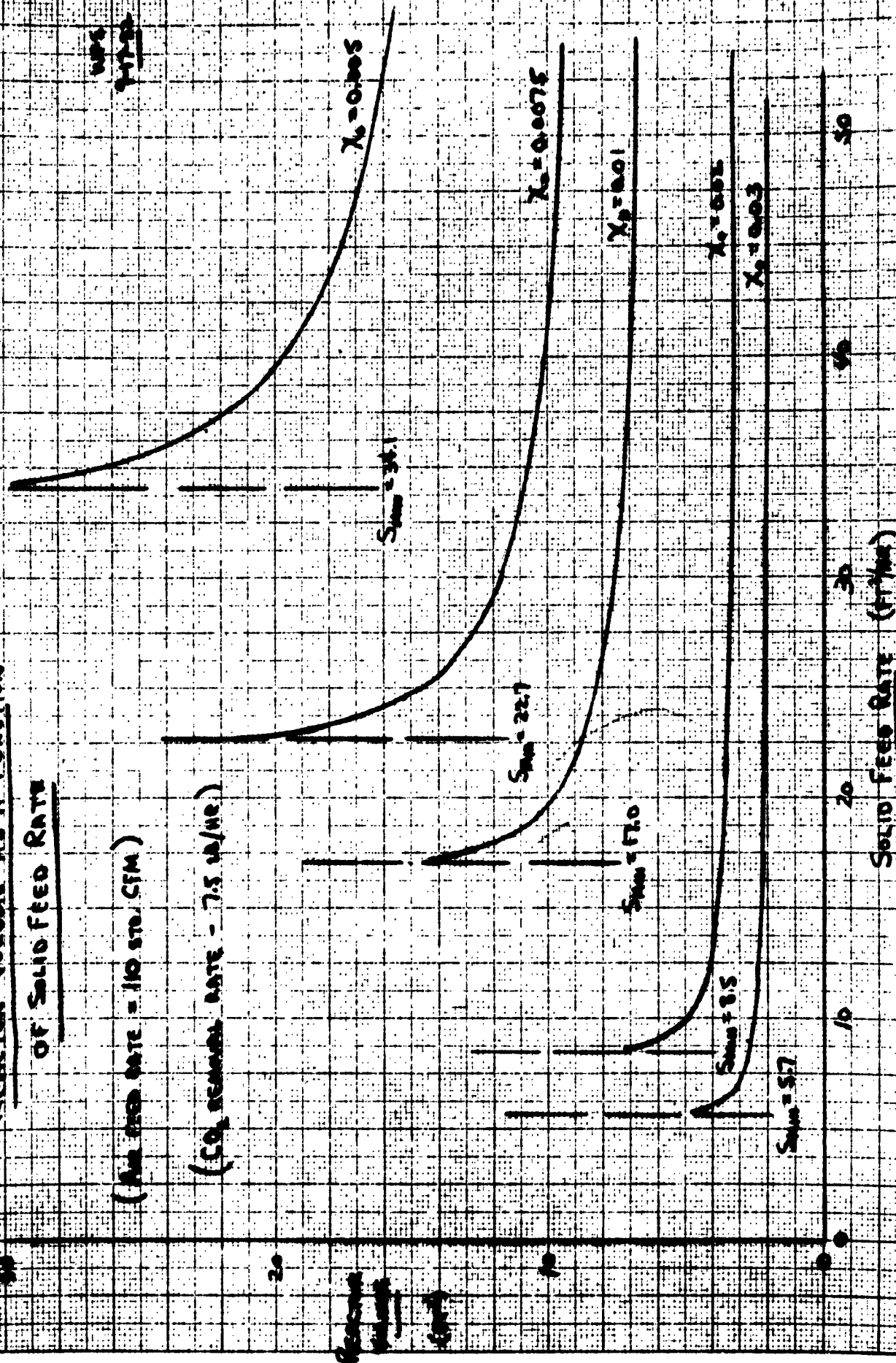
EXPERIMENTAL

In order to determine the feasibility of using the silver oxide-carbon dioxide reaction as the basis of a regenerative CO_2-removal process, it has been necessary to perform a series of small-scale experiments. These preliminary tests have been designed to provide answers to several important questions.

(1) Is the reaction reversible, and can it be repeated several times using the same sample of silver oxide?

(2) What are the variables affecting the rate of the absorption step?

(3) What physical form of silver oxide is best for CO_2 removal -- pure, or deposited on an inert carrier?

(4) What are the variables affecting the rate of the desorption step?

At the present writing, questions (1) and (2) have been fairly well answered, but further work will be necessary to determine answers for questions (3) and (4) satisfactorily. Experimental work is continuing and should result in satisfactory answers and a final process design in the near future.

Experiments with silver oxide have all been carried out in an apparatus similar to that sketched in Figure 12. This is a small-scale unit, one which provides considerable information in a relatively short time, and the data obtained should be applicable to the operation of a larger unit as well. The unit was operated with a fixed solid bed and an inlet gas of constant composition, which is identical with the operating conditions specified in Case I under Mathematical Development. Therefore, it is likely that the experimental results will fit the mechanism suggested in this development. Case II is more difficult to obtain in practice, and as yet no experiments have been run under this procedure.

An air-CO_2 mixture of known and constant composition is required for the inlet gas stream. Such a mixture is obtained by pumping CO_2 and air (in the desired pressure ratio) into the mix-

FIGURE 12
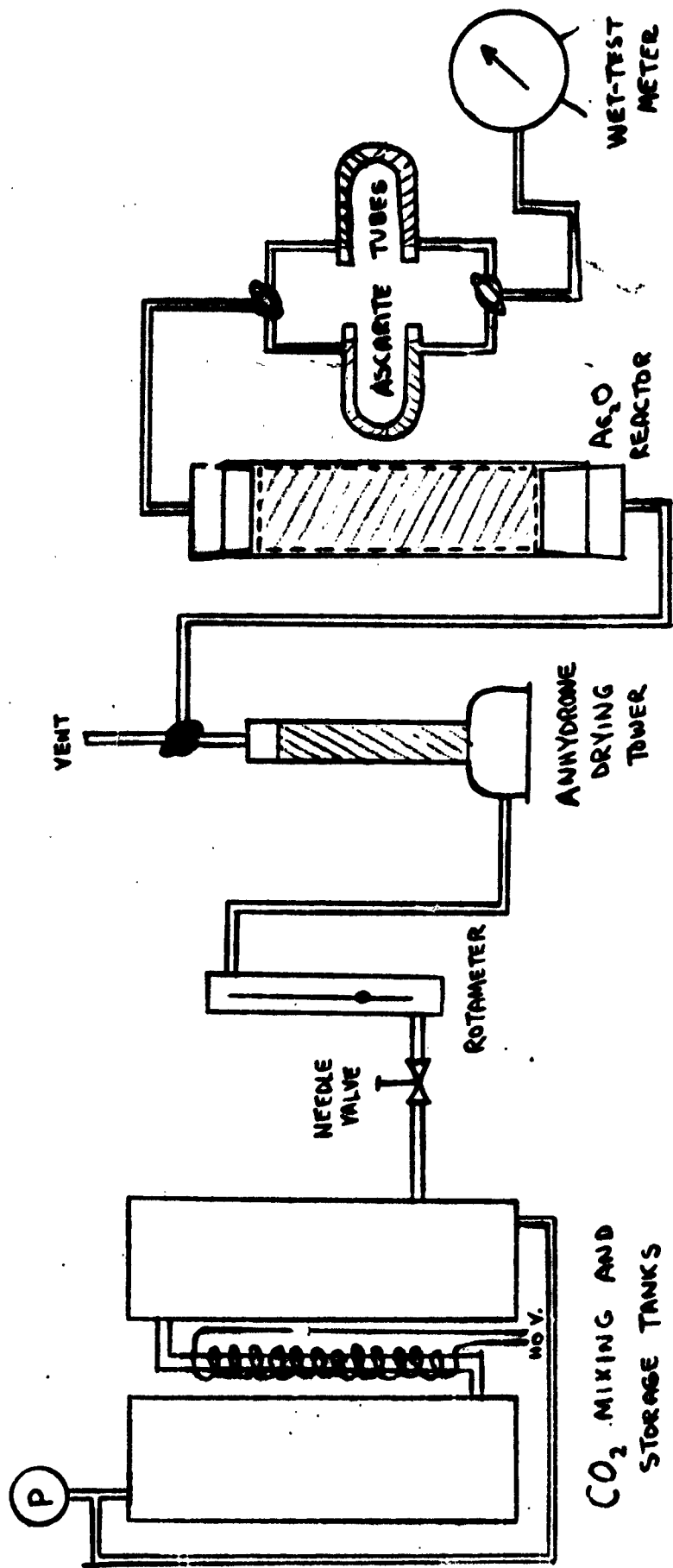
FLOW SHEET FOR Ag_2O EXPERIMENTS

WET-TEST METER

ASCARITE TUBES

Ag_2O REACTOR

VENT

ANHYDRONE DRYING TOWER

ROTAMETER

NEEDLE VALVE

CO_2 MIXING AND STORAGE TANKS

WFS
9-16-52

P

continued until the silver oxide is essentially saturated with CO_2, as indicated by a constant CO_2 output rate. Then the basket containing the silver oxide is weighed and placed in the oven, where it is held overnight at 125°C and < 5 mm Hg, to decompose the carbonate and reform the active silver oxide.

Data from fourteen runs made to date, using three different samples of Ag_2O, are summarized in Table II. In addition, typical plots of the total CO_2 absorbed as a function of time are included in Figures 13 through 17, for all of the runs using Ag_2O sample A. (Similar plots have been made for the runs employing the other Ag_2O samples, but they are not included here.) It can easily be seen that the repeatability of the reaction is only fair. In general, it seems that the first run with any particular sample shows very good CO_2 removal. Subsequent runs show considerably less removal, but with much less of a trend toward lower values after the second run in any set. It is likely that this high capacity for the first run is due to adsorbed NaOH not completely washed off. Therefore, the true capacity is that exhibited by later runs, which seems to be falling off only slightly with use.

Reference to the experimentally determined CO_2 absorption data indicates that in all cases the run seems to have been made up of two distinct periods. In the early stages CO_2 is being absorbed at a relatively high and varying rate. Later in the run a considerably lower magnitude constant rate period is reached. Such a result would be expected if the absorption were taking place by two simultaneous processes: (1) Reaction of the CO_2 with surface layers of Ag_2O, according to the mechanism of Case I, and (2) Reaction of additional CO_2 with internal layers of Ag_2O, limited by diffusion. To determine the portion of the CO_2 absorption attributable to the mechanism of Case I, it seems a logical approximation merely to subtract the constant rate contribution, as determined graphically from the data. When this is done, the curves labelled "modified data" are obtained. It will be assumed that these curves represent fairly well the CO_2 absorption due to reaction with the available surface layers of Ag_2O, by the mechanism of Case I.

Further calculations have been made on the data of series A,

TABLE II

EXPERIMENTAL DATA – CO_2 ABSORPTION ON Ag_2O

Sample No.	A-1	A-2	A-3	A-4	A-5	B-1	B-2	B-3	B-4	B-5	B-6	B-7	D_B^1	D_B^2	D_B^2	D_B^2
Date	6/12/52	6/20/52	6/24/52	7/1/52	7/3/52	6/17/52	6/20/52	6/25/52	6/26/52	7/8/52	7/10/52	7/16/52	7/18/52	7/22/52	7/24/52	8/1/52
Temperature (°F)	88.0	73.5	85.0	82.5	84.0	86.0	73.5		88.0	82.0	81.0	79.0	85.2	91.0	86.0	83.0
Pressure (mm)	746.3	747.2	740.2	745.0	748.7	743.8	746.3		743.2	750.0	746.5	748.0	748.0	747.3	755.0	751.6
% CO_2	2.86	2.86	2.86	2.86	2.86	2.86	2.86		2.86	2.86	2.86	2.86	2.86	1.30	1.30	1.29
Rotameter	1.0	1.0	1.0	1.0	1.0	0.75	0.75		0.75	0.75	0.75	0.75	1.0	1.0	0.75	0.90
Wt. Before (gm)	70.025	70.425	70.752	70.584	70.579	73.100	73.491	run N.G.	73.461	73.398	73.399	73.378	75.463	76.024	76.234	76.998
Wt. After (gm)	70.829	70.696	71.034	70.823	70.784	73.885	73.718		73.672	73.584	73.642	73.584	76.110	76.328	76.516	76.603
H_2O Lost (gm)	—	—	—	—	—	—	—		—	—	—	—	0.029	0.020	0.005	0.027
Apparent CO_2 (gm)	0.804	0.271	0.282	0.239	0.205	0.785	0.227		0.211	0.186	0.243	0.206	0.676	0.322	0.297	0.390
Constant Rate (gm CO_2/min)	-0.0041	0.0042	0.0034	0.0032	0.0055	not calculated	0.0032	leak in system	not calculated	0.0040	0.0029	0.0030	not calculated	not calculated		
Avg. Inlet Rate	0.0685	0.0700	0.0672	0.0682	0.0690		0.0528			0.0529	0.0522	0.0527				
Corr. Inlet Rate	0.0644	0.0658	0.0638	0.0650	0.0635		0.0496			0.0489	0.0493	0.0497				
Initial Absorption Rate	0.0460	0.0460	0.0440	0.0445	0.0460		0.0440			0.0420	0.0460	0.0460				
Asymptote (total gm CO_2)	0.7350	0.2100	0.2600	0.1840	0.1600		0.1950			0.1400	0.1250	0.1550				
Initial Outlet y/y_0	0.307	0.307	0.317	0.322	0.281		0.116			0.145	0.110	0.076				

Sample A – 42.515 gm alumina, 4.378 Ag_2O (apparent)

(series ended when solder on basket melted)

Sample B – 43.822 gm alumina, 4.754 gm Ag_2O (apparent)

(series ended when more Ag_2O was added to alumina for D_B series)

Sample D_B – Sample B plus 1.976 gm Ag_2O (apparent)

(series ended when oil heated up into oven – smoke poisoned Ag_2O-alumina)

FIGURE 13

ABSORPTION DATA - RUN A-1

CONSTANT RATE = 0.0041 GM/MIN

ACTUAL DATA

(MODIFIED DATA WOULD BE ASYMPTOTIC TO 0.7350 GM.)

TOTAL CO_2 ABSORBED (GM)

INITIAL RATE = 0.0460 GM/MIN

TIME (MIN)

WFG
9-16-52
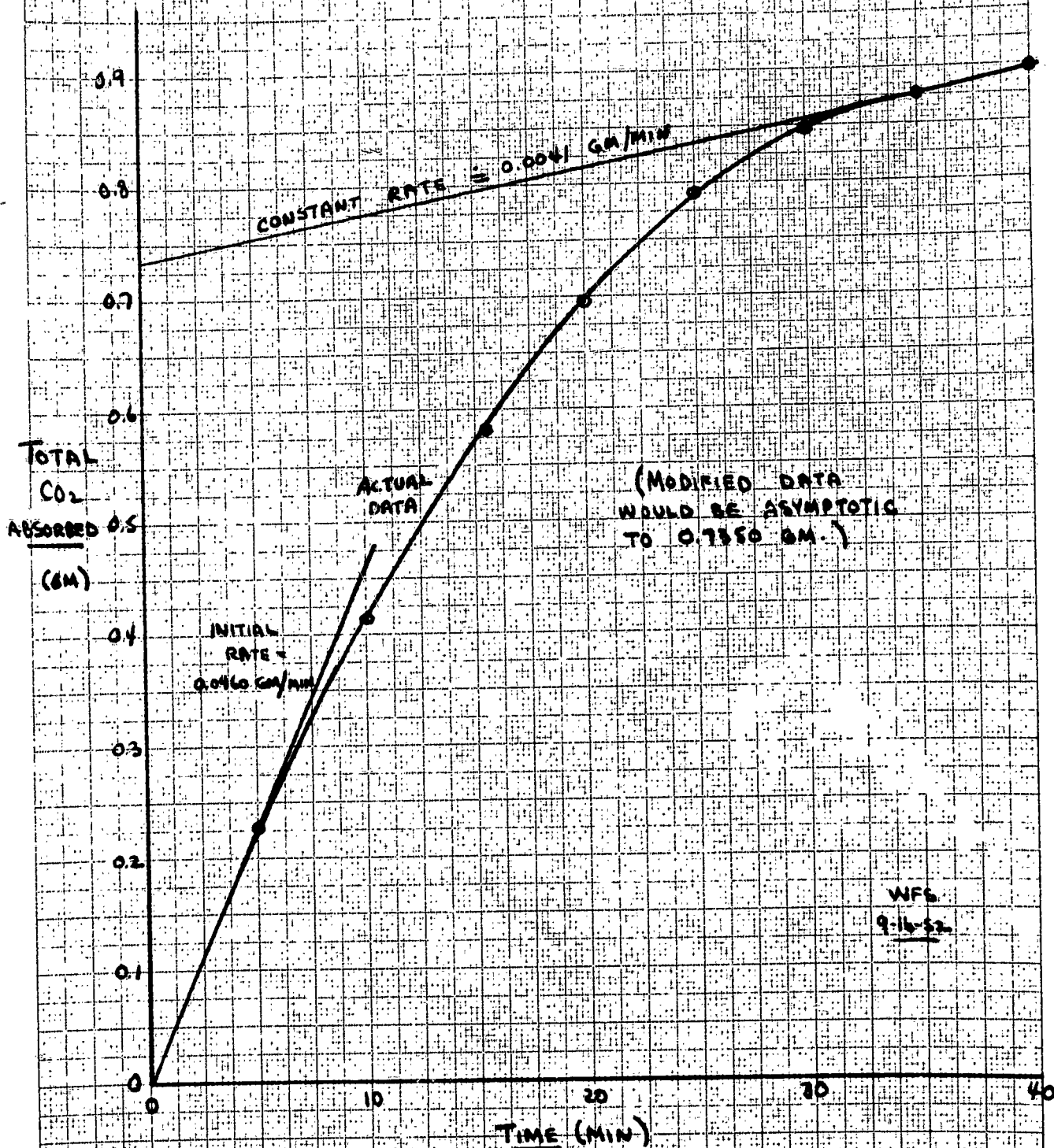
FIGURE 14

ABSORPTION DATA - RUN A-2
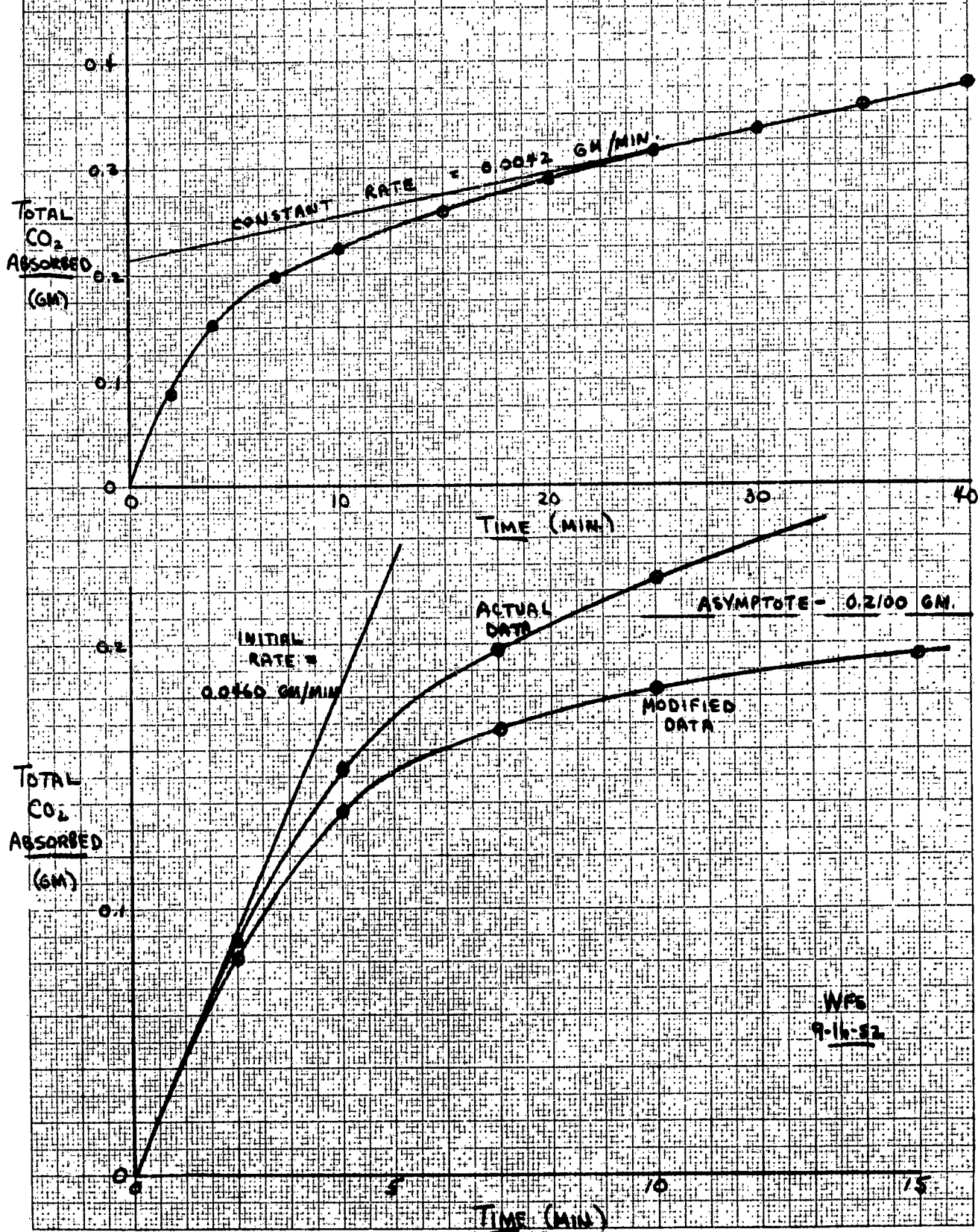
FIGURE 15

ABSORPTION DATA - RUN A-2

CONSTANT RATE = 0.0034 GM/MIN

ACTUAL DATA

ASYMPTOTE = 0.2600 GM.

MODIFIED DATA

INITIAL RATE = 0.0440 GM/MIN

WFS
9-16-32
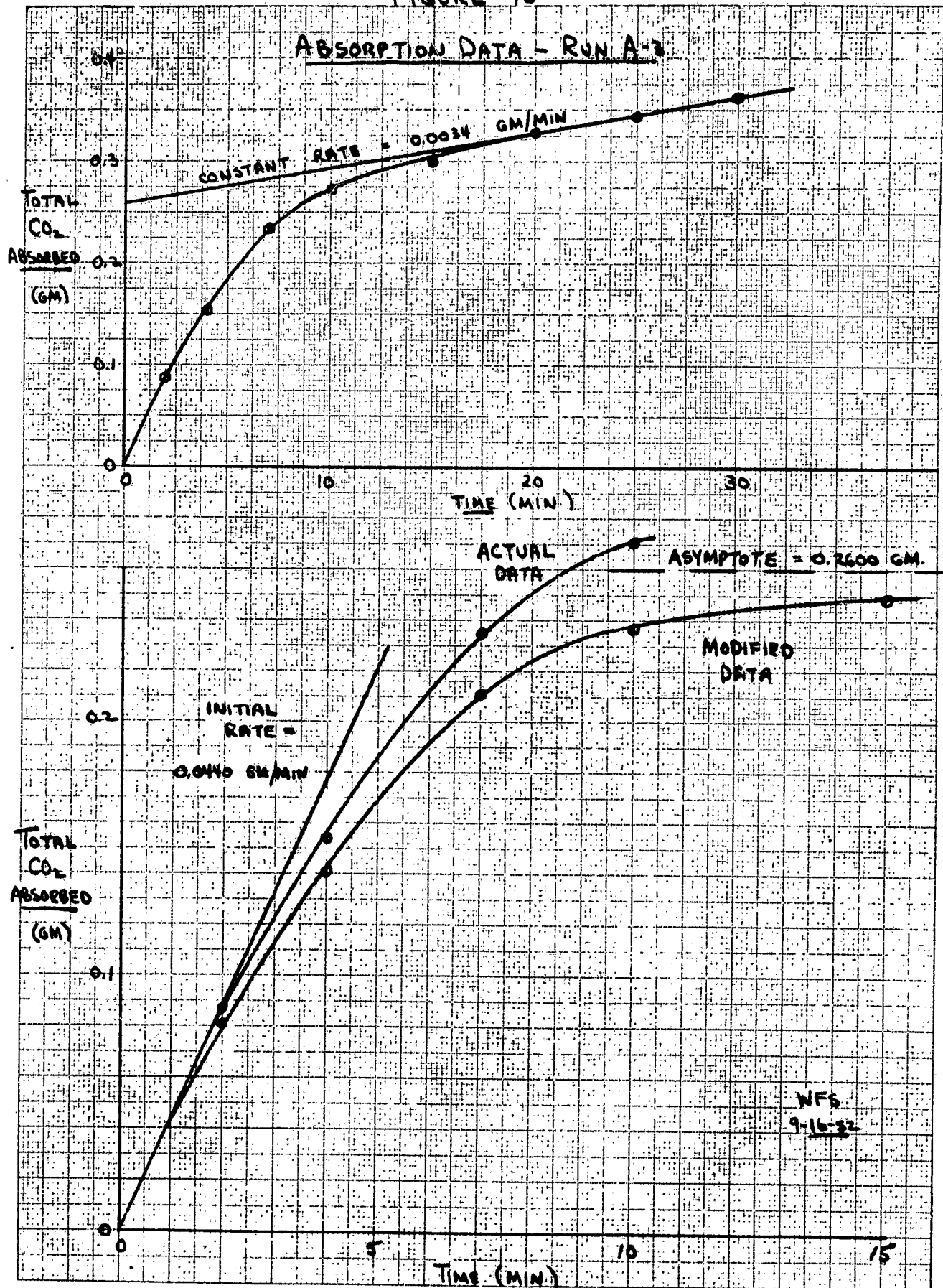
FIGURE 16

ABSORPTION DATA - RUN A-4
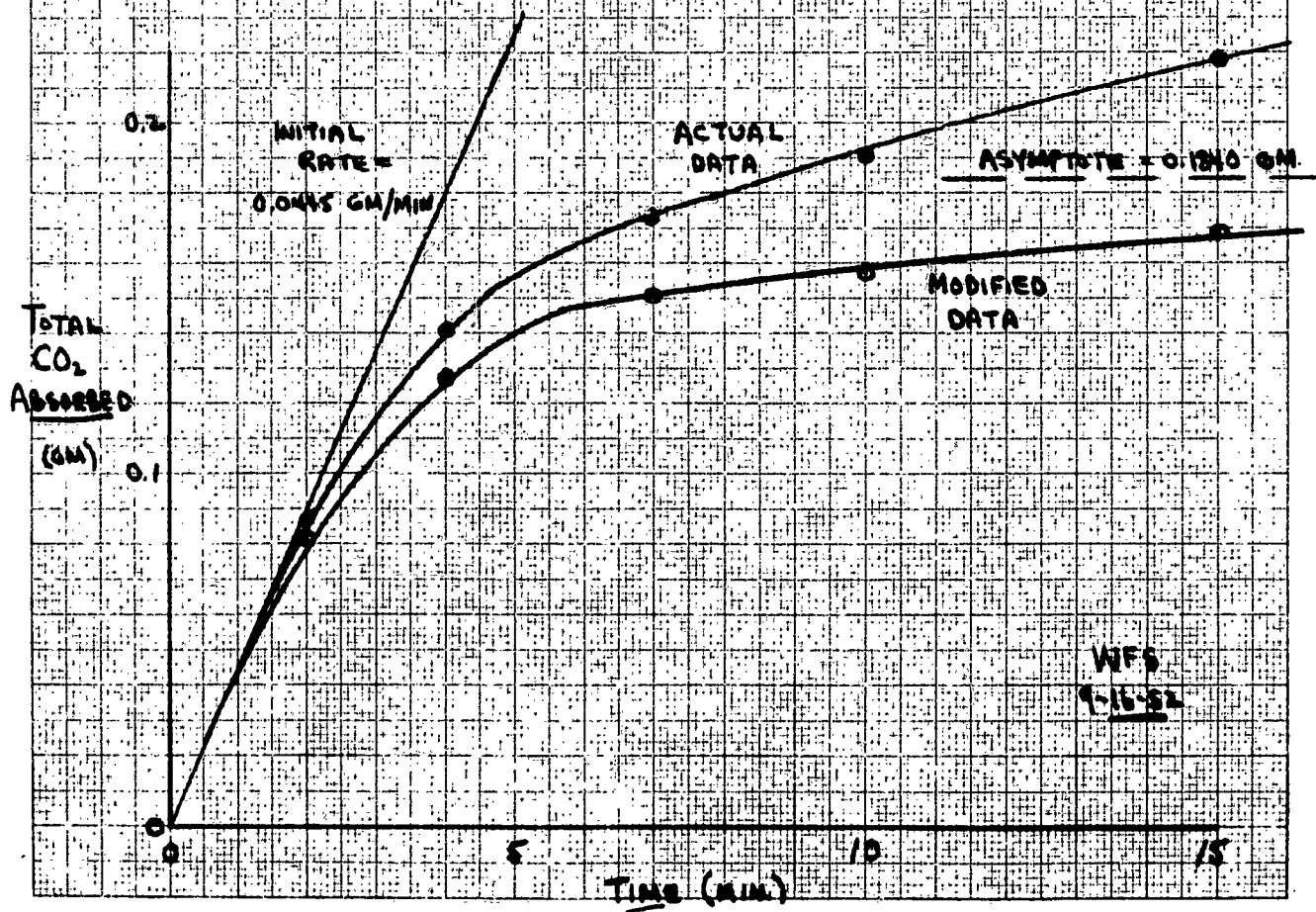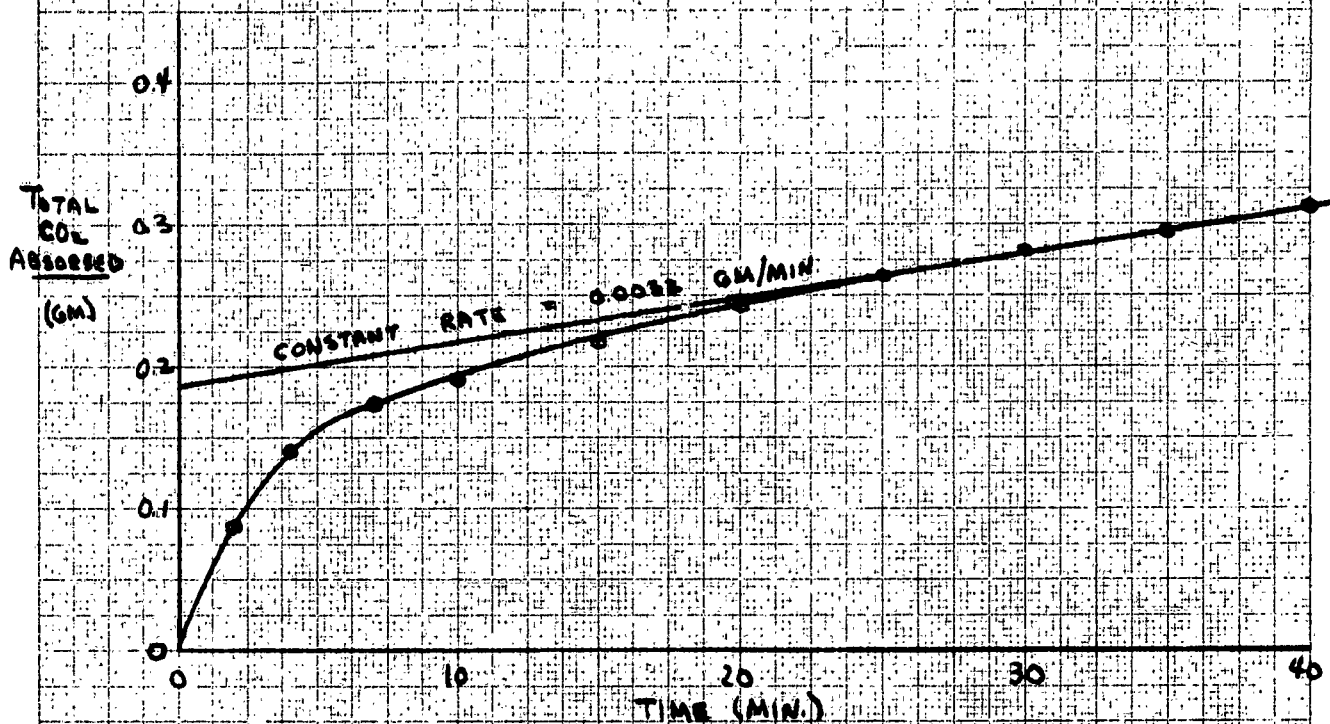
FIGURE 17

ABSORPTION DATA - RUN A·5
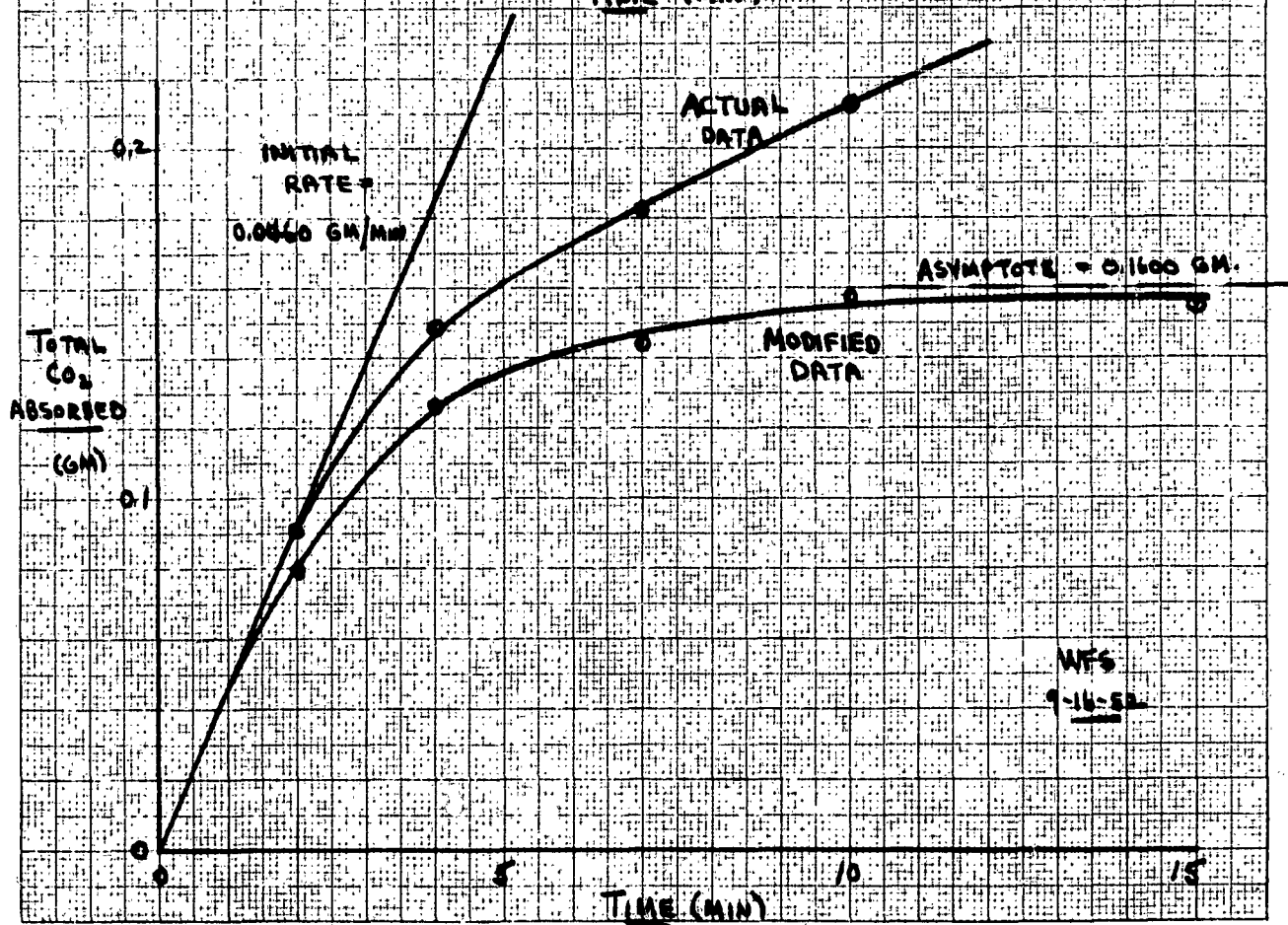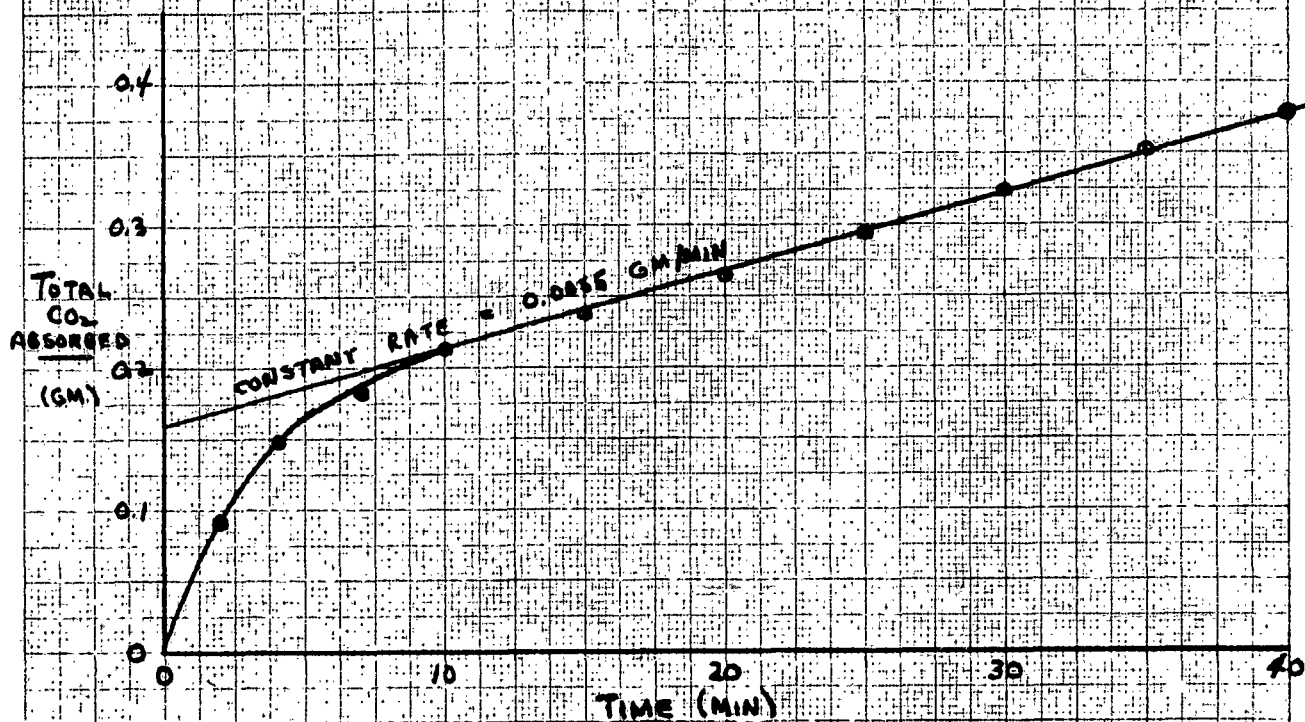
using the modified data as explained above, to give effective values of CO_2 inlet rates. Knowing the CO_2 outlet rates, from weighings of the ascarite tubes, it is possible to calculate values of $(y/y_o)_{avg.}$ for each sample interval. This has been done for all of the runs, and the results are summarized in Table III. The relationship used is as follows:

$$\left(\frac{y}{y_o}\right)_{avg.} = \frac{1}{\frac{gm\ CO_2\ in}{gm\ CO_2\ out}\ (1 - y_o) + y_o}$$

TABLE III

CALCULATED VALUES OF $(y/y_o)_{avg}$

Sample Interval	Outlet $(y/y_c)_{avg.}$ Values			
	A-2	A-3	A-4	A-5
t = 0	0.307	0.317	0.322	0.281
0-2	0.394	0.389	0.416	0.372
2-4	0.585	0.527	0.660	0.650
4-7	0.845	0.647	0.885	0.906
7-10	0.927	0.869	0.962	0.981
10-15	0.962	0.963	0.965	?
15-20	0.977	0.963	0.973	0.998
20-25	0.981	?	0.986	0.996
25-30	?	0.990	0.998	0.990
30-35	0.999	---	0.978	?
35-40	0.997	---	0.995	?

At this point it seems logical to check the applicability of the mechanism proposed in the section on Mathematical Development. Calculations have resulted in values of $(y/y_0)_{avg.}$ at the reactor outlet as a function of time, with all other variables held as constant as possible.

That is:

M = constant $\therefore j = e^M = A$

N = constant $\times t$ $\therefore h = e^N = \left[e^{k_A \cdot y_0} \right]^t = B^t$

Define: $y/y_0 = Y$

Therefore: $Y = \dfrac{A B^t}{1 + A(B^t - 1)}$

$Y(1 - A) = A B^t (1 - Y)$

$\dfrac{Y}{1 - Y} = \dfrac{A}{1 - A} B^t$

$\log \dfrac{Y}{1 - Y} = \log \dfrac{A}{1 - A} + t \log B$

Define: $Y' = \dfrac{Y}{1 - Y}$ $A' = \log \dfrac{A}{1 - A}$ $B' = \log B$

Therefore: $\log Y' = A' + B' t$

When the function $\log \dfrac{y/y_0}{1 - y/y_0}$ is plotted versus t, a straight line will result if the experimental data follow the equations of the proposed mechanism. In addition, the slope and intercept of this line can be used to calculate the values of x_0 and k_A for the particular run. This function has been calculated and plotted for each of the runs using Ag_2O sample A. A typical plot, for Run A-2, is included here, as Figure 18. From this plot it can be seen that a straight line does result, for the data of the first ten minutes or so. After this time, the slope falls off considerably, probably because of errors in calculation when values of y/y_0 begin to approach 1.0. For a first approximation of the constants of the mechanism equation, the straight line portion of the early part of the run has been considered as representative and the best straight line fitted to the available five data points. This procedure has also been followed on the other runs of series A. Results are tabulated in Table IV, where average values of k_A and x_0 are also shown. Similar calculations

are in progress for the runs of series B and D_B. Results of these calculations and of additional experimental runs will be presented in the next report.

FIGURE 18

CHECK OF MECHANISM EQ.
(LOG Y' VS. TIME)

(DATA OF RUN A-2)

$$Y' = \frac{y/y_0}{1 - y/y_0}$$

WF6
4-17-52

$\log_{10} Y'$

TIME (MIN)

-45-
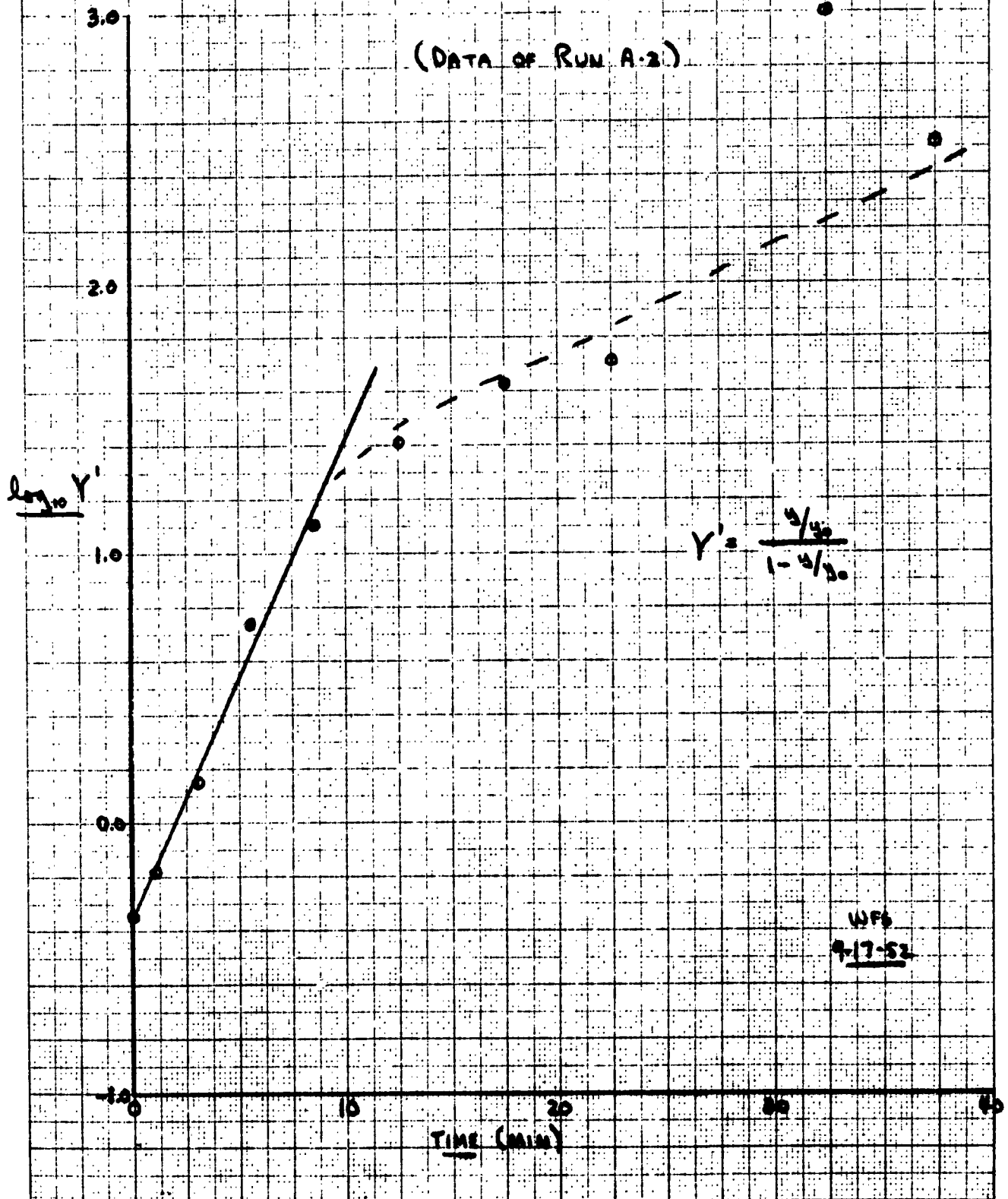
TABLE IV

CHECK OF MECHANISM - DATA

Time	A-2 y/y_0	A-2 log Y	A-3 y/y_0	A-3 log Y	A-4 y/y_0	A-4 log Y	A-5 y/y_0	A-5 log Y
0	0.307	-0.354	0.317	-0.333	0.322	-0.323	0.281	-0.414
1	0.394	-0.187	0.389	-0.196	0.416	-0.147	0.372	-0.227
3	0.585	0.149	0.527	0.047	0.660	0.288	0.650	0.269
5.5	0.845	0.737	0.647	0.263	0.885	0.886	0.906	0.979
8.5	0.927	1.104	0.869	0.822	0.962	1.403	0.981	1.713

slope = 10.66 (hr)
intercept = -0.35

slope = 7.82 (hr)
intercept = -0.35

slope = 12.65 (hr)
intercept = -0.33

slope = 15.30 (hr)
intercept = -0.43

avg. slope = 11.61 (hr)
avg. intercept = -0.365

$$Y = \frac{y/y_0}{1 - y/y_0}$$

avg. value of k_A = 950 atm^{-1}-hr^{-1}
avg. value of x_0 = 0.00575 lb mol/ft^3

} for series A

CONCLUSIONS

Sufficient experimentation has been carried out on the silver oxide process to allow several conclusions to be drawn. First, the process seems to be feasible for use as a regenerative system of CO_2-removal, since several successive absorption-desorption cycles can be carried out on one sample with only a small decrease in capacity. A longer series of cycles will be necessary to support this conclusion definitely, however. Second, the most important variable in the absorption step seems to be the initial concentration of oxide available on the surface of the solid. If this quantity can be increased, the size of equipment required for the process can be materially decreased. It should be noted that it is the concentration of oxide <u>available</u> on the solid surface which is important. Therefore, there will probably be little to be gained by the use of pure silver oxide, since the quantity of oxide on the surface will not be materially different from that available on an alumina-supported sample of similar size. Future runs with pure Ag_2O will be necessary to prove this definitely, however.

The mechanism equations derived and presented in this report will be of considerable value in indicating the relative effects of the variables involved in the absorption step. In combination with similar equations for the desorption step, they will permit calculation of equipment sizes, feed rates, etc., so that the optimum process design will result. Such a complete design will form a major part of the write-up on the silver oxide process for the next report.

SECTION II

LOW TEMPERATURE ABSORPTION, CO_2 SOLUBILITY

INTRODUCTION

The search for suitable absorbents for use in the low temperature regenerative system of CO_2 removal is continuing. Previous data in this phase have been presented in earlier reports. Samples representing several classes of compounds are being evaluated as possible absorbents. At present, the most promising class of compounds is the esters. Consequently, more attention is being focused on compounds of this general classification. Also, this class of compounds will be evaluated to determine what trends may exist within the class.

Much additional work must be done before any one compound can be selected as the best absorbent for the low temperature process.

Experimental Procedure

The method for determining CO_2 solubility presently being used is the "open" method as described in the tri-monthly report of this project for the period January 1 to March 31, 1952. This method consists of bubbling the CO_2 through the solvent.

It has been necessary to modify the analytical procedure due to the fact that esters hydrolyze. The earlier procedure involved a volumetric analysis in which a known weight of sample was treated with a known excess of $Ba(OH)_2$. The barium hydroxide then reacted with the carbon dioxide to form barium carbonate. The excess of barium hydroxide was then determined by titrating with standard acid. Thus the amount of carbon dioxide in the solution was determined. However, if this procedure is applied to the esters, the esters will hydrolyze and produce an acid, which will then react with the barium hydroxide and in the calculations will appear as carbon dioxide, thus producing erroneous values for CO_2 solubility.

The procedure now used is to treat the sample with an excess of $Ba(OH)_2$. This reacts as before to produce barium carbonate, which precipitates. This precipitate is then filtered, washed, dried, and weighed to determine the amount of carbon dioxide which was present in the sample. The esters still hydrolyze to produce

an acid which also reacts with the barium hydroxide. However, as long as the barium salt produced is soluble, it does not appear in the weight of precipitate and hence causes no errors.

Data

The samples tested and the results obtained appear in Table V. This table lists the molecular weight of each solvent. The second and third columns list the temperature and pressure for each sample. The fourth column lists the mole fraction of CO_2 experimentally determined as present in the sample. The calculated value of γ is reported in the fifth column. This value of γ is calculated from the equation $\gamma = y\,p/x\,P$, where

γ = activity coefficient of CO_2 in solution

y = mole fraction of CO_2 in gas phase

x = mol fraction of CO_2 in liquid phase

p = total pressure of gas

P = vapor pressure of pure CO_2 at temperature of solution

The last column of the table reports the mole fraction of CO_2 which would exist in solution at a total gas pressure of 760 mm Hg and at the given temperature, assuming the calculated value of γ to apply.

This table extends the results previously reported in the tri-monthly report of this project (Jan. 1 - March 31, 1952). In the case of tributyl phosphate, these data correct the previous results for a better interpretation of the blank then being applied. Also it may be noticed that, in view of the present work, two values for toluene previously reported have been omitted as unreliable. The values for octyl acetate reported here differ widely from those previously reported. The earlier values were obtained by another experimental method which appears less reliable than the method now being used; and the present values are believed to be more accurate.

CONCLUSIONS

The survey of absorbents for use in the low temperature absorption system is not complete; but the class of compounds known as esters show the most promise. Consequently more attention is being placed in compounds of this class.

The results show that γ increases as temperature decreases for all compounds tested to date. It was at first believed that γ would approach 1.00 as temperature decreased, due to composition effects. The effect of composition on γ is expressed by Margules' equation as follows:

$$\ln \gamma_1 = x_2^2 \left[A + 2 (B - A) x_1 \right]$$

where: γ_1 = activity coefficient of CO_2 in solution

x_1 = mole fraction of CO_2 in solution

x_2 = mole fraction of absorbent in solution

A and B are constants dependent upon absorbent, temperature, and pressure.

This equation states that as x_1 increases and x_2 decreases, the value of γ should approach 1.00 as a limit. The present results, therefore, show that the temperature effect on A and B is quite large and overcomes the effect of composition change. The result is that the values of γ for saturated solutions always increase as the temperature decreases.

The values of γ are an indication of any deviation of the actual solutions from ideal solutions. A value of γ = 1.00 corresponds to an ideal solution; and the lower the value of γ is, the higher the absorption (mole fraction) of CO_2 will be. The molecular weight of the solvent is necessary to correct absorption values from mol fraction to weight per cent. Consequently, a compound possessing both a low molecular weight and a low value of γ is desired.

It would also be desirable to obtain a compound whose γ decreases with decreasing temperatures, since this will predict a larger change in CO_2 solubility with temperature. Unfortunately, this positive value of $d\gamma / dt$ does not appear to exist; and a

small negative value will probably have to be accepted. Hence, the important criteria of good solubility are a low value of and a low molecular weight; of secondary importance is the criterion of a positive or small negative value of $d\gamma/dT$.

TABLE V

CO_2 SOLUBILITY IN ORGANIC SOLVENTS

Solvent	Temperature	Baro. Press. mm Hg	CO_2 Mol. Fract. at Baro. Press.	$\gamma = \dfrac{Y \cdot P}{x \cdot P}$	CO_2 Mol. Fract. at 760 mm Hg
Decalin m. w. = 138.24	82°F	745.8	0.00713	2.03	0.00727
	82°F	744.4	0.00682	2.12	0.00696
	82°F	744.4	0.00677	2.14	0.00691
Alkazene -- 42 m.w. = 263.98	82°F	745.8	0.00695	2.09	0.00708
	82°F	744.4	0.00750	1.93	0.00766
			0.00779	2.13	0.00694
	-23°C	738.3	0.0145	3.78	0.0150
	-34°C	746.7	0.0133	4.37	0.0186
Dichloro-isopropyl-ether m.w. = 171.01	80.4°F	742.0	0.0160	0.920	0.0164
			0.0153	0.963	0.0157
	77.8°F	746.8	0.0152	1.02	0.0155
			0.0156	0.990	0.0159
	72.2°F	742.8	0.0165	0.992	0.0169
			0.0165	0.992	0.0169
	59.5°F	742.3	0.0187	1.03	0.0191
			0.0182	1.06	0.0186
	63.2°F	742.3	0.0185	0.995	0.0189
			0.0177	1.04	0.0181
	67.3°F	744.5	0.0171	1.02	0.0175
			0.0168	1.04	0.0171
	+14°C	752.6	0.0202	1.00	0.0204
			0.0200	1.01	0.0202
	+0.5°C	741.7	0.0256	1.10	0.0262
			0.0256	1.09	0.0262
	-10°C	749.5	0.0340	1.11	0.0345
			0.0344	1.10	0.0349
	-32.0°C	750.7	0.0579	1.30	0.0586
			0.0592	1.27	0.0599
	-34°C	746.7	0.0606	1.32	0.0617
	-36°C	752.9	0.0656	1.32	0.0663
	-47.0°C	745.5	0.0913	1.41	0.0931
			0.0788	1.45	0.0905
	-48°C	747.4	0.0762	1.77	0.0775
			0.0786	1.71	0.0799
Butyl-Cellosolve m.w. = 118.11	80.4°F	742.2	0.0120	1.28	0.0123
			0.0123	1.20	0.0126
	77.2°F	746.8	0.0125	1.24	0.0127
			0.0115	1.34	0.0117
	72.2°F	742.8	0.0131	1.25	0.0134
			0.0129	1.27	0.0132
	59.5°F	742.3	0.0159	1.22	0.0163
			0.0145	1.35	0.0148

Solvent	Temperature	Baro. Press. mm Hg	CO_2 Mol. Fract. at Baro. Press.	$\gamma = \frac{y \cdot p}{x \cdot P}$	CO_2 Mol. Fract. at 750 mm Hg
Butyl-Cellosolve (continued)	63.2°F	742.3	0.0138	1.33	0.0141
			0.0138	1.33	0.0141
	67.3°F	744.5	0.0136	1.29	0.0139
			0.0131	1.34	0.0134
	+14°C	752.6	0.0160	1.26	0.0162
			0.0152	1.33	0.0153
	+0.5°C	741.7	0.0205	1.36	0.0210
			0.0203	1.38	0.0208
	-10°C	749.5	0.0283	1.34	0.0287
			0.0287	1.31	0.0291
	-32.0°C	750.7	0.0469	1.50	0.0475
			0.0487	1.54	0.0493
	-34°C	746.7	0.0495	1.61	0.0504
	-35°C	753.1	0.0544	1.54	0.0549
			0.0537	1.55	0.0542
	-47°C	745.5	0.0804	1.60	0.0820
			0.0799	1.61	0.0815
	-48°C	747.4	0.0828	1.62	0.0842
			0.0846	1.59	0.0861
Propylene glycol m. w. = 76.06	80.4°F	742.0	0.00328	4.49	0.00336
			0.00256	5.75	0.00262
	77.2°F	746.8	0.00353	4.37	0.00359
			0.00317	4.87	0.00323
	72.2°F	742.8	0.00338	4.84	0.00346
			0.00329	4.98	0.00337
	67.3°F	744.5	0.00347	5.04	0.00354
			0.00341	5.13	0.00348
	63.2°F	742.3	0.00369	4.99	0.00378
			0.00358	5.14	0.00367
	59.5°F	742.3	0.00393	4.92	0.00402
			0.00386	5.01	0.00395
Toluene m.w. = 92.06	72.4°F	744.7	0.00886	1.85	0.00904
			0.00965	1.70	0.00985
			0.00928	1.76	0.00947
	-37°C	749.1	0.0302	2.95	0.0306
	-38.5°C	749.1	0.0320	2.94	0.0320
	-48°C	743.0	0.0426	3.14	0.0436
			0.0395	3.39	0.0404
2-Ethylhexyl chloride m.w. = 148.67	78°F	751.3	0.0145	1.06	0.0147
			0.0136	1.13	0.0138
	26°C	751.3	0.0141	1.08	0.0143
			0.0138	1.10	0.0140
	74°F	748.2	0.0149	1.06	0.0151
			0.0154	1.05	0.0156
	69.5°F	744.9	0.0151	1.13	0.0154
			0.0148	1.15	0.0152

Solvent	Temperature	Baro. Press. mm Hg	CO_2 Mol. Fract. at Baro. Press.	$= \frac{Y P}{x P}$	CO_2 Mol. Fract. at 760 mm Hg
2-Ethylhexyl acid m.w. = 144.21	78°F	751.3	0.0180	0.855	0.0182
			0.0192	0.799	0.0195
	26°C	751.3	0.0229	0.666	0.0231
			0.0208	0.730	0.0211
	74°F	748.2	0.0231	0.697	0.0235
			0.0216	0.747	0.0219
	69.5°F	744.9	0.0240	0.708	0.0245
			0.0231	0.737	0.0235
2-Ethylhexanol m.w. = 130.23	78°F	751.3	0.00847	1.82	0.00857
			0.00960	1.60	0.00971
	26°C	751.3	0.00879	1.73	0.00889
			0.00863	1.76	0.00873
	74°F	748.2	0.00838	1.92	0.00851
			0.00817	1.97	0.00830
	69.5°F	744.9	0.00868	1.96	0.00886
			0.00889	1.91	0.00907
Ethyl Aceto Acetate m.w. = 130.14	+13°C	751.4	0.0255	0.813	0.0257
			0.0262	0.791	0.0265
	+0.5°C	741.7	0.0333	0.841	0.0341
			0.0325	0.862	0.0333
	-2°C	754.7	0.0356	0.856	0.0358
			0.0339	0.899	0.0341
	-7°C	748.0	0.0404	0.857	0.0410
	-10°C	749.5	0.0440	0.857	0.0446
			0.0430	0.878	0.0436
	-32°C	750.7	0.0833	0.900	0.0843
			0.0811	0.924	0.0821
	-38°C	748.4	0.0998	0.924	0.101
			0.0975	0.946	0.0990
	-47.0°C	745.5	0.0964	1.34	0.0983
			0.111	1.16	0.113
Octyl Acetate m.w. = 172.26	80.5°F	749.0	0.0250	0.574	0.0263
	79.5°F	748.9	0.0273	0.551	0.0277
	81°F	747.1	0.0232	0.645	0.0236
	+14°C	752.6	0.0303	0.667	0.0306
			0.0305	0.662	0.0308
	-10°C	749.5	0.0521	0.724	0.0528
			0.0538	0.701	0.0546
	-32°C	751.8	0.0939	0.799	0.0949
			0.0944	0.795	0.0955
	-47°C	745.5	0.135	0.959	0.137
			0.117	1.10	0.119
Tributyl Phosphate m.w. = 266.32	85°F	747.4	0.0346	0.405	0.0352
	77.5°F	746.5	0.0335	0.460	0.0341
	73.2°F	748.6	0.0340	0.479	0.0345
	72.4°F	749.7	0.0389	0.424	0.0394

Solvent	Temperature	Baro. Press. mm Hg	CO_2 Mol. Fract. at Baro. Press.	$=\dfrac{y\,P}{x\,P}$	CO_2 Mol. Fract. at 760 mm Hg
Tributyl Phosphate (continued)	71.4°F	752.1	0.0342	0.490	0.0346
			0.0317	0.528	0.0320
	70.7°F	746.8	0.0336	0.500	0.0342
	69.7°F	749.1	0.0348	0.490	0.0353
			0.0340	0.502	0.0345
	-19°C	734.3	0.0846	0.570	0.0876
			0.0842	0.572	0.0872
	-23°C	738.3	0.0910	0.603	0.0937
	-34°C	746.7	0.125	0.642	0.127
		737.5	0.126	0.624	0.130
			0.127	0.621	0.131
		753.0	0.127	0.635	0.128
			0.120	0.673	0.121
	-36°C	747.0	0.143	0.602	0.145
	-38.5°C	749.1	0.139	0.653	0.141
	-48°C	743.0	0.199	0.671	0.204
			0.191	0.701	0.195
Triethyl Phosphate m.w. = 192.14	74.6°F	748.7	0.0256	0.627	0.0260
			0.0253	0.634	0.0257
	80°F	746.3	0.0248	0.600	0.0253
		746.2	0.0262	0.568	0.0267
			0.0255	0.584	0.0260
	73.6°F	742.8	0.0274	0.587	0.0280
			0.0258	0.623	0.0264
			0.0260	0.619	0.0266
			0.0258	0.623	0.0264
	71.8°F	747.1	0.0267	0.620	0.0272
			0.0276	0.600	0.0281
			0.0268	0.618	0.0273
	+13°C	751.4	0.0306	0.677	0.0309
			0.0308	0.671	0.0312
	-10°C	749.5	0.0589	0.640	0.0598
			0.0611	0.618	0.0619
	-14°C	750.7	0.0666	0.637	0.0675
			0.0651	0.652	0.0659
	-32°C	751.8	0.112	0.670	0.113
	-34°C	746.7	0.114	0.699	0.116
	-38°C	748.4	0.131	0.703	0.133
			0.130	0.712	0.132

SECTION III

FREEZING-OUT OF CARBON DIOXIDE

INTRODUCTION

In the last tri-monthly report (April 1 - June 30 1952) a preliminary treatment of the 'freeze-out' method of carbon dioxide removal was presented. During the past three months this method has been developed further to a point where the major problems are practically solved and the process appears entirely feasible.

The removal of carbon dioxide from air in closed atmospheres by a continuous process in which the carbon dioxide is frozen out of the air stream has several advantages over other processes. No storage space is required for chemicals or other supplies which are necessary in non-regenerative methods. No oxygon or nitrogen is removed along with the carbon dioxide as is the case when physical absorption is used. Power requirements are not excessive and space requirements are modest. The only significant materials and utilities required are sea water for cooling and electric power for compression. In addition to removing carbon dioxide from the atmosphere, this process reduces the humidity of the air to a low value.

DESCRIPTION OF PROCESS

A schematic flow diagram of this carbon dioxide 'freeze-out' process is shown in Figure 19. This shows the foul air containing 1% CO_2 and with a relative humidity of 65% entering the process at 80°F and 1 atma. This air stream enters the first compressor (P-1) at a rate of 500 lbs./hr. This inlet stream consists of 7.59 lbs/hr of CO_2, 7.05 lbs/hr of H_2O, and 485.36 lbs/hr of dry, CO_2-free air. After the first stage of compression the air is cooled with sea water. During this cooling some of the water vapor is liquefied and removed from the stream. Further compression and cooling removes more water.

The high pressure foul air leaving the second sea water cooler (HE-2) is passed through a gas-to-gas heat exchanger (HE-3) where it is cooled to about 35°F. In this exchanger additional water is condensed out and flashed to the low pressure side of the exchanger. The foul air with most of the water removed is next sent to a reversing heat exchanger (HE-4) where more of the water vapor is removed by freezing out on the exchanger surface.

The operation of this reversing exchanger is shown in more detail in Figure 20. During the first half of the cycle, the high pressure foul air is passed down one side of the exchanger depositing ice as it is cooled to about -150°F. (This temperature is just above the temperature at which CO_2 starts to freeze out.) While the high pressure air is depositing ice on one side of the exchanger, ice is being removed from the other side by passing low pressure purified air through it. After a suitable period of operation, during which ice builds up on the high pressure side and the low pressure side is derimed, the reversing valves are switched. This sends the high pressure air down the side which has just been derimed and the low pressure purified air back through the side which has fresh rime deposits. This reversing action is indicated in Figure 20. It should be noted at this time that all the water which is condensed in the sea water coolers is permanently separated from the air. On the other hand,

the water removed in these two heat exchangers (HE-3 and HE-4) is re-evaporated into the purified gas stream.

From the reversing heat exchanger (HE-4) the high pressure air next passes through side (3) of HE-6 (see Figure 19) where it is cooled slightly by raising the temperature of the exchanger to nearly -150°F. During this heating of HE-6 side (4) is being evacuated to remove CO_2. After passing through side (3) the high pressure air is sent through side (2) of HE-5 where it is cooled to about -220°F by passing countercurrent to the low pressure air which has just left the expansion turbine. In cooling to about -220°F the high pressure air is purified by the removal of 99% of the CO_2 and most of the residual water. The CO_2 and H_2O are removed by being frozen out on the heat exchanger surface in the same manner that water is deposited in the reversing heat exchanger (HE-4). After a suitable interval of time during which side (2) is receiving rime deposits and side (4) is being derimed, the valves are switched to allow the high pressure stream leaving HE-4 to pass successively through sides (1) and (4). This change allows side (2) to be defrosted by heating and evacuation and side (4) to receive the rime deposits. After the same interval the valves are switched back. This reversing operation should prevent excessive plugging of the heat exchangers by removing all the rime that has been deposited in the previous cycle. However if by this procedure it is found that adequate deriming is not taking place, then a four step reversing procedure in which each of the four sides of HE-5 and HE-6 successively passes

    1) high pressure air at about -150°F,
    2) high pressure air being cooled to about -220°F,
    3) CO_2 removal by evacuation,
and 4) low pressure air,

will definitely provide complete deriming in each cycle. In this case the high pressure air will pass through two sides in the following rotation:

1) side (3) and side (2)
2) side (1) and side (3)
3) side (4) and side (1)
4) side (2) and side (4).

The high pressure air at about -220°F (now containing only 0.01% CO_2 and a negligible amount of H_2O) next passes through an expansion turbine where some power and considerable cooling is achieved. (HE-7 shown on the flow sheet is not a separate heat exchanger for operation below 11 atmospheres when it merely indicates that heat leak exists.) The air leaves the turbine at about 1 atma and between -270 and -312°F depending upon the pressure on the inlet side (-270°F for about 3 atm inlet pressure and -310°F for about 11 atm).

The low pressure air leaving the turbine (now cold and purified) is passed back through side (1) of HE-5 (or one of the other sides of HE-5 or HE-6 depending upon which part of the cycle is in operation) where it picks up heat from the high pressure air which is being cooled to about -220°F. After leaving this heat exchanger the low pressure air stream may be split with part of it recycled back through the exchanger (HE-5). This recycling is not necessary if the two-step reversing procedure is used for the operation of HE-5 and HE-6. It may or may not be necessary for the four-step reversing procedure depending upon the effectiveness of the deriming by evacuation and heating.

The low pressure air next passes through the reversing heat exchanger (HE-4) where it picks up the ice deposits left by the high pressure air. Again some recycling may be necessary to insure complete deriming of this exchanger. From HE-4 the low pressure air passes through HE-3 where it picks up the water removed from the high pressure air and where it is heated up to 80°F and discharged to the atmosphere. This purified air contains only 0.01% CO_2 and has a relative humidity of about 3%.

POWER AND SPACE REQUIREMENTS

The results of detailed calculations indicate that the required power for processing 500 pounds per hour of foul air is between 12 and 20 kilowatts as is summarized below.

High Pressure Side atma	Required Power, kilowatts				
	Compression	Evacuation	Pumping etc.	Turbine	Net
5	14.0	0.2	0.8	-2.0	13.0
11	22.4	0.2	0.8	-2.7	20.7

These figures are based upon compressors and turbines designed to occupy small volumes. Efficiencies of 70% were assumed for both compression and for expansion.

A summary of the space requirements indicates that a total volume of between 40 and 80 cubic feet should be sufficient. A breakdown of this estimate is given below.

	Volume, cubic feet
Heat exchangers, bare	3 - 6
insulation	2 - 4
Compressors	5 - 10
Turbine	0.3 - 1
Piping, valves, controls	10 - 20
Free Space	20 - 39
Total	40 - 80

These figures are based upon equipment designed especially for conditions requiring small volumes. The heat exchangers, compressors, and turbine were carefully evaluated while the remaining items were roughly estimated.

OPERATING CONDITIONS

The operating temperatures, pressures and compositions of of the various parts of the process shown in Figure 19 depend largely upon physical and thermal properties of the fluid-solid system air-CO_2-H_2O. They also depend upon the properties of available sea water, the desired atmospheric conditions of the region supplying the foul air, and the desired composition of the fresh air. In order to investigate the effect of the many process variables on the power and space requirements, it was necessary to consider as primary variables the operating pressure, P_2, and the amount of CO_2 removed. In order to restrict the problem it was decided to consider removal of 99% of the entering CO_2. This choice was made since preliminary calculations indicated that the power and space requirements would be practically independent of amount of CO_2 removed, as long as about 95% or more CO_2 was removed. Since the optimum operating pressure was not known, it was decided to investigate pressures, for P_2, up to 20 atmospheres. With these choices of primary variables the operating temperatures were fairly definitely established. Each of these temperatures and pressures is discussed in a following paragraph.

Inlet temperature, T_1. The inlet temperature was arbitrarily chosen as 80°F to represent a reasonable basis.

Inlet pressure, P_o. For the same reason the inlet pressure was chosen as 1 atmosphere.

Inlet composition. A relative humidity of 65% and a CO_2 concentration of 1.0% by volume were chosen as comfortable conditions which should be maintained.

Compressor discharge pressure, P_1. Depending upon the operating pressure, P_2, and the type of compressor selected, one, two, or possibly three stages of compression may be required. For one stage operation, $P_1 = P_2$. For two stage operation, $P_1 = \sqrt{P_2}$ where both pressures are expressed in atmospheres.

Compressor discharge temperature, T_2. The discharge temperature is principally a function of the pressure P_1, and of the efficiency of the compression. This function is plotted in the left hand

side of Figure 21 where three curves labeled $P_1 = P_2$ are plotted. These curves show how T_2 varies with P_1 and compression efficiency. T_2 is also presented in Table VII for values of P_1 between 2.24 atm and 6.81 atm.

Sea Water temperature, T_{14}. An analysis of reported sea water temperatures at various latitudes, longitudes, seasons, and depths indicated that 80°F was an acceptable figure to use for the purposes of this study. Table VI is a listing of surface temperatures throughout the world for two seasons of the year and temperatures at 200 and 400 meters below the surface, these submerged temperatures being almost independent of the season.

Sea water temperature, T_{16}. The temperature of the sea water leaving the heat exchanger, HE-1, was chosen as 90°F, which represents a 10°F rise in temperature.

Compressed air temperature, T_3. It was assumed that the air could be cooled to within 10°F of the water temperature. This made T_3 equal to 90°F.

Compressor discharge temperature, T_4. This discharge temperature depends upon the pressure, P_2, and compressor efficiency as well as P_1 and T_3. T_4 as a function of P_2 and compression efficiency is plotted in Figure 21 and listed in Table VII.

Sea water temperature, T_{15}. Same as T_{16}.

Compressed in temperature, T_5. Same as T_3. T_5 is shown as a function of P_2 in Table VIII and Figure 22.

Temperature of foul air leaving HE-3, T_6 and T_6'. This temperature was set as 35°F to be a few degrees above the freezing point of water, 32°F.

Temperature of foul air leaving HE-4, T_7. In order to limit the deposition of solid CO_2 to HE-5 and HE-6, the temperature T_7 must be higher than the temperature at which a mixture of air and 1% CO_2 is in equilibrium with solid CO_2. This temperature is tabulated in Table IX, plotted in Figure 23 as a function of pressure. It is also shown in Figure 22 and Table VIII.

Temperature of high-pressure clean air leaving HE-5, T_8.

In order to remove 99% of the CO_2 from the foul air, the temperature of the air stream must be reduced until it is at the temperature at which a mixture of air and 0.01% CO_2 is in equilibrium with solid CO_2. This temperature, T_8, is plotted in Figures 22 and 23 and given in Table VIII as a function of pressure. This is also the temperature of the air inlet to the expansion engine for pressures below about 11 atm. In order to prevent liquid air from forming in the expansion engine, the temperature of the inlet stream must be that shown as T_8' or higher. For pressures above 11 atm., T_8' is higher than T_8, and the stream must be heated (by HE-7 or other means). This indicates that compression to more than 11 atmospheres is of no advantage. These temperatures were obtained assuming 70% efficiency in the expansion engine.

Temperature of clean air leaving turbine, T_9.

Assuming expansion to 1 atm. at 70% efficiency in the expansion engine, the temperature leaving the turbine, T_9, was calculated from T_8. T_8' was obtained from T_9 for the higher pressures by using -312.8°F for T_9.

Temperature of clean air leaving HE-3, T_{13}.

The temperature of the clean air discharged from the process was assumed to be 80°F, which is 10°F cooler than T_5. This represents conservative design conditions and in operation may be considerably different.

Temperature of clean air leaving HE-4, T_{12}.

An energy balance around HE-3, assuming no heat leak and allowing for revaporization of condensate, fixes T_{12} as shown in Figure 22 and Table VIII. During actual operation, it may be as much as a few degrees lower due to heat leak.

Temperature of clean air entering HE-4, T_{11}'.

The temperature of clean air entering HE-4 must be high enough to remove the ice deposits in the reversing exchanger. This temperature is related to T_7 as shown in Figure 24. For temperatures of T_{11}' lower than indicated on Figure 24, the low-pressure clean air will not derime the exchanger. In order to insure complete deriming, temperature T_{11}' has been chosen higher than shown in Figure 24. It is tabulated in Table VIII as calculated from 75% of the difference shown in Figure 24. In order to obtain this temperature, a recycle stream as shown in Figure 19 is necessary.

Temperature of clean air leaving HE-5, T_{11}. An energy balance around HE-4, assuming no heat leak in either HE-4 or HE-3, indicates the temperature for T_{11} which is shown in Figure 22 and Table VIII. In actual operation T_{11} will be lower, perhaps several degrees, due to heat leak.

Temperature of clean air entering HE-5, T_{10}'. If the two step deriming cycle satisfactorily prevents build up of solid CO_2 and solid H_2O in HE-5 and HE-6, then no recycle stream is required and $T_{10}' = T_{10}$. However, if the four step reversing procedure is necessary T_{10}' must be higher than T_{10} and related to T_8 as shown in Figure 24. In order to insure deriming of these exchangers, T_{10}' as plotted in Figure 22 and tabulated in Table VIII was calculated by using 75% of the permissible difference shown in Figure 24.

Temperature of clean air leaving turbine, T_{10}. An energy balance around HE-5 and HE-6, assuming no heat leak in any one of HE-3, HE-4, HE-5, HE-6, and neglecting the energy effects associated with the evacuation part of the cycle, indicates for T_{10} the temperatures plotted in Figure 22 and shown in Table VIII. At this time it can be noticed that T_9 and T_{10} represent the same stream and that the difference between T_9 and T_{10} is a quantitative measure of the permissible heat leak in the exchangers.

Temperature, T_{17}, and Pressure, P_3, for evacuation. In order to remove CO_2 by evacuation the pressure must be reduced and/or the temperature raised by an amount at least as much as indicated by the equilibrium phase relationships of the air-CO_2 system. Figure 25 shows these relationships in terms of the process variables. The temperature rise, $T_{17}-T_8$, is plotted against the pressure factor P_2/P_3. For removing 99% of the CO_2, two lines are presented, one for $P_2 = 10$ atm and one for $P_2 = 5$ atm. One line ($P_2 = 10$ atm) is presented for removing 98% CO_2.

In the preceding paragraphs are presented the underlying assumptions and reasons for establishing the various conditions of the process. It should be pointed out that, for this phase

of the problem, no consideration was given to pressure drop in the flow of air through the several exchangers and associated piping. This simplification has but little effect on the temperatures obtained and practically no effect on the conclusions of this study.

In making the energy balances to establish some of the process temperatures and to determine the heat exchanger duties, the enthalpies of the several streams were calculated. These enthalpies have been plotted in Figure 26 and tabulated in Table X. These values were based on individual enthalpies for air (Figure 27), for CO_2 (Figure 28) and for water (Keenan and Keyes, Steam Tables).

In the process described above the water condensed in HE-3 and the rime deposited in HE-4 were revaporized in the low pressure clean air. Calculations were also made assuming that these quantities were discarded. The resulting temperatures are given in Table XI and Figure 29.

SELECTION OF EQUIPMENT

Compressors. A survey of available industrial compressors
indicated that practically all models occupy a relatively
large volume (50 to 80 cubic feet total volume) and are there-
fore unsuited for the proposed process. The rotary lobe type
(Elliott-Lysholm) as discussed in recent literature (Engineering
155 97-100, Jan. 29, 1943; SAE Journal 51 June 1943; Mechanical
Engineering 68 514-8, June 1946; NDRC, Division 11, Summary
Technical Report, Vol. 1, 1946) appears rather promising. It
is estimated that a single stage compressor of this type capable
of compressing 500 pounds per hour of air with a compression
ratio of 2.5 or 3 can be designed to occupy a volume about 2.5
or 3 cubic feet (including drive). These compressors operate
at about 70% efficiency (see Figure 30).

Turbine. Based on reports of Swearingen (Chemical Engineering
Progress 43 85-90 Feb. 1947) and Rushton (NDRC, Division 11,
Summary Technical Report, Vol. 1, 1946) it is estimated that
for the proposed process a turbo-expander can be built which
will occupy less than one cubic foot (about 0.3 cu. ft. for
expansion from 5 atmospheres). This expander would operate with
an efficiency of about 70-80%.

Heat Exchangers. In connection with the recent development
of compact equipment for the production of oxygen, two types of
heat exchangers have been used. The ribbon-packed annular exchanger
(Trumpler and Dodge, Chem. Eng. Progress 43 75-84, February 1947)
originated by Collins, and the sandwich type exchanger (Simpelaar
and Aronson, Trans ASME 72 955-965, Oct. 1950) both have a con-
siderably greater transfer surface to volume ratio than commercial
heat exchangers. Either type could be used for the proposed
process. Since the sandwich type exchanger has been more thoroughly
tested and since it is of simpler construction, it was the basis
for this work.

This heat exchanger consists essentially of thin copper

fins furnace bonded between brass plates. The exchanger is mani-
folded so that one fluid will flow in one direction through every
alternate passage and the other fluid will flow in the opposite
direction through the intermediate passages. This arrangement
of surface provides over 300 sq. ft. of effective surface per
cubic foot of heat exchanger volume and corresponds to over 3.5
sq. ft. per pound of metal.

For the specific design considered in this problem, the
recommended equations and data of Simpelaar and Aronson were
restricted and applied to a 3/32" strip fin throughout these
calculations. The properties and necessary data associated with
this particular fin were obtained from the above article. The
distinct advantage of such type of heat exchange equipment over
the conventional shell and tube types lies in the unusually high
heat transfer coefficients attainable. In this connection, gas
film coefficients as high as 60 Btu/(hr)(ft^2)($^\circ$F) are ordinary
against values of 3 to 5 commonly considered for the conventional
shell-tube type exchangers. Conservative pressure drop con-
siderations for both the warm and cold sides indicate that with
the exclusion of end effects (entrance and exit plus piping),
the total pressure drops through the finned-heat exchangers are
as follows:

Heat Exchanger	Pressure Drop, psi	
	Warm Side	Cold Side
HE-1	0.393	- - -
HE-2	0.218	- - -
HE-3	0.248	1.17
HE-4	0.550	2.61
HE-5	0.135	0.63
HE-6	0.135	
	1.679	4.41

Warm Side: ΔP = 1.68 psi.
Cold Side: ΔP = 4.41 psi

These values were reached by considering heat exchangers

of one passage flow throughout and assuming a pressure of 73.5 psia for the unprocessed air through heat exchangers HE-3, HE-4 and HE-5. The cold side pressure drop most likely cannot be decreased unless more than one gas passage is selected for the exchangers.

Heat transfer coefficients for a 3/32" strip fin were evaluated from the j-factor relationship proposed by the above investigators. This relationship is presented below:

$$j_h = \frac{h}{gd}\left[\frac{c_p\mu}{k}\right]^{2/3} = 0.245/(Re)^{0.4}$$

where A = total heat-transfer area which is equal to the sum of the surface of the fins and that of the wall.

c_p° = heat capacity of air, considered as 0.24 Btu/(lb)(°F)

D_e = equivalent passage diameter, $D_e = \dfrac{4}{\dfrac{A}{A_c}\cdot\dfrac{1}{L}}$, ft

G = core, air mass velocity, lb/(hr)(ft^2 of A$_c$)

h = surface heat transfer coefficient based on total heat transfer area, Btu/(hr)(ft^2)(°F)

j_h = heat transfer factor (dimensionless)

L = length of flow passage

Re = Reynolds number $\dfrac{D_e G}{\mu}$

$\dfrac{c_p\mu}{k}$ = Prandtl group, assumed for air to be 0.74

μ = viscosity, lb/(hr)(ft)

The strip fins are 3/32" wide (direction of fluid flow), 0.485" long (distance between plates), 0.004" thick and are 3/32" apart in the direction of fluid flow and .082" apart perpendicular to fluid flow and the rows of fins are staggered.

The following physical characteristics were obtained from the specific heat exchanger employed by Simpelaar and Aronson

in their article (page 959).

Passage details: (Number = 18, height = 0.485", width = 12", length = 90" = 7.5 ft) Total Area (fins plus wall): A = 1858 sq ft Free Cross Sectional Area: A_c = 0.70 sq ft

$$\frac{A}{A_c} = \frac{1858}{0.70} = 2655$$

$$\frac{A}{A_c} \cdot \frac{1}{L} = \frac{2655}{7.5} = 354$$

$$D_e = \frac{4}{\frac{A}{A_c} \cdot \frac{1}{L}} = \frac{4}{354} = 0.0113 \text{ ft.}$$

Heat transfer surface/passage per foot of length (h = 0.485", w = 12", l = 12")

$$\frac{1858}{18 \times 7.5} = 13.7 \text{ sq ft of fin plus wall surface/passage}$$

per foot of length

HE-3 is selected to illustrate the calculation procedure. For this case unprocessed air at 73.5 psia containing carbon dioxide and water vapor is being cooled from 90 to 35°F countercurrently with processed air at substantially atmospheric pressure, the temperature of which rises from 25 to 80°F. The purpose of this exchanger is a twofold one: to cool the air stream to 35°F and simultaneously condense water vapor. This liquid condensate in turn is to be revaporized in the processed air stream. For this particular case the total exchanger duty is 117,977 - 108,706 = 9271 Btu/hr. The temperature difference, for this case, calculates to be 10.0°F. Consequently UA = 9271/10 = 927 Btu/(hr)(ft^2)(°F).

The length and total fluid volume necessary for this heat exchanger at the above given pressure of 73.5 psia are directly related to the number of passages. Arbitrarily cases dealing with 1, 2, 3 and 4 passages for each fluid stream were selected and the calculation procedure is presented below:

Heat Exchanger, HE-3:

High pressure side, P_2 = 73.5 psia

Air flow going from T_5 to T_6

Temperature = 90°F to 35°F $(T_{avg} = 62°F)$

Viscosity = $\mu = 4.477 \times 10^{-2}$ lbs/ft x hr

Air Rate W = 485.36 + 7.59 + 0.42 + 2.54/2 = 494.64 lbs/hr

Passage. w = 12", h = 0.485, L = ?

Strip fin: Thickness = 0.004", h = 0.458, L = 3/32"

$a_c = A_c/h = 0.70/18 = 0.039$ ft^2 of cross-sectional free area/passage

$D_e = 0.113$

$$\frac{c_p \mu}{h}^{2/3} = (0.75)^{2/3} = 0.818$$

n, No. of Passages	A_c ft^2	$G = W/A_c$ (lb/(hr)(ft^2)	$\frac{D_e G}{\mu}$	$\left[\frac{D_e G}{\mu}\right]^{0.4}$	$j_h = \frac{0.245}{(Re)^{0.4}}$	$h_w = j_h \frac{c\,G}{(Pr)^{2/3}}$
1	0.0389	12,716	3210	25.3	0.00969	36.2
2	0.0778	6,358	1605	19.15	0.0128	23.9
3	0.1167	4,238	1070	16.25	0.01508	18.75
4	0.1556	3,179	802	14.5	0.0169	15.76

Low Pressure side, $P_o = 14.7$ psia

Air flow going from T_{12} to T_{13}

Air Rate = W = 485.36 + 0.42 + (2.96 - 0.42) = 488.32 lbs/hr

Temperature = 25°F to 80°F $(t_{avg} = 52°F)$

$$\mu = 4.31 \times 10^{-2} \text{ lb/hr x ft}^2$$

n, No. of Passages	A_c ft^2	$G = W/A_c$ lb/(hr)(ft^2)	$\frac{D_e G}{\mu}$	$\left[\frac{D_e G}{\mu}\right]^{0.4}$	$j_h = \frac{0.245}{(Re)^{0.4}}$	$h_c = j_h \frac{c\,G}{(Pr)^{2/3}}$
1	0.0389	12,553	3291	25.5	0.00960	35.4
2	0.0778	6,276	1645	19.45	0.0126	23.2
3	0.1167	4,184	1097	16.45	0.01489	18.25
4	0.1556	3,138	823	14.7	0.01665	15.31

No. of Passages	$\frac{1}{h_w}$	$\frac{1}{h_{oo}}$	$\frac{1}{U}$	U	A = 927/U	L = A/13.7h
1	0.02762	0.02825	0.05587	17.90	51.79 ft^2	3.78
2	0.04184	0.04310	0.08494	11.77	78.76	2.87
3	0.05333	0.05479	0.10812	9.25	100.2	2.44
4	0.06345	0.06532	0.12877	7.77	119.3	2.18

n, No. of Passages	Volume, cu ft*		
	Warm Side	Cold Side	Total
1	0.147	0.147	0.294
2	0.223	0.223	0.446
3	0.285	0.285	0.285
4	0.339	0.339	0.678

The variation of the heat exchanger length and fluid volume is dependent upon the absolute pressure of the unprocessed air (warm side). These variables are incorporated and related to the number of gas passages and appear in Figures 31-35 for heat exchangers HE-1, HE-2, HE-3, HE-4 and HE-5.

A compilation of conditions that might be selected for the operation of a cycle point to a total exchanger volume of from 3 to 6 cubic feet. In this connection, the maximum length necessary for a one passage arrangement is that of exchanger HE-4 which is 12 feet. This value reduces to 6.8 feet for a four-passage arrangement. If a one passage arrangement is to be chosen for this heat exchanger, it may be possible to consider two or three separate one-pass exchangers of shorter length, whose total effective length is 12 feet. The lengths of the other exchangers are not critical and vary from 0.72 to 4.8 feet.

---

*Note: The exchanger volumes calculated correspond to those occupied by the fluid alone and do not include the fin and wall partitions. In order to calculate the total volume (fluid plus fins) these values must be multiplied by the factor representing the total cross sectional area divided by the free cross sectional area or $\left[\frac{0.485 \times 12}{144}\right]$ /0.0389 = 1.039.

CONCLUSIONS

The study has shown the feasibility of the process of freezing out the CO_2 since the size and power requirements are both reasonable. This concludes the phase of the work currently authorized.

Future work in the problem would involve the setting up of experimental equipment for confirming the results obtained and for observation of any factors which may have been minimized.

Problems that have to be investigated in this experimental phase would be:

1. Determination of heat leaks.
2. Determination of cycle times and coordination of the various parts of the cycle.
3. Time lag in initial start up.
4. Determination of problems involved in CO_2 formation in expansion engine.
5. Balance of refrigeration requirements in heat exchange reversing procedures.
6. Investigation of the actual CO_2 condensing and subliming conditions and confirming the heat transfer coefficients.
7. Checking of the process in general.
8. Mechanical operational problems, valving particularly, under the pressures and low temperatures involved.

TABLE VI

SURFACE TEMPERATURE OF THE OCEANS

Latitude	0	20	40	60	80	100	120	140	160	180	160	140	120	100	80	60	40	20	Season	Depth (M)
		← E										W ←								
60	7	—	—	—	—	—	—	2	—	—	—	—	—	—	—	—	3	8	Feb.	
	13	—	—	—	—	—	—	15	9	6	9	—	—	—	—	4	8	12	Aug.	
	9	—	—	—	—	—	—	6	—	3	—	—	—	—	—	3	5	8		200
	2	—	—	—	—	—	—	—	—	3	—	—	—	—	—	2	3	0		400
40	13	14	—	—	—	—	0	6	9	11	9	12	—	—	—	15	16	14	Feb.	
	25	25	30	—	—	—	25	25	21	20	21	19	—	—	—	24	24	21	Aug.	
	—	—	—	—	—	—	—	5	6	10	6	9	—	—	—	18	17	13		200
	—	—	—	—	—	—	—	1	—	6	—	—	—	—	—	10	16	12		400
20	23	—	26	23	—	—	24	25	25	25	25	22	21	25	26	25	23	19	Feb.	
	23	—	30	24	—	—	28	28	28	27	28	24	25	22	29	28	26	24	Aug.	
	14	—	—	16	—	—	15	22	21	20	21	16	10	18	20	20	19	15		200
	8	—	—	13	—	—	10	14	13	11	13	8	8	12	15	13	12	12		400
0	23	—	27	28	28	28	27	28	28	27	27	28	29	25	27	—	27	27	Feb.	
	23	—	24	27	27	28	28	28	28	28	23	28	23	22	23	—	26	24	Aug.	
	14	—	14	14	14	13	13	20	21	21	20	20	17	18	13	—	12	13		200
	8	—	10	10	10	10	10	9	9	9	9	9	10	12	10	—	8	9		400
20	23	20	27	27	26	25	29	15	28	26	26	15	15	15	17	18	25	26	Feb.	
	18	22	24	23	22	22	23	12	24	23	24	12	11	11	11	12	23	21	Aug.	
	13	15	16	20	19	18	17	12	21	20	21	12	11	10	12	12	16	16		200
	9	11	12	14	15	12	10	9	13	14	13	9	9	9	9	10	11	10		400
40	17	20	17	17	16	15	15	15	17	18	18	16	15	15	17	17	17	16	Feb.	
	13	13	13	13	11	11	11	12	13	13	13	12	10	11	11	13	11	11	Aug.	
	9	15	9	11	11	10	11	9	13	12	12	9	10	10	8	10	10	10		200
	6	11	8	10	11	10	9	10	10	9	9	9	9	10	6	10	5	7		400
50	-1	-1	-1	-1	-1	1	-1	0	-1	4	-1	3	2	4	5	3	0	0	Feb.	
	-1	-1	-1	-1	-1	1	-1	-1	1	-1	1	0	-1	-1	1	0	-1	-1	Aug.	
	0	4	1	1	1	1	1	2	2	2	2	2	2	2	3	2	0	0		200
	2	2	2	1	1	1	1	2	2	2	2	2	2	2	3	2	1	1		400

Longitude → E ← W

less than -1 to 1

less than -1 to 0 C

TABLE VII

TEMPERATURE AND ENTHALPY CHANGE OF AIR STREAM FROM COMPRESSORS

Pressure Atm		Temperature °F						Enthalpy Change Btu/# 70% Efficiency	
		T_2			T_4				
		Efficiency			Efficiency				
P_1	P_2	100%	85	70	100	85	70	Per Stage	Total
2.24	5	220	245	281	231	256	292	48	96
2.45	6	242	266	309	253	277	320	55	110
2.65	7	260	284	331	271	295	342	61.5	123
2.83	8	272	300	349	283	360	311	66	132
3.00	9	283	315	365	294	326	376	70	140
3.16	10	293	329	382	304	340	393	73.5	147
3.32	11	302	341	396	313	352	407	76.4	152.8
3.37	15	337	380	439	348	391	450	86.8	173.6
4.47	20	373	418	484	384	429	496	98.5	197
5.00		395	448	524				107.8	107.8
6.81		470	537					135	135

TABLE VIII

AIR STREAM TEMPERATURE °F FOR 99% CO_2 REMOVAL WITH
CONDENSATE AND RIME REVAPORIZED BY CLEAN AIR STREAM

	1	3	5	10	15	20
Foul air, operating pressure, atm	1	3	5	10	15	20
Foul air, inlet to H.E. 1, T_1, T_2	80.0	90.0	90.0	90.0	90.0	90.0
Foul air, outlet from H.E. 1, T_3	80.0	365.0	524.0	393.0	450.0	496.0
Foul air, inlet to H.E. 2, T_4	80.0	90.0	90.0	90.0	90.0	90.0
Foul air, outlet from H.E. 2, inlet to H.E. 3, T_5	80.0	80.0	80.0	80.0	80.0	80.0
Clean air, outlet from H.E. 3, T_{13}	35.0	35.0	35.0	35.0	35.0	35.0
Foul air, outlet from H.E. 3, inlet to H.E. 4, T_6	25.0	25.0	25.0	24.8	24.5	24.1
Clean air, inlet to H.E. 3, outlet from H.E. 4, T_{12}	-187.5	-175.8	-169.0	-158.9	-153.2	-149.4
Foul air, outlet from H.E. 4, inlet to H.E. 5, T_7	-189.4	-181.6	-177.8	-172.1	-166.8	-167.5
Clean air, 75% of minimum inlet to H.E. 4, T_{11}	-199.5	-188.8	-182.9	-176.1	-174.0	-172.4
Clean air, inlet to H.E. 4, outlet from H.E. 5, T_{11}	-236.0	-227.5	-223.7	-218.9	-216.8	-216.7
Clean air, inlet to expansion engine, T_8					-201.2	-186.0
Clean air, minimum inlet to expansion engine T_8'						
Clean air, 75% of minimum inlet to H.E. 5, T_{10}	-237.4	-231.3	-229.6	-227.4	-227.0	-227.8
Clean air, maximum required outlet from expansion engine, T_{10}		-258.9	-257.0	-259.5	-266.4	-275.5
Clean air, outlet from 70% efficient expansion engine, T_9	-236.0	-268.9	-287.9	-309.2	-312.83	-312.63

Note: At 11.08 atm T_8' coincides with T_8

TABLE IX

INLET AIR STREAM EQUILIBRIUM TEMPERATURES

Condition	Per Cent CO_2 Removed	Temperature - °F	
		At 1 atm Pressure	At 13.6 atm Pressure
T_7	0	-187.5	-154.3
T_8	36	-193.0	-161.7
T_8	68	-201.2	-172.7
T_8	84	-209.3	-183.6
T_8	92	-216.3	-192.7
T_8	96	-223.7	-201.5
T_8	98	-230.0	-209.1
T_8	99	-236.0	-217.2
T_8	99.5	-242.0	-223.8
T_8	99.75	-247.2	-230.9
T_8	99.875	-252.5	-237.0

Note: Curves are based upon the equilibrium temperatures of CO_2 under its own vapor pressure and corrected for total pressure.

TABLE X

TOTAL ENTHALPY OF HIGH PRESSURE AIR STREAM IN BTU/HR

Pressure - atm	1	3	5	10	15	20
Inlet to H.E. 3 at T_5	122799	120344	117977	116104	115331	114844
Outlet from H.E. 3 at T_6 assuming H_2O present as a vapor at T_{13}	116324	113875	111503	109615	108805	108271
Outlet from H.E. 3 at T_6 (including condensate)	110863	109173	108706	108227	107880	107572
Inlet to H.E. 4 at T_6	110848	109160	108698	108223	107878	107570
Outlet from H.E. 4 at T_7 assuming H_2O present as a vapor at T_{12}	84441	84011	84240	84591	84538	84336
Outlet from H.E. 4 at T_7 (including rime)	81837	83151	83724	84333	84366	84207
Inlet to H.E. 5 at T_7	82159	83257	83788	84365	84387	84223
Outlet from H.E. 5 at T_8 (including solid CO_2, 92% CO_2 removed)	76924	77751	78009	77853	77396	76573
Inlet to expansion engine at T_8 (92% CO_2 removed)	76925	77732	77981	77811	77346	76521
Outlet from H.E. 5 at T_8 (including solid CO_2, 99% CO_2 removed)	74418	75013	75070	74556	73517	72216
Inlet to expansion engine at T_8 (99% CO_2 removed)	74459	75036	75085	74562	73518	72217

Basis: Air (oxygen and nitrogen): Saturated liquid 1 atm pressure (141.7°R) enthalpy = 46.33 Btu/#
entropy 0.0 Btu/#°R

Water: Saturated liquid at 32°F; enthalpy = 0.0 Btu/#, entropy = 0.0 Btu/#°R
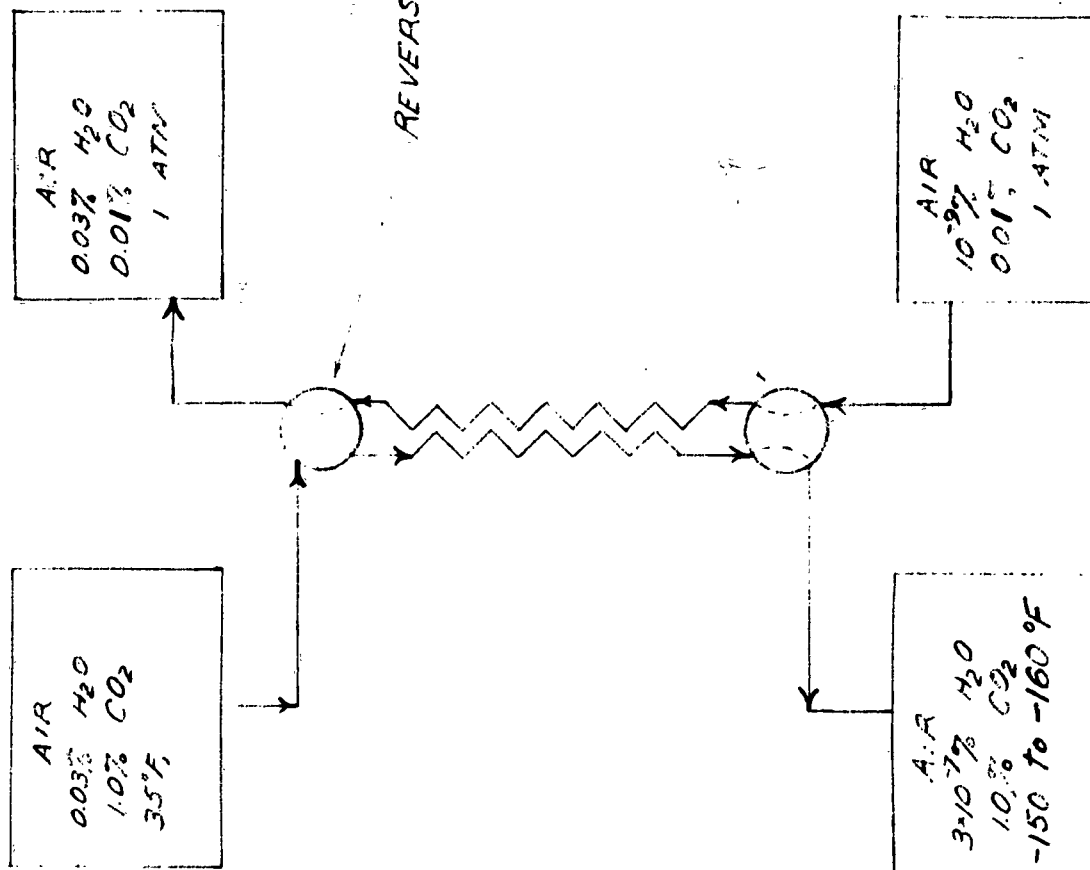CO_2: Saturated liquid at 32°F; enthalpy = 180.0 Btu/#, entropy = 1.0 Btu/#°R

TABLE XI

AIR STREAM TEMPERATURES °F FOR 99% CO_2 REMOVAL

WITH CONDENSATE AND RIME DISCARDED

Foul air, operating pressure, atm	1	3	5	10	15	20
Foul air, inlet to H.E. 1, T_2	80.0	365.0	524.0	393.0	450.0	496.0
Foul air, outlet from H.E. 1, T_3	80.0	90.0	90.0	90.0	90.0	90.0
Foul air, inlet to H.E. 2, T_4	80.0	90.0	90.0	90.0	90.0	90.0
Foul air, outlet from H.E. 2 inlet to H.E. 3, T_5	80.0	80.0	80.0	80.0	80.0	80.0
Clean air, outlet from H.E. 3, T_{13}	90.0	35.0	35.0	35.0	35.0	35.0
Foul air, outlet from H.E. 3, inlet to H.E. 4, T_6	35.0	-15.1	1.1	13.0	16.6	18.1
Clean air, inlet to H.E. 3, outlet from H.E. 4, T_{12}	-22.5	-175.8	-169.0	-158.9	-153.2	-149.4
Foul air, outlet from H.E. 4, inlet to H.E. 5, T_7	-187.5	-181.6	-177.8	-172.1	-168.8	-167.5
Clean air, 75% of minimum inlet to H.E. 4, T_{11}						
Clean air, inlet to H.E. 4, outlet from H.E. 5, T_{11}	-189.4	-235.3	-210.7	-189.8	-183.2	-180.4
Clean air, inlet to expansion engine, T_8	-266.4	-227.5	-223.7	-218.9	-216.8	-216.7
Clean air, minimum inlet to expansion engine, T_8'	-236.0				-201.2	-186.0
Clean air, 75% of minimum inlet to E.E. 5, T_{10}	-237.4	-231.3	-229.6	-227.4	-227.0	-227.8
Clean air, maximum inlet to outlet from expansion eng., T_{10}	-331.8	-305.2	-284.7	-273.2	-275.6	-282.5
Clean air, outlet from 10% efficient expansion engine, T_9	-236.0	-268.9	-287.9	-309.2	-312.83	-312.83

Note: At 11.08 atm T_8' coincides with T_8

BILL OF MATERIAL

ITEM	REC'D	SPECIFICATIONS	MATERIAL

FOUL AIR
1% CO_2
65% Relative Humidity
T_1 = 80°F
P_o = 1 Atm.
Rate: Total, 500 lbs./hr.
CO_2 7.59 lbs./hr.
H_2O 7.05 lbs./hr.
Air   485.36 lbs./hr.

Sea
Water
T_{14}

Sea
Water
T_{14}

FRESH AIR
0.015% CO_2
Ca. % Rel.Hum.
P_o = 1 Atm.
T_{13} = 80°F

CO_2 Discharge

CO_2 Discharge

H.P. = ?

Turbine

CHEMICAL ENGINEERING DEPARTMENT
NORTHWESTERN TECHNOLOGICAL INSTITUTE
EVANSTON, ILLINOIS

TITLE: CO_2 Removal by Freezing

DR. BY:	DATE: 8-31-52
CHKD BY:	SCALE: None
APPD. BY:	ASS'BLY NO:

DRAWING NO. 605-1

PROJECT: 130

FIG: 19

B

BY	ALTERATIONS	DATE

TOLERANCES:—ALL FRACTIONAL DIMENSIONS ± 1/64"
ALL DECIMAL DIMENSIONS ± .005"
UNLESS OTHERWISE SPECIFIED

GLENNON & KERN, CHICAGO

FIG: 20

(b) DURING SECOND HALF OF CYCLE

REVERSING VALVES

AIR
0.03% H₂O
0.01% CO₂
1 ATM

AIR
10⁻²% H₂O
0.01% CO₂
1 ATM

AIR
0.03% H₂O
1.0% CO₂
35°F

AIR
3×10⁻²% H₂O
1.0% CO₂
-150 to -160°F

(a) DURING FIRST HALF OF CYCLE

CHEMICAL ENGINEERING DEPARTMENT
NORTHWESTERN TECHNOLOGICAL INSTITUTE
EVANSTON, ILLINOIS

TITLE: Reversing Exchanger	
DR. BY: MJK	DATE: June 18, 1952
CH'KD BY:	SCALE: None
APPD. BY:	ASS'BLY NO:
DRAWING NO. 602-1	

PROJECT: 130

A

GLENNON & KERN, CHICAGO

FIG. 21

CO_2 FREEZE-OUT METHOD

Temperatures of air stream from compressors
$P_0 = 1$ atm, $T_1 = 80°F$, $T_3 = 90°F$
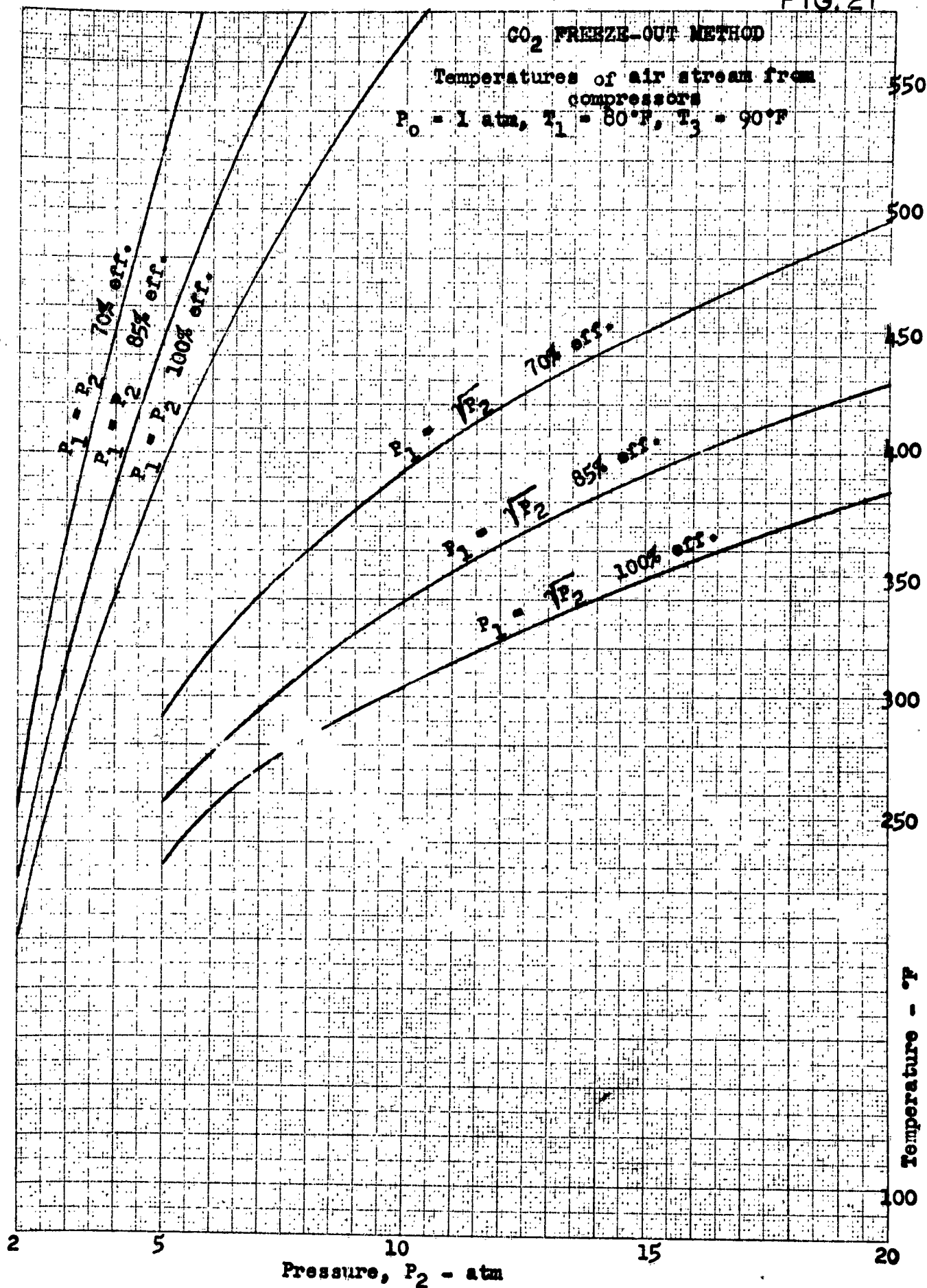
Pressure, P_2 — atm

Temperature — °F

FIG. 22

CO₂-FREEZE-OUT METHOD

Air Stream Temperatures

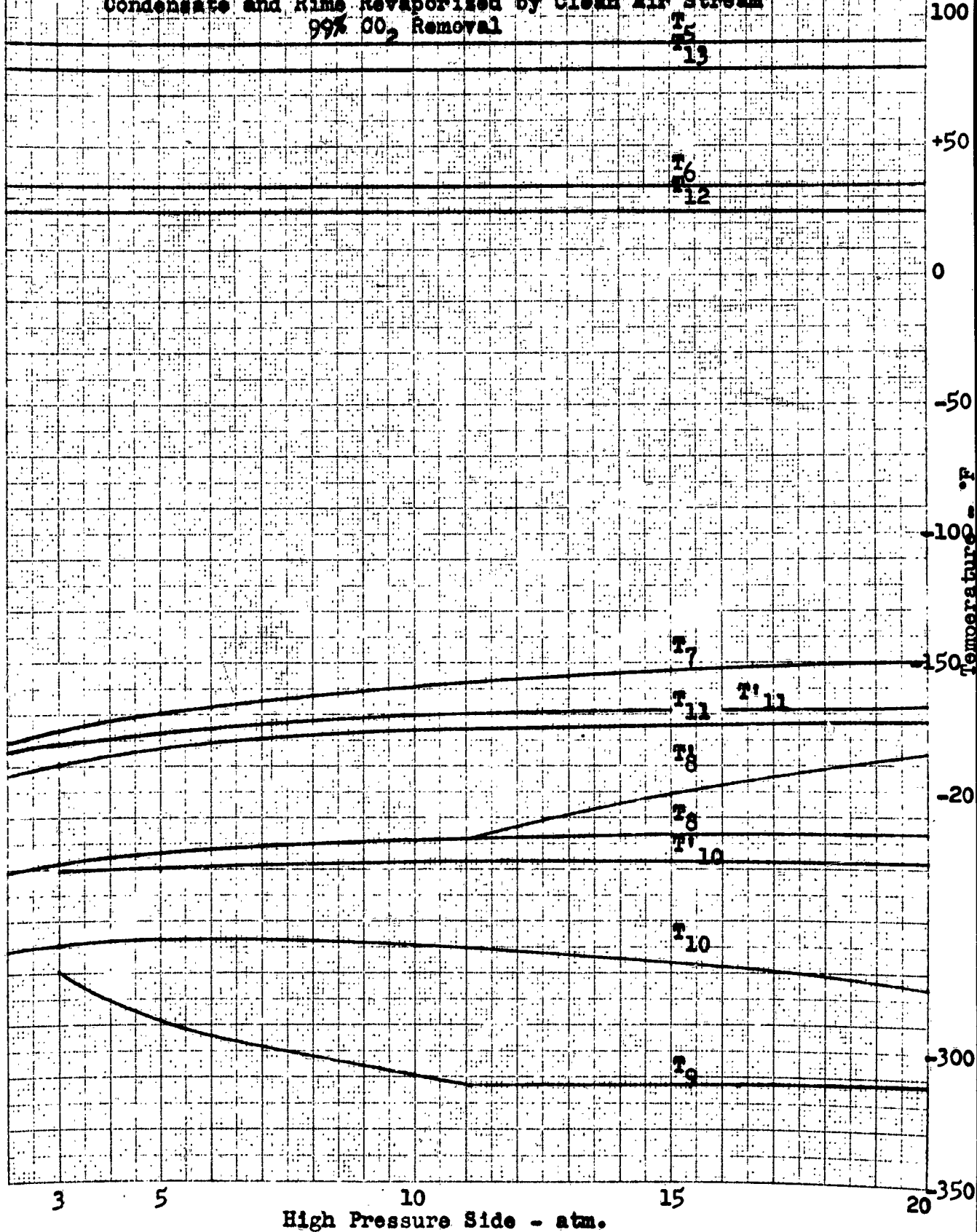Condensate and Rime Revaporized by Clean Air Stream
99% CO₂ Removal

FIG 23

SOLID CO₂ – AIR EQUILIBRIUM
Temperature vs. Pressure
Parameters: CO₂ Content of Air Stream

Total Pressure – atmospheres

FIG. 24

DERIMING STREAM TEMPERATURE

P_2 = Pressure on high pressure side.
P_o = Pressure on low pressure side
T_7 or T_8 = Temperature on high pressure side
T_{11} or T_{10} = Temperature on low pressure side

Pressure Ratio P_2/P_o = 20

Maximum Temperature Difference, °F

$T_7 \div T_{11}'$ or $T_8 \div T_{10}'$, °F
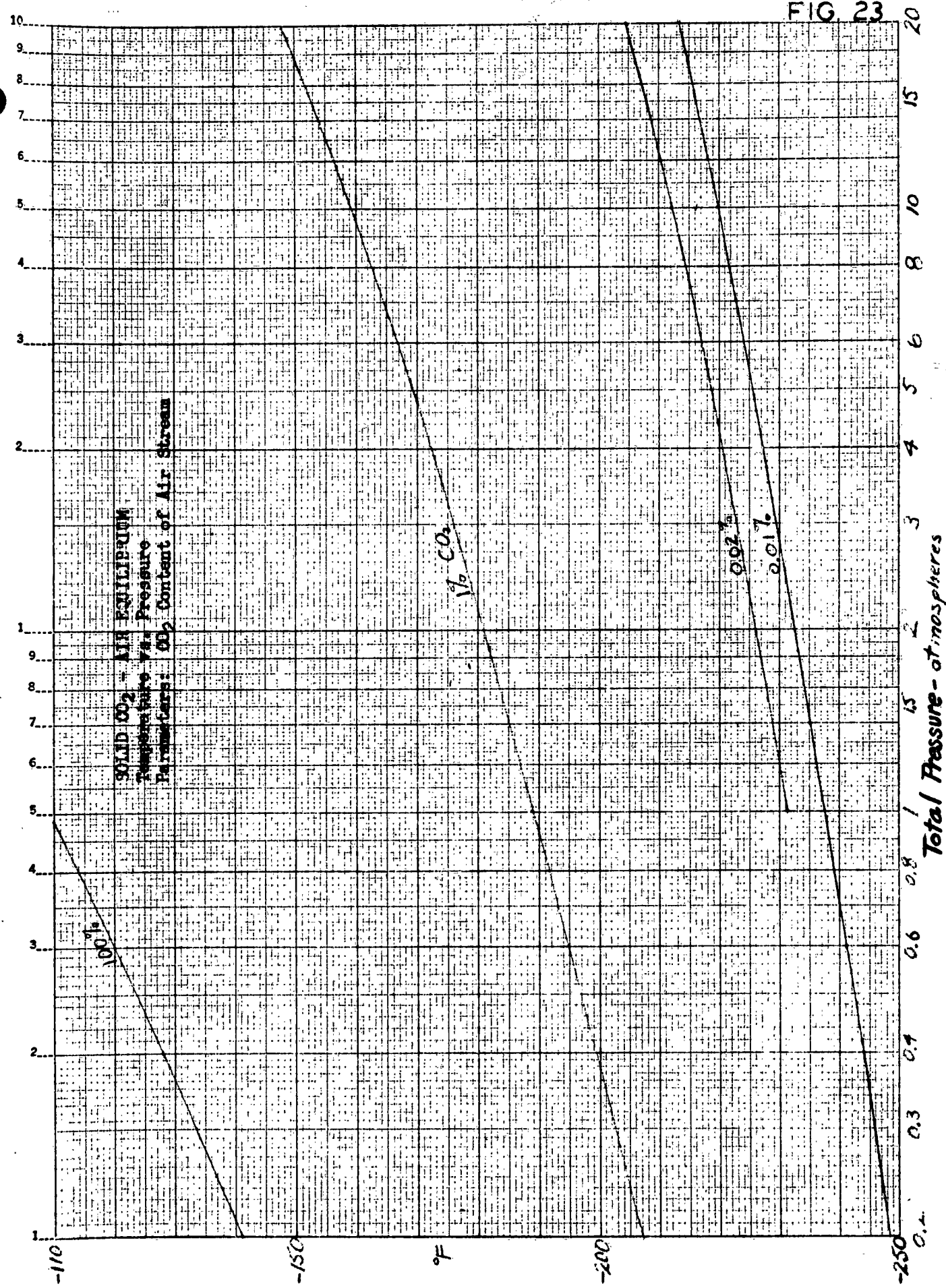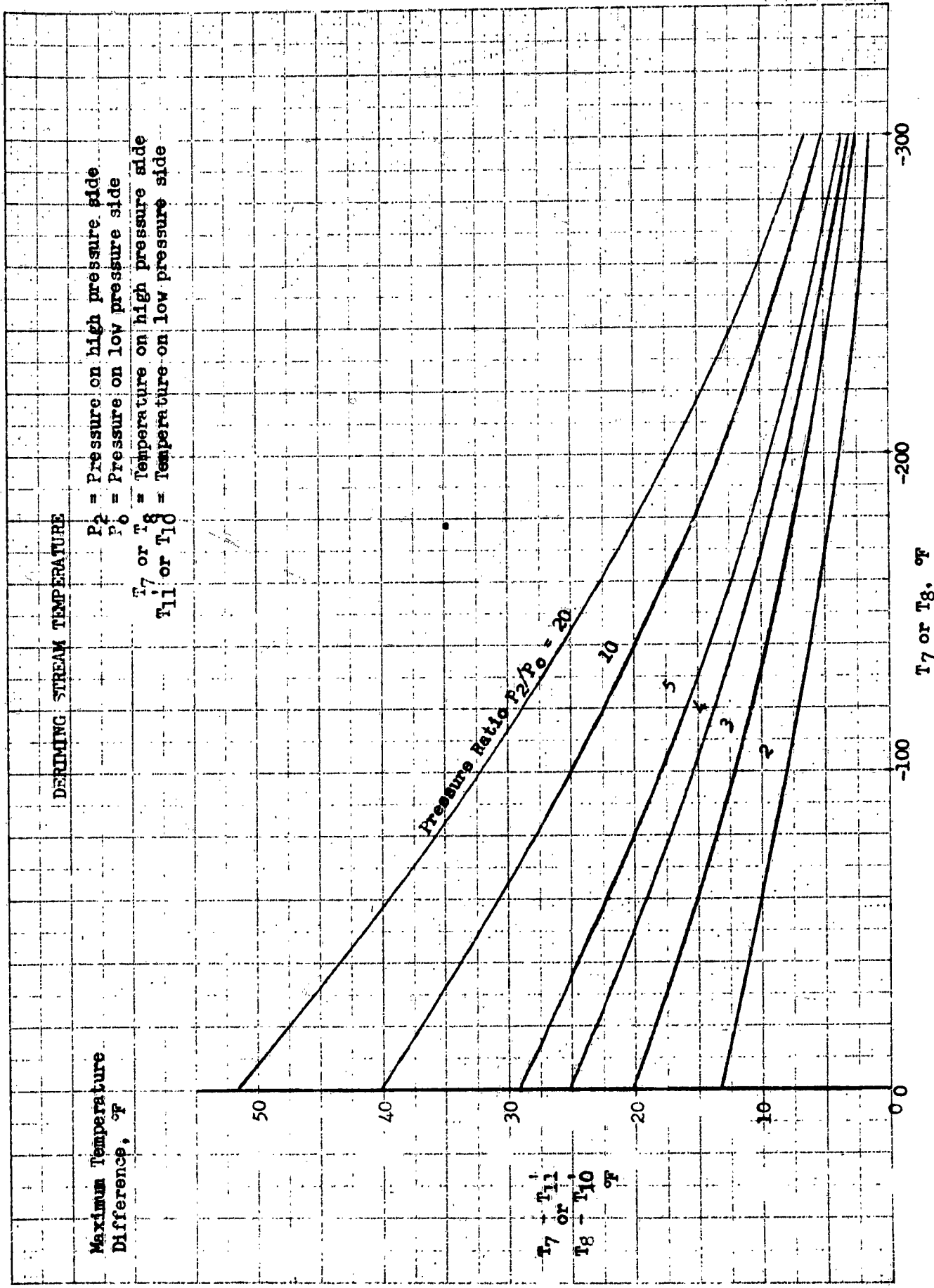
FIG. 25

HEAT EXCHANGER DERIMING
Basis: Initial CO_2 Content of Air is 1%
100% CO_2 in Deriming System
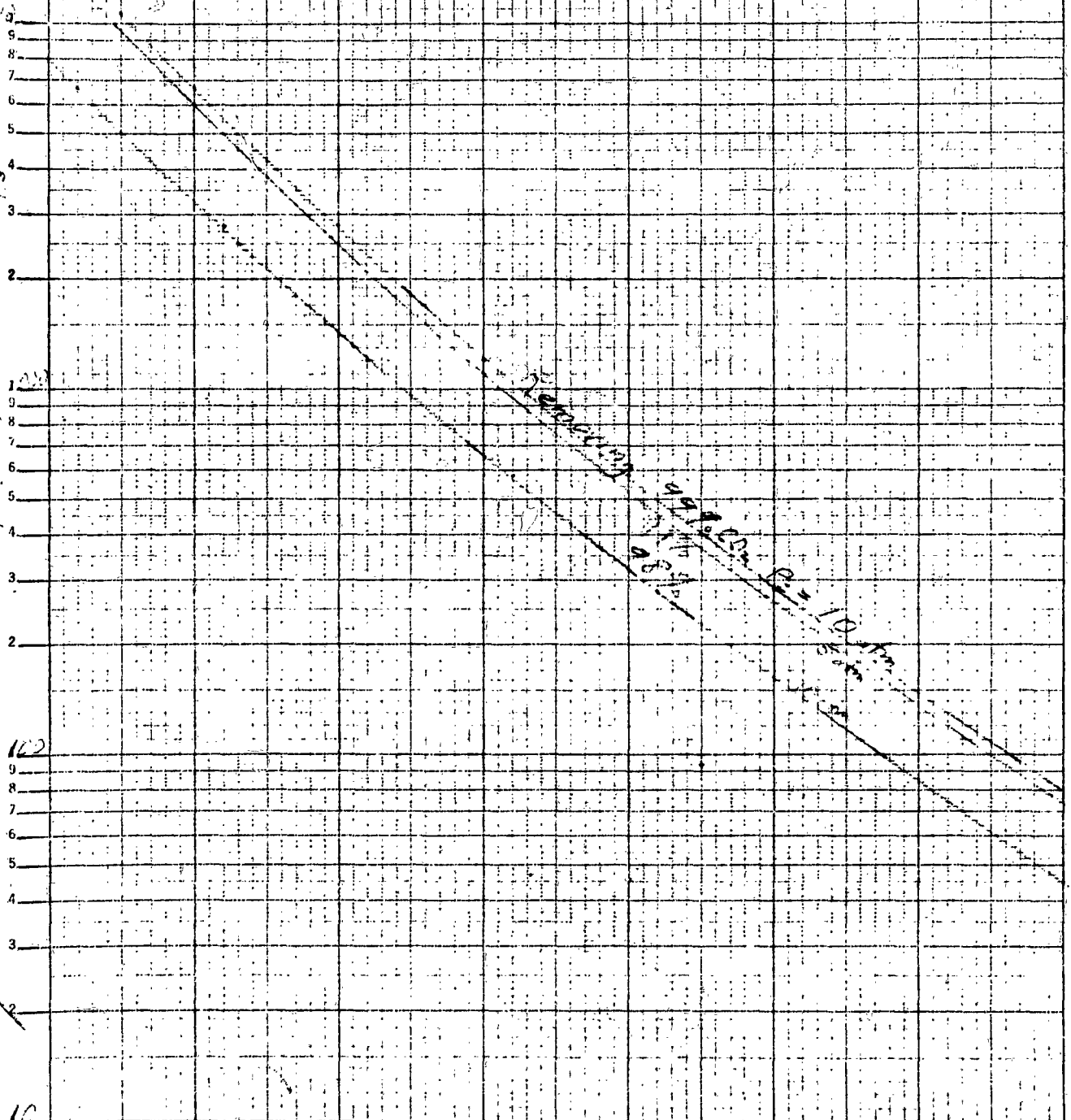P_2: High pressure in operating part of cycle
P_3: Low pressure in deriming part of cycle
T_8: Coldest end of CO_2 exchanger operating section
T_{17}: Minimum temp. for deriming part of cycle
Parameters: Pressure P_2
: % CO_2 removal

Temp. Rise °F $T_{17} - T_8$

FIG. 26

CO_2 FREEZE-OUT METHOD

Total Enthalpy of Air Stream
Basis: Initial Air Stream
500#/hr (7.06 # H_2O, 7.59 # CO_2)

H of air stream entering H.E. 3 at T_5 = 90°F

H of air stream leaving H.E. 3 at T_6 = 35°F (assuming H_2O is present as vapor at T_{13} = 80°F)

H of air stream leaving H.E. 3 and entering H. E. 4 at T_6 = 35°F

H of air stream leaving H.E. 4 at T_7 (assuming rime is present as a vapor at T_{12})

H of air stream leaving H. E. 4 and entering H.E. 5 at T_7

H of air stream leaving H.E. 5 and entering expansion engine (92% CO_2 removed)

H of air stream leaving H.E. 5 and entering expansion engine (99% CO_2 removed)

Enthalpy, H, — Btu/hr x 10^{-3}

125

120

115

110

85

80

75

70

Pressure = atm.

2   3   4   5   10   15   20

FIG. 27

Temperature °R

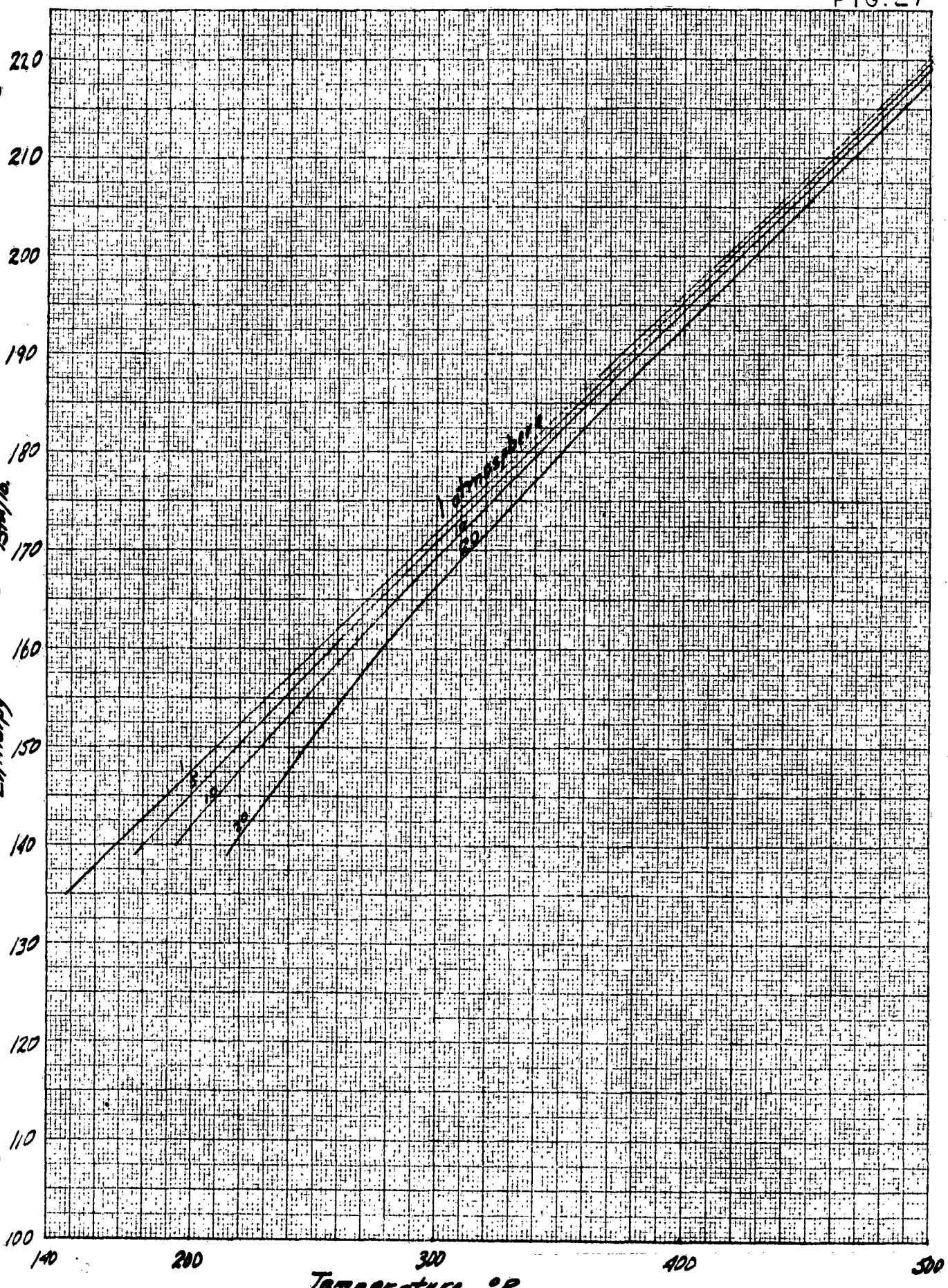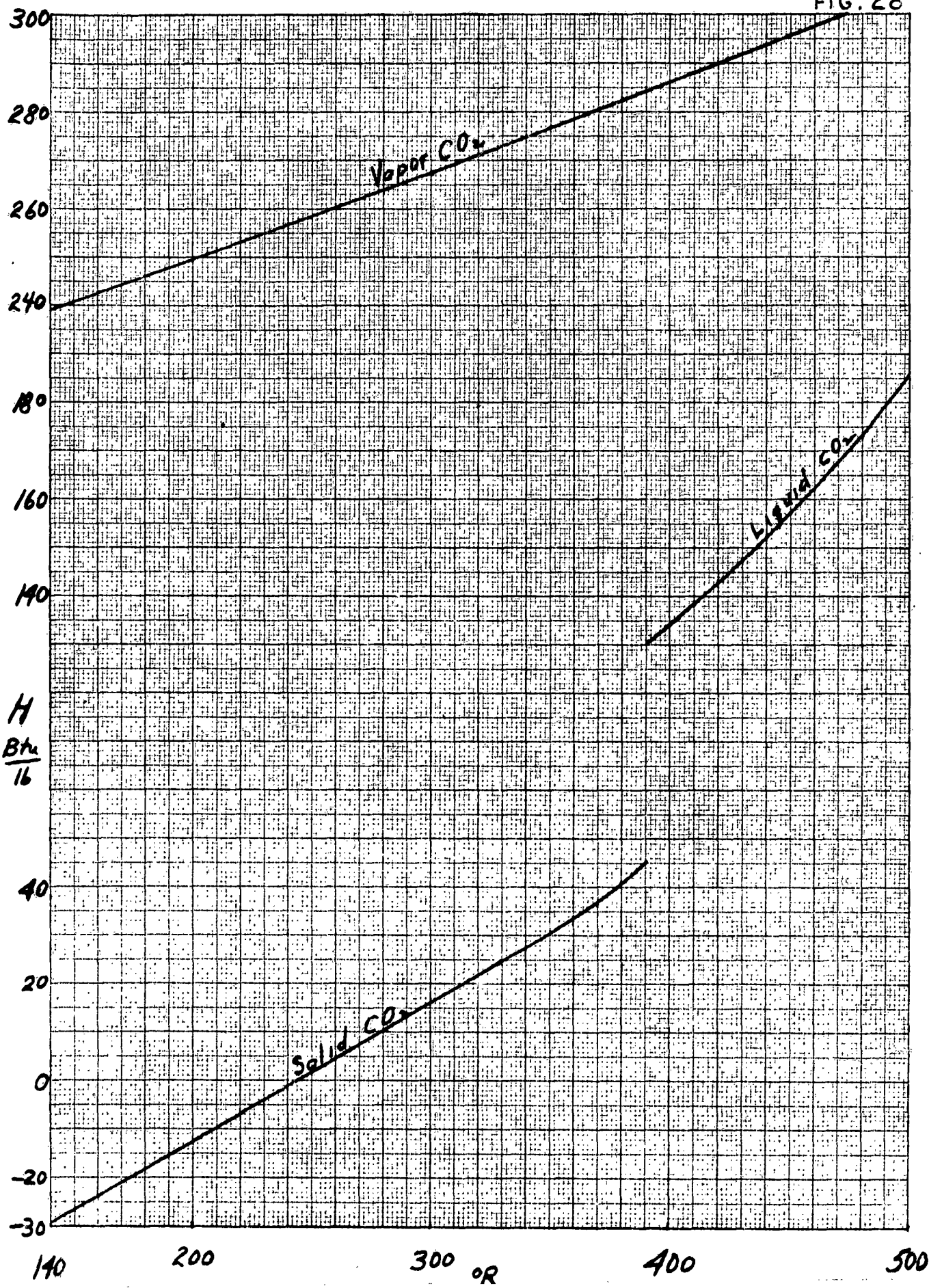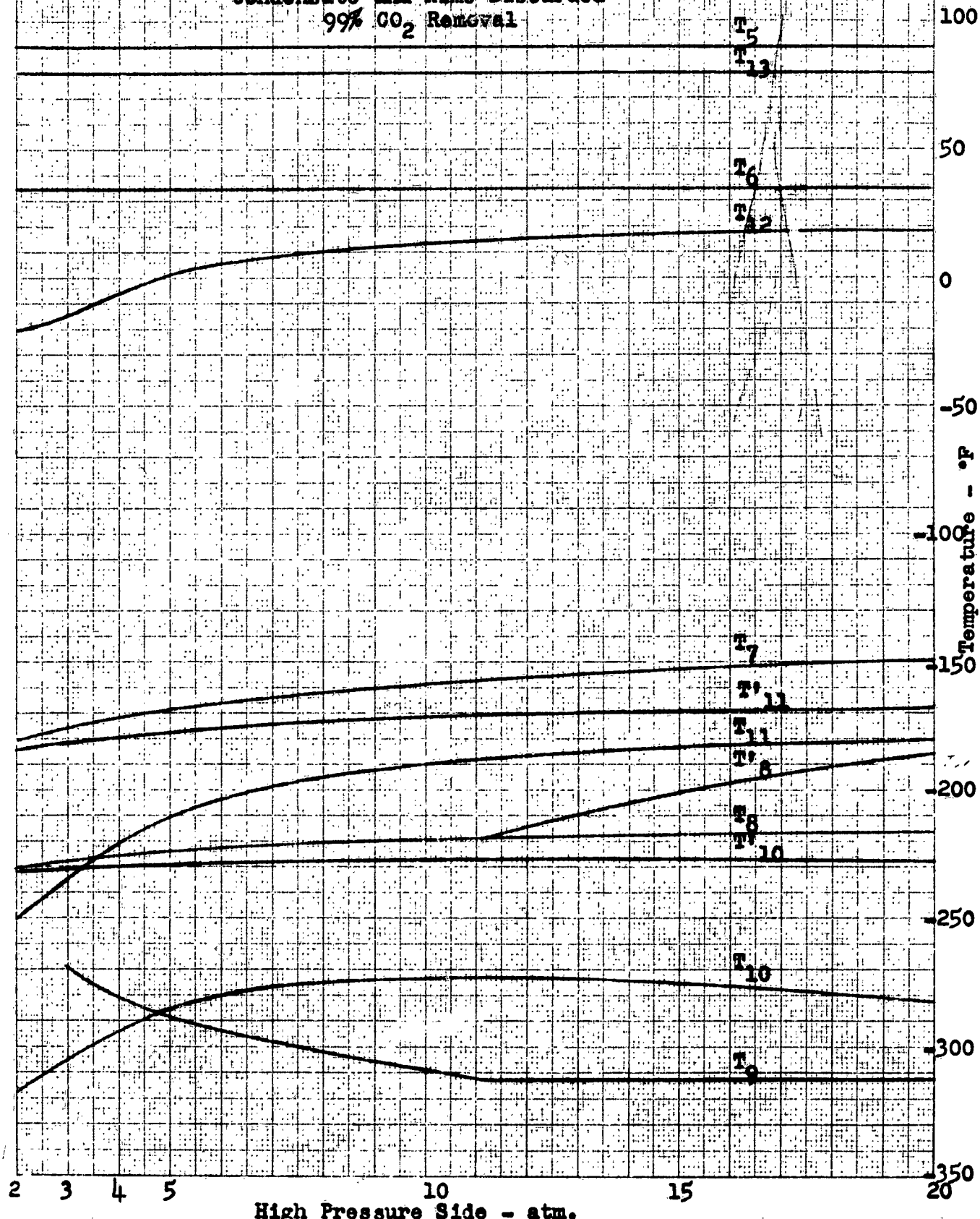FIG. 28

FIG. 29
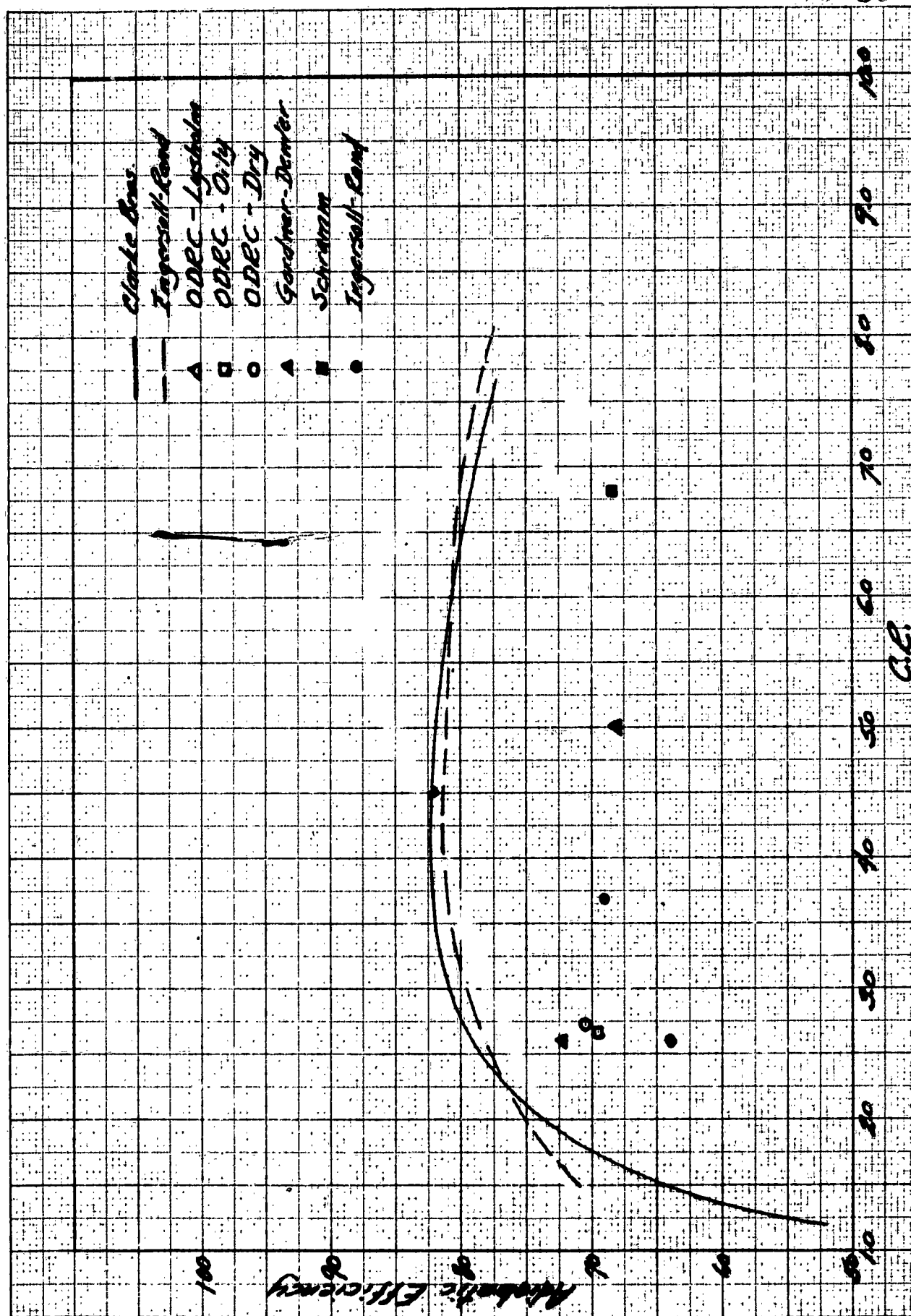
CO₂-FREEZE-OUT METHOD

Air Stream Temperatures
Condensate and Rime Discarded
99% CO₂ Removal

FIG. 30

FIG. 31

Brazelton ~ Thodos   Sept. 9, 1952.

FIG. 32

Brazelton~Thodos Sept. 9, 1952

Water Cooled Heat Exchanger HE-1

Use 3" strip fin ~0.183" height, 6" width

Air $T_2 \longrightarrow 90°F$
Water $90° \longleftarrow 80°F$

FIG 33

Brazelton ~ Thodos   Sept. 9, 1952

FIG. 54

Air to Air Heat Exchanger HE-1

$\frac{3}{32}$" strip fin, height = 0.485", width = 12"

Warm Side (unprocessed air) —— $T_6 = 95°F$ —— $-169.0 \leq T_7 \leq -149.4°F$

Cold Side (processed air) —— $241 \leq T_8 \leq 25.0°F$ —— $-177.8 \leq T_{11} \leq -161.5°F$

Volume (unprocessed plus processed air passages), ft^3

Length of Exchanger, ft

Number of Passages

P_2, Inlet Air Pressure, psia

Number of Passages

FIG. 35

Brazelton - Rhodes   Sept. 12, 1952

Air to Air Heat Exchanger HE-5

$\frac{3}{32}"$ strip fin ; height = 0.485" , width = 12"

Warm Side [unprocessed air] — 159.0 ≤ T_1 ≤ 146.4°F ——— -223.7 ≤ T_8 ≤ -216.7°F

Cold Side [processed air] — 182.9 ≤ T_2 ≤ 173.1°F ——— -229.6 ≤ T_6 ≤ -221.8°F

Volume [unprocessed plus processed air passages], ft³

Number of Gas Passages

Length of Exchanger, ft.

P_2, Inlet Air Pressure, psia

Number of Gas Passages